Governing the Speed of a Light Signal in Optical Fibers: Brillouin Slow and Fast Light

PAR

Sang Hoon CHIN

ÉCOLE POLYTECHNIQUE
FÉDÉRALE DE LAUSANNE

Suisse
2009

To my parents

To my wife Uhhee Song

To my son See-Won and my daughter Rose

Abstract

Dynamic control of the speed of a light signal, based on stimulated Brillouin scattering in optical fibers, was theoretically studied and also experimentally demonstrated as the core object of this thesis. To date, slow light based on stimulated Brillouin scattering has shown the unmatched flexibility to offer an efficient timing tool for the development of all-optical future router. Nevertheless, the seeming perfect Brillouin slow light suffered from three major obstacles: naturally narrow signal bandwidth, strong change of signal amplitude, and significant signal distortion. The essential contribution of this work has been mostly dedicated to resolve all those impairments so as to make Brillouin slow light a completely operating all-optical delay line for practical applications. Actually, high capability of tailoring the spectral distribution of the effective Brillouin resonance makes possible to resolve partially or completely all those problems.

First of all, a broadband spectral window was passively obtained in between two Brillouin gain/loss resonances by simply appending two segments of fibers showing different Brillouin frequency shifts. The global Brillouin gain of the concatenated fibers manifests a gain/loss doublet resonance showing a broad window in between gain/loss peaks. In practice, this configuration has a crucial advantage that it removes the need of the pump modulation, generally used to create a polychromatic pump source. Therefore, a broadband Brillouin slow and fast light was simple realized with a reduced distortion.

Secondly, the signal amplification or attenuation associated to the signal delay was completely compensated by superposing Brillouin gain and loss resonances with identical depth but different width. As a result, the Brillouin gain led to effectively a spectral hole in the center of the broadband absorption and opened a transparent window while the sharp change in the refractive index was preserve. This way it makes possible to realize zero-gain Brillouin slow light. This configuration was also exploited to produce Brillouin fast light with a total absence of signal loss, simply by swapping the spectral position of the two pumps.

At last, a signal was continuously delayed through a Brillouin fiber delay line without any distortion. Due to the strong induced dispersion, pulse broadening is a major

difficulty in all slow light systems and it is impossible to compensate such broadening using a linear system. Therefore, a conventional Brillouin slow light system was combined with a nonlinear optical fiber loop mirror that gives a nonlinear quadratic transmission. Using this configuration, the inevitable pulse broadening was completely compensated at the output of the loop and a signal was delayed up to one symbol without any distortion

Brillouin slow light systems were further studied in the spectral domain. For a given Brillouin resonance the spectrum of a light pulse was optimized to better match the Brillouin bandwidth. When the time envelope of a pulse was properly shaped, it was clearly observed that the spectral width of the pulse became minimized while preserving the pulse duration. This way the maximum time delay through Brillouin slow light could be enhanced for a fixed pulse width.

Brillouin fast light was even realized in total absence of any pump source, which is a plain requirement for the generation of Brillouin slow or fast light. This self-generated delay line, key contribution of this thesis, relies on both spontaneous and stimulated Brillouin scattering in optical fibers. In this implementation, a light signal was strongly boosted above the so-called Brillouin threshold, so that most power of the signal was transferred to a backward propagating wave, namely the generation of amplified spontaneous Stokes wave. Since the center frequency of the intense Stokes wave is below the signal frequency by exactly Brillouin shift of the fiber used, this wave led to a Brillouin loss band centered at the signal frequency. Consequently, the signal experienced fast light propagation and the propagation velocity of the signal was self-controlled, simply by varying the signal input power. This technique has many practical advantages such as its high simplicity of the configuration and an invariant signal power in the output of this delay line. Additionally, this system self-adapts the signal bandwidth as the spectrum of the amplified Stokes wave matches the spectral distribution of the signal.

An alternative method to generate all-optical delay line was proposed instead of slow light. This scheme makes use of the combination of wavelength conversion and group velocity dispersion. This type of delay line was mainly aimed at improving the storage capability of delaying element. The wavelength of a signal was simply and efficiently converted at a desired wavelength using cross gain modulation in semiconductor optical amplifiers. Then the converted signal was delivered to a high dispersive medium and arrived at the end of the medium with relative time delay due to the group velocity dispersion. A fractional delay of 140 was continuously produced through this delay line for a signal with a duration of 100 ps, preserving signal bandwidth and wavelength.

The effect of slow light on linear interactions between light and matter was experimentally investigated to clarify the current scientific argument regarding slow light-

enhanced Beer-Lambert absorption. It was predicted that real slowing of the light group velocity could enhance the molecular linear absorptions so as to improve the sensitivity of this type of sensing. However, the experimental results unambiguously show that material slow light (slow light in traveling wave media) does not enhance the Beer-Lambert absorption.

Keywords

Version abrégée

L'étude théorique et la démonstration expérimentale du contrôle dynamique de la vitesse d'un signal lumineux, basé sur la diffusion Brillouin stimulée dans les fibres optiques, représente l'essentiel de ce travail de thèse. À ce jour, la lumière lente obtenue par la diffusion Brillouin stimulée a démontré une souplesse inégalée pour réaliser la fonction de temporisation destinée au développement des futurs routeurs tout-optiques. Néanmoins, malgré ses atouts évidents, la lumière lente Brillouin présente trois défauts majeurs: une bande passante du signal naturellement étroite, une forte altération de l'amplitude du signal et une distorsion significative de l'enveloppe du signal. La contribution essentielle de ce travail réside dans la résolution de ces problèmes, afin de réaliser avec la lumière lente Brillouin une ligne de retard tout-optique pour des applications pratiques. En fait, la possibilité de modifier la distribution spectrale effective de la résonance Brillouin permet de résoudre partiellement ou complètement tous ces problèmes.

En premier lieu, une fenêtre spectrale large-bande a pu être obtenue, de manière passive, entre deux résonances Brillouin en gain ou perte, en juxtaposant simplement deux segments de fibres avec des décalages fréquentiels Brillouin différents. Le gain Brillouin global des fibres concaténées se présente sous la forme d'une double résonance gain/perte présentant un large intervalle spectral entre les pics gains/pertes. Dans la pratique, cette configuration a l'énorme avantage de supprimer le besoin de moduler la pompe - modulation généralement utilisée pour créer une pompe polychromatique. Une lumière lente et rapide Brillouin large bande a été réalisée de façon simple avec une distorsion réduite en utilisant cette configuration.

Deuxièmement, l'atténuation ou l'amplification du signal, associées à la création de l'effet retard sur le signal, ont été entièrement compensée en superposant des résonances en gain et perte Brillouin d'égale amplitude, mais de largeur différente. Par conséquent, le gain Brillouin superposé à la perte conduit pratiquement à la formation d'un trou spectral au centre de la large bande d'absorption, créant ainsi une fenêtre de transparence tout en

préservant la variation accentuée de l'indice de réfraction. De cette façon, il est possible de réaliser une lumière lente Brillouin à gain nul. Cette configuration est également exploitée pour produire de la lumière Brillouin rapide avec une totale absence d'atténuation du signal, en échangeant simplement la position spectrale des deux pompes.

Enfin, un signal a été continûment retardé sans aucune distorsion par le biais d'une ligne de retard Brillouin fibrée. En raison de la forte dispersion induite, l'élargissement de l'impulsion est une pénalité majeure dans tous les systèmes de lumière lente et il est impossible de compenser un tel élargissement en utilisant un système linéaire. Pour y remédier, un miroir non linéaire, réalisé avec une boucle de fibre optique, a été associé à un système conventionnel à base de lumière lente Brillouin, pour donner une transmission quadratique non-linéaire. En utilisant cette configuration, l'inévitable l'élargissement de l'impulsion a été entièrement compensé à la sortie de la boucle et un signal a pu être retardé sans aucune distorsion sur une durée équivalente à un symbole.

Les systèmes à lumière lente Brillouin ont également été étudiés dans le domaine spectral. Pour une résonance Brillouin donnée, le spectre d'une impulsion lumineuse a été optimisé pour mieux correspondre à la largeur utile de la résonance Brillouin. Lorsque l'enveloppe temporelle d'une impulsion est correctement mise en forme, il a été clairement observé que la largeur spectrale de l'impulsion est minimisée tout en préservant la durée temporelle de l'impulsion. De cette manière, le retard maximal par la lumière lente Brillouin peut être potentiellement augmenté pour une largeur d'impulsion fixée.

Une lumière rapide Brillouin a pu même être obtenue en l'absence totale de toute pompe, le pompage étant jusqu'ici considéré comme une condition sine qua non pour la production de lumière lente ou rapide Brillouin. Cette ligne à retard auto-générée repose sur les diffusions Brillouin spontanée et stimulée dans les fibres optiques. Pour cette mise en œuvre, un signal lumineux a été fortement amplifié au-dessus du seuil Brillouin, de sorte que la majeure partie de la puissance du signal a été transférée à une onde contrapropagative, à savoir la génération d'ondes de Stokes spontanée amplifiée. Puisque la fréquence centrale de l'onde Stokes intense est décalée en-dessous de la fréquence du signal d'une valeur correspondant exactement au décalage Brillouin de la fibre utilisée, cette onde conduit à la formation d'une résonance de perte Brillouin centrée sur la fréquence du signal. Par conséquent, le signal se trouve en condition pour une propagation en lumière rapide et la vitesse de propagation du signal a pu être autocontrôlée, en faisant simplement varier le niveau du signal d'entrée. Cette technique a de nombreux avantages pratiques, tels une grande simplicité de la configuration et une puissance de signal constante en sortie de la ligne à retard. En outre, ce système adapte automatiquement la bande passante de la résonance de

perte au signal, puisque le spectre de l'onde Stokes amplifiée correspond à la distribution spectrale du signal.

Une autre méthode pour générer des lignes à retard tout-optiques a été proposée en lieu et place de la lumière lente. Ce procédé utilise une combinaison de conversion de longueur d'onde et de dispersion de vitesse de groupe. Ce type de ligne à retard vise principalement à améliorer la capacité de stockage d'un élément à retard. La longueur d'onde d'un signal a pu être simplement et efficacement convertie vers la longueur d'onde désirée en utilisant l'intermodulation de gain des amplificateurs optiques à semi-conducteurs. Puis, le signal converti est injecté dans un milieu hautement dispersif pour obtenir à la sortie du milieu un retard temporel relatif dû à la dispersion de la vitesse de groupe. Un retard normalisé de 140, continûment ajustable, a été produit par le biais de cette ligne à retard pour un signal d'une durée de 100 ps, sans modification de la largeur de bande du signal et de sa longueur d'onde.

L'effet de la lumière lente sur les interactions linéaires entre la lumière et la matière a été expérimentalement étudié afin de clarifier l'actuelle conjecture scientifique pour savoir si la lumière lente augmente l'absorption moléculaire de type Beer-Lambert ou pas. Il a été prédit que le ralentissement de la vitesse de groupe de la lumière pourrait renforcer l'absorption linéaire moléculaire de façon à améliorer la sensibilité de ce type de détection. Toutefois, les résultats expérimentaux montrent clairement que la lumière lente de type matériel (lumière lente produite lorsqu'une onde traverse un matériau) ne renforce pas l'absorption de type Beer-Lambert.

Mots clés

optique nonlinéaire, optique fibre, optique fibre nonlinéaire, diffusion Brillouin, propagation d'impulse, amplificateurs et oscillateurs

Acknowledgement

It is my great pleasure to take an opportunity to acknowledge those people who gave me precious help during my Ph.D study. They are quite broadly ranged. They could be around my academic life and also around my private life. Actually, I don't know who I have to start from, but let me start from academic area. Prof. Luc Thévenaz, my wonderful supervisor, must be the first who I have to appreciate. First of all, he gave me this great chance to make Ph.D work at EPFL in Switzerland and guided me always to the right direction. Technical discussion with him was always fruitful, and showed me some challenges and motivations to work. The most important thing is that any second during the discussion was precious and worth doing it. To tell the truth, during discussion I always felt like I am growing up. I believe that he is an extraordinary scientist and it is him who made me a scientist. In addition, he was a very good counselor about family life. Since I have a family, actually I had two jobs, working as a student at school during day and working as a husband and a father of a boy at home during evening. He always gave me good advice about what a family is supposed to be.

Officially, I have only one supervisor, but personally, I have a second supervisor for my Ph.D work. He is Prof. Miguel González-Herráez at Alcala in Spain, one of the juries in my Ph.D exam. During my Ph.D work, he was always next to me, not physically but through email we spent a lot of time to deeply discuss about my experimental results and to devise new ideas. When I didn't follow the discussion well, he didn't save his time before he made me understood the physics behind experiments and mathematical analysis like Luc did. I like to give special thanks to him. And, also, I like to thank all juries in my Ph.D exam, Prof. René Salathé at EFFL, Prof. Jacob Khurgin at Johns Hopkins University in USA and Dr. Romuald Houdré at EFPL. I learned a lot from their questions and comments. They made me look at my work at different angles. It was very nice. Moreover, I like to thank Prof. Moche Tur at Tel Avi University in Israel. I had a discussion with him, just 4 days before my exam, about my presentation for Ph.D exam. I got very precious wisdoms and comments, which improved the quality of my presentation by order of magnitude.

I remember the moment when I just arrived at Luc's laboratory. Frankly speaking, I was so afraid of all electrical equipments and optical components because I was not at all familiar with such stuff and even I didn't know how to operate and which can be helpful for my experiments. Whenever I got in such trouble my brothers (Dario Alasia, Jean-Philippe Besson and Mario Mattiello) came to me to solve all problems, showing me clear explanation. The valuable friendship with them gave me tremendous pleasure while living in Switzerland. One of my best moments at school was a coffee break with them, speaking about our lives, our babies, our bright futures and our dreams. I never forget them. There are still many people who I have to thank. Paulou Pierrette, secretary of photonics doctoral school, helped me a lot when I settled down my new life in Switzerland. She spent lots of time to find an apartment for me. I really appreciate it. Of course, all members of our group (Jean-Charles, Stella, Isabelle and Nikolay) deserve appreciated. I enjoyed a lot having lunch and coffee with them. Two technicians, Frédo and Pascal, were very kind to me, supporting all electronic elements I needed. Also, I like to thank Holger Ficher, Sébastien Equis and José Dintinger for hanging out and also technical discussion, and all people in the laboratory NAM as well.

Today I am so sad since I can not share this pleasure with my parents. Both of them passed away, especially my father passed away just two weeks before the deadline for the submission of my dissertation. For this moment I had sunk into mental chaos, but now everything is ok. In fact, this event makes me much stronger and work harder. I really appreciate their way to raise me. They taught me how to interact with people and how to behave among people from school, society, etc. They always said, "Save money, energy, whatever. Be honest and don't tell a lie. The honest is your best friend and it will bring people to you." Yes, of course, it is very easy to say, but not easy to act so. But, I saw them living this way. Neither of them was working in academic fields. Actually, in my family, I am the only one who did Ph.D study. They don't know the nature of the academic life, but always encouraged me a lot for my study and appreciated my decision whatever I made by myself. They were really good teachers in my life, ever. Also, I like to appreciate my brother and sisters' help and support. They always encouraged me in my whole life and gave me their confidence.

My sweet wife should deserve wonderful thanks, during the last three years and half, for rolling up my sleeves and for letting me concentrate on my work. It is for sure difficult to live abroad without any family, but only with her husband who is not taking care of home very well but only working for Ph.D. Even, having a baby (See-Won) and raising him was mainly her task in Switzerland. I tried to help her as much as possible, but I don't think that it

was enough help for her. So, through this time, I like to thank her again and I like to say to her, "I LOVE YOU." Also, I like to give many thanks to my first son, See-Won for not making huge accidents (^^;). Also, my parents-in-law spent bunch of time to pray for my success. I really appreciate it.

I must thank Heui-sook Weman, the mother of Léo and the wife of Helges Weman. Their help was endlessly flowing into my family. Actually, thanks to them we didn't have any time, even a second to feel lonely and to be bored. First of all, their regular invitation for dinner was fantastic and always delicious. My wife enjoyed a lot the foods when she was pregnant. That's why my son is very healthy today, I guess. ^^. Actually, the meal is only just tiny part during dinner. Talking about the life, Korea's politics, international cultures and so on was really great. We learned a lot while talking together. It is true that Heui-sook is not only a good cook, but also a very good counselor about how to build up my family. I really appreciate whatever she did for my family. Also, I like to thank many Korean people from EPFL and the church. Especially, the bible study with Korean people, living in Lausanne, was memorial event.

Contents

List of Figures

List of Tables

Chapter 1

Introduction

The physics of wave propagation in a dispersive medium has a long history that goes back to more than a century. Lord Rayleigh introduced the concept of group velocity when he discovered that dispersive materials could modify the propagation velocities of wave packets, and predicted the possibilities to make the group velocity faster than the phase velocity in sound waves. The transformation of this theory from sound to light wave led to the apparent contradiction with the fundamental principles of special relativity and causality. Such a problem has been already mentioned by A. Sommerfeld in 1910's and extensively debated in the scientific community. To resolve this problem, A. Sommerfeld and L. Brillouin introduced the concept of signal velocity that must be distinguished from group velocity. They noted that a signal undergoes severe distortion while propagating through a material with large anomalous dispersion, so that group velocity turns meaningless in terms of information propagation. Thus they concluded that a signal can not propagate at a velocity, faster than c (c being the light velocity in vacuum).

Slow light has been coined in modern science for a phenomenon that allows a light signal to propagate with a reduced group velocity. Although slow light was initially motivated by scientific curiosity, this technique has been rapidly developed for many potential applications for which slow light has been identified as a solution. As a matter of fact, the possibility to exert an optical control on the group velocity of an optical signal could have important implications in modern applications such as high capacity data networks and their associated modern technologies: all-optical signal processing, optical buffering and quantum computing, just to mention a few. Over the last decade, successful experiments on slow light propagation has been demonstrated with an astonishing control of the group velocity, namely the velocity at which a signal travels in a material, from nearly stopping it to exceeding the vacuum velocity c or even reaching negative velocities.

So far, slow light has been realized in a wide variety of materials with different physical phenomena, i.e. ultra-cold or -hot atomic gases [1-5], crystalline solids [6,7], micro-cavities [8,9], semiconductors [10,11], optical fibers [12-15] and photonic crystal structures [16,17]. Apparently a wide diversity of slow light schemes has been demonstrated, but it must be pointed out that all schemes are characterized by one common feature: the presence of one or multiple strong resonances to obtain sufficient dispersion in the media. Besides, some recent works have already explored the fundamental limits of the maximum time delay achievable in slow light devices. For instance, fractional delay (the ratio of time delay to signal duration) or delay-bandwidth product and significant distortion imposed onto the temporally delayed signals after passing through a slow light device have been studied to evaluate the potential applications in telecommunication systems.

L. Hau *et al*. demonstrated, in 1999, the first pioneering slow light propagation in ultra-cold atomic gases as cold as 450 nK to obtain a Bose-Einstein condensate [1]. The light velocity was spectacularly reduced down to 17 m/s, equivalent to the speed of a bike, in the vicinity of a narrowband electromagnetically induced transparency (EIT). The extreme environmental conditions were, however, soon identified as a scientific challenge to be solved by the photonic community. M. Bigelow *et al*. proposed, in 2003, a novel solution to overcome this issue, using a solid crystal [7]. They created a spectral hole as narrow as 612 Hz FWHM within the absorption band of alexandrite crystal, using the quantum effect of coherent population oscillations (CPO). Then they spectrally placed a signal in the center of the spectral hole and observed successfully, at room temperature, both ultra-slow and superluminal propagation of light in a solid crystalline. Although this technique resulted in remarkable reduction of the group velocity, it seems still far from acceptable for real application systems since it operates at a very well-defined wavelength and the achievable time delay in this system is very limited to around 10 % of the signal duration. Besides, the bandwidth of the spectral hole restricted inherently the signal bandwidth to the kHz range. Therefore, the scientific challenge to generate practical control of signal delay remains still fascinating.

A significant step towards real applications was achieved by Song *et al*. in 2005 when slow light was experimentally and efficiently realized in an optical fiber using stimulated Brillouin scattering (SBS) [13]. It has been then experimentally proved that Brillouin slow light can readily reproduce most of the former results in slow and fast light, showing group velocities from as slow as 71000 km/s to superluminal or even negative group velocities. One can argue that the scale of reduction in group velocity through Brillouin slow light is much far from being as large as the reduced group velocities observed in the slow light systems based on electric transitions such as EIT or CPO. However, after introducing

the concept of fractional delay, this argument was no more issued since fractional delay has been the parameter of interest for real applications.

To date, Brillouin slow light systems have proved to be an unmatched and unprecedented flexible timing tool as a result of their unique spectral tailoring capability. What makes Brillouin slow light a particularly attractive delay line lies in the high flexibility of SBS, essentially the possibility to be achieved in any type of optical fiber and at any wavelength. Moreover, Brillouin slow light presents some inherent advantages: room temperature operation, high potential for large signal bandwidths, simple tabletop configuration, and seamless integration in fiber optic communication systems. Despite the apparent perfection of Brillouin slow light, this scheme requires novel solutions to resolve intrinsic problems. First, since the linewidth of natural Brillouin resonance is as narrow as 30 MHz, the signal bandwidth in optical communication systems is strictly restricted up to 50 Mbit/s. Second, the amplitude of the delayed signal is strongly amplified or attenuated by the associated Brillouin gain or loss, respectively. Third, the signal suffers from significant distortion, expressed by signal broadening, since the signal experiences frequency-dependent gain and phase distortion through slow-light. Signal distortion is an intrinsic deadlock in any kind of slow light system.

The objective of this thesis work has been to propose possible solutions to the three major bottlenecks in SBS delay-lines: signal bandwidth, signal amplification and signal distortion, so as to enable the full exploitation of Brillouin slow light for all-optical signal delaying and processing. In this thesis, several novel configurations were introduced to realize broadband Brillouin slow light, nearly zero-gain Brillouin slow light and non-distorted Brillouin slow light. Moreover, it is found that the achievable signal delay via Brillouin slow light was clearly enhanced when a signal shape is optimized, so that the spectral width of the signal is minimized to precisely match the bandwidth of a given Brillouin gain resonance. Departing from typical Brillouin slow light systems, it could be clearly observed that the propagation velocity of signal could be speeded up using an extremely simple configuration and in absence of any distinct pump source. This scheme is referred to as self-advanced Brillouin fast light. In addition, an alternative delaying technique was devised in order to match the real data rate in telecommunication systems (up to tens of Gbit/s), which makes use of the combination of wavelength conversion and group velocity dispersion in a material. Finally, the effect of slow light on linear light-matter interaction was experimentally investigated to verify the recent scientific question if slow light can enhance the Beer-Lambert absorption while light propagates through a gas cell.

Organization of this thesis

The content of this dissertation is addressed in four distinct chapters and a conclusion.

Chapter.2 defines and addresses the different characteristic velocities of a light signal for a better understanding of the underlying concepts behind slow light. In the second part, an analytical description of the propagation of a light signal in a dispersive medium is discussed. The evolution of the signal envelope during propagation is obtained by a representation in the Fourier domain. In the last part, the types of spectral resonances, which can be obtained in optical fibers for the generation of slow light, will be briefly reviewed.

Chapter 3 is devoted to the physics of Brillouin scattering in a material. The generation of spontaneous scattering will be described in terms of the thermodynamic nature and then stimulated Brillouin scattering will be presented as a parametric process of two counter-propagating optical waves and acoustic wave.

Chapter 4 is the core of this thesis. The essential contributions of this thesis work to Brillouin slow light systems are experimentally demonstrated to propose adequate solutions for resolving the critical issues related to signal bandwidth, signal amplification and signal distortion. The actual limitations of Brillouin slow light are also briefly discussed. Another approach to realize an all-optical tunable delay-line is followed, resulting in very large signal delays suitable for high speed network systems.

Chapter 5 is dedicated to clarify the possibilities of slow light to enhance the linear interactions between light and matter.

Chapter 6 will present the conclusions and perspectives of this fascinating technique.

Bibliography

[1]   L. V. Hau, S. E. Harris, Z. Dutton, and C. H. Behroozi, "Light speed reduction to 17 meters per second in an ultracold atomic gas," Nature, **397**, 594-598 (1999).

[2]   M. M. Kash, V. A. Sautenkov, A. S. Zibrov, L. Hollberg, G. R.Welch, M. D. Lukin, Y. Rostovtsev, E. S. Fry, and M. O. Scully, "Ultraslow group velocity and enhanced nonlinear optical effects in a coherently driven hot atomic gas," Phys. Rev. Lett. **82**, 5229-5232 (1999).

[3]   C. Liu, Z. Dutton, C. H. Behroozi and L. V. Hau, "Observation of coherent optical information storage in an atomic medium using halted light pulses," Nature, **409**, 490-493 (2001).

[4]   M. D. Stenner, D. J. Gauthier and M. A. Neifeld, "The speed of information in a fast-light optical medium," Nature, **425**, 695-698 (2003).

[5]   L. J. Wang, A. Kuzmich and A. Dogariu, "Gain-assisted superluminal light propagation," Nature, **406**, 277-279 (2000).

[6]   A. V. Turukhin, V. S. Sudarshanam, M. S. Shahriar, J. A. Musser, B. S. Ham, and P. R. Hemmer, "Observation of ultraslow and stored light pulses in a solid," Phys. Rev. Lett. **88**, 023602 (2002).

[7]   M. S. Bigelow, N. N. Lepeshkin and R. W. Boyd, "Superluminal and slow light propagation in a room-temperature solid," Science, **301**, 200-202 (2003).

[8]   A. Yariv, Y. Xu, R. K. Lee and A. Scherer, "A coupled resonator optical waveguide: a proposal and analysis," Opt. Lett. **24**, 711-713 (1999).

[9]   J. E. Heebner and R. W. Boyd, "Slow and fast light in resonator-coupled waveguide," J. Mod. Opt. **49**, 2629-2636 (2002).

[10] P. C. Ku, F. Sedgwick, C. J. Chang-Hasnain, P. Palinginis, T. Li, H. Wang, S. W. Chang and S. L. Chuang, "Slow light in semiconductor quantum wells," Opt. Lett. **29**, 2291-2293 (2004).

[11] J. Mork, R. Kjaer, M. van der Poel and K. Yvind, "Slow light in a semiconductor waveguide at gigahertz frequencies," Opt. Express, **13**, 8136-8145 (2005).

[12] N. Brunner, V. Scarani, M. Wegmuller, M. Legré, and N. Gisin, "Direct measurement of superluminal group velocity and signal velocity in an optical fiber, Phys. Rev. Lett. **93**, 203902 (2004).

[13] K. Y. Song, M. G. Herráez, and L. Thévenaz, "Observation of pulse delaying and advancement in optical fibers using stimulated Brillouin scattering," Opt. Express, **13**, 82-88 (2005).

[14] J. E. Sharping, Y. Okawachi, and A. L. Gaeta, "Wide bandwidth slow light using a Raman fiber amplifier," Opt. Express, **13**, 6092-6098 (2005).

[15] D. Dahan and G. Eisenstein, "Tunable all optical delay via slow and fast light propagation in a Raman assisted fiber optical parametric amplifier: a route to all optical buffering," Opt. Express, **13**, 6234-6249 (2005).

[16] A. Y. Petrov and M. Eich, "Zero dispersion at small group velocities in photonic crystal waveguides," Appl. Phys. Lett. **85**, 4866-4868 (2004).

[17] Y. A. Vlasov, M. O'Boyle, H. F. Hamann, and S. J. McNab, "Active control of slow light on a chip with photonic crystal waveguides," Nature, **438**, 65-69 (2005).

Chapter 2

Optical signal propagation in a dispersive medium

Prior to the discussion about the recent progress that leads to a control of the speed of a light signal, it is important to consider how to define the characteristics of the velocity of a light wave propagating in a dispersive medium. In early works [1,2], the light speed has been characterized in at least eight different ways: phase velocity, group velocity, information (or signal) velocity, centro-velocity, energy velocity, relativistic velocity, ratio-of-units velocity, correlation velocity and even more. This section, however, will introduce the first three velocities which are the most useful quantities for real photonic communication systems, and in particular group velocity will be discussed in detail.

2.1 Signal propagation

Let us consider the light propagation in an optical waveguide. Once either the electric or magnetic field experiences a perturbation at some point in space, an electromagnetic wave is generated and travels from that point. Like all electromagnetic phenomena, the propagation of light is completely governed by the classical Maxwell's equations. For a nonconducting medium without free charges these equations are given as [3,4]:

$$\nabla \times E = -\partial B / \partial t \quad , \quad B = \mu_o H + M \tag{2.1}$$

$$\nabla \times H = -\partial D / \partial t \quad , \quad D = \varepsilon_o E + P \tag{2.2}$$

$$\nabla \cdot D = 0 \tag{2.3}$$

$$\nabla \cdot B = 0, \tag{2.4}$$

where E and H represent the electric and magnetic field vectors, respectively, and D and B correspond to electric and magnetic flux densities. By applying a curl operator to Eq.(2.1)

and Eq.(2.2) the electric and magnetic fields can be decoupled in these equations and thus a light wave can be derived for a single field E or B. As a result, the propagation equation for optical fields can be written as:

$$\nabla^2 E = -\frac{1}{c^2}\frac{\partial^2 E}{\partial t^2}, \qquad \frac{1}{c^2} = \mu_o \varepsilon_o , \qquad (2.5)$$

where the light velocity c in vacuum is determined by the electric and magnetic permittivity of the waveguide material, ε_o and μ_o, respectively. In isotropic and dielectric media, the vacuum constants ε_o and μ_o must be replaced by the corresponding constants for the medium ε and μ. Thereby, the propagation speed of the optical fields in a material is given by $v = (\mu\varepsilon)^{-1/2}$. This allows the introduction of the index of refraction n, which represents the ratio between the light speeds in vacuum and in a medium, $n=c/v$. A particular well known solution of the second order differential equation Eq.(2.5) in an homogeneous medium is a monochromatic plane wave:

$$E(z,t) = \mathrm{Re}\{E_o \exp[i(\omega t - k\,z)]\}, \qquad (2.6)$$

where ω and k are the angular frequency and wavevector, respectively. The wavelength λ is usually described as the measured distance over which a wave propagates in one complete cycle, $\lambda = 2\pi/k$. The wave equation (2.5) describes the propagation of an electric field E along the longitudinal axis z. At a given time the amplitude of this field varies sinusoidally with the distance z, as shown in Figure.2.1, and at a given point z in space the electric wave varies harmonically with time t.
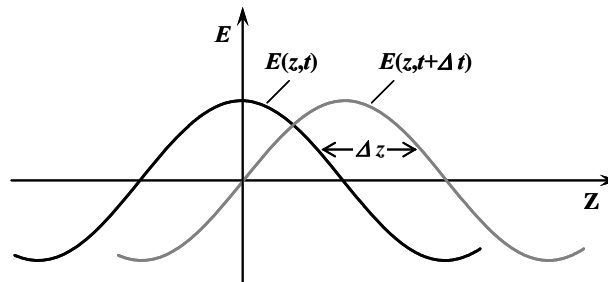
Figure 2.1: Waveforms of plane wave propagating in space at times t and $t+\Delta t$.

2.1.1 Phase and group velocity

Phase velocity

It must be pointed out that a monochromatic plane wave represented by a simple cosine function has essentially an infinite duration and its spectral content is given by a Dirac distribution $\delta(\omega_o)$ since it contains only one angular frequency ω_o. Let us assume that a

monochromatic plane wave propagates through a medium with refractive index n. The phase of this wave is straightforwardly given by:

$$\phi = \omega_o t - kz,$$ (2.7)

and the phase velocity is in general defined as the velocity at which particular points of constant phase travel through the medium for the plane wave. Thus it is given as:

$$v_p = \frac{\omega_o}{k} = \frac{c}{n}.$$ (2.8)

If the phase is known at defined positions at a given time, the phase of a light wave propagating over a certain depth in the medium can be recovered at a later time using the phase velocity. In order words, the phase velocity indicates only how the phase of the monochromatic plane wave is delayed in the medium.

Group velocity

A light signal such as an optical pulse has totally different properties when compared to a sinusoidal wave in terms of duration and spectral distribution. A pulse can be simply constructed by multiplying Eq.(2.6) by a bell-shaped function. This way a Gaussian-shaped pulse can be obtained by:

$$E(0,t) = \mathrm{Re}\left\{ E_o \exp\left[-\frac{1}{2}\left(\frac{t}{t_o}\right)^2 + i\omega_o t \right] \right\},$$ (2.9)

where t_o is a factor related to the duration of the Gaussian envelope. Figure.2.2 depicts its temporal envelope and spectrum compared to those of a monochromatic wave, where the
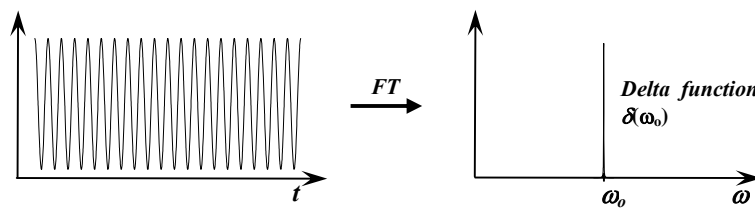
Figure 2.2a: On left temporal evolution of the electric field of a monochromatic plane wave that is an infinite sine wave and on right its spectrum obtained by a Fourier transform (*FT*), showing a Dirac distribution $\delta(\omega_0)$ with zero spectral width.
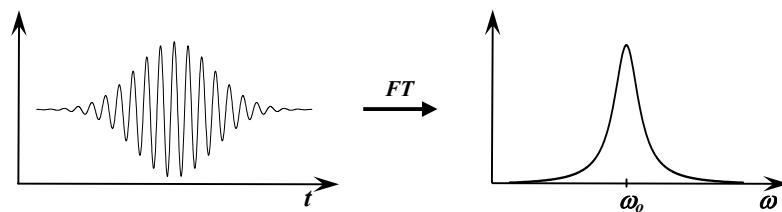
Figure 2.2b: On left temporal evolution of the electric field of a Gaussian shaped pulse representing an optical signal, and on right its spectrum is presented, showing a Gaussian distribution with a spectral width proportional to Γ^{-1}

spectra of the waves are simply obtained by a Fourier transform of the envelope function of the signal. It is important to discuss the spectral components of a light signal. Once again a monochromatic plane wave contains only one angular frequency ω_o, whereas a light signal naturally requires a full set of frequency components. Therefore, the electric field of the signal is given by the superposition of the electric fields of a set of monochromatic waves:

$$E(z,t) = \sum_m E_m \exp\left[i(\omega_m t - k_m z)\right]. \tag{2.10}$$

When the waves are all added up in phase the peak of the signal appears and moves forward at group velocity v_g, as shown in Figure.2.3.

$$E_1 = \sin\left(\omega_1 t - k_1 z\right)$$
$$+$$
$$E_2 = \sin\left(\omega_2 t - k_2 z\right)$$
$$+$$
$$E_3 = \sin\left(\omega_3 t - k_3 z\right)$$
$$+$$
$$\vdots$$
$$=$$
$$E = \sum_m \sin\left(\omega_m t - k_m z\right)$$

$$\left|E(z,t)\right|^2$$
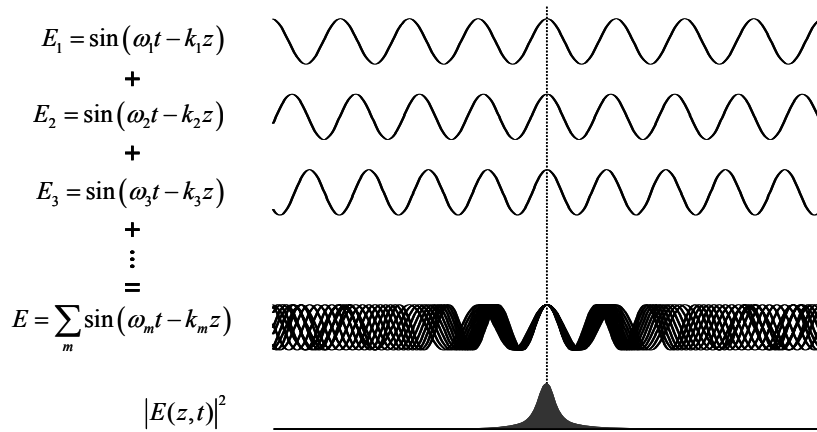
Figure 2.3: Schematic representation of the generation of an optical signal. The peak of the signal appears at the position, where a large number of frequency components are all in phase.

When electromagnetic fields interact with atoms and molecules in a material the optical response of the medium depends in general on the angular frequency ω. Thereby, the index of refraction $n(\omega)$ becomes a function of the angular frequency. Such a phenomenon is designated as material dispersion. In addition, the confinement of light in a waveguide structure gives rise to another type of dispersion, referred to as waveguide dispersion, since the propagation constant β is dependent on the angular frequency. Now let us launch an optical signal into a dispersive medium. What will be the effect of dispersion on the signal? If the medium has a negligibly small dispersion or is vacuum the signal will travel without any distortion through the medium at the phase velocity as a sinusoidal wave does. Otherwise, in a dispersive medium phase velocity does not describe properly the process of signal propagation. This distinction between phase velocity and group velocity was first discovered by L. Rayleigh [5]. More details on signal propagation in the dispersive medium will be discussed in section 2.2.

To mathematically understand how a signal propagates through a medium, one may start from the basic expressions for the wavevector $k=2\pi/\lambda$ and the wavelength $\lambda=2\pi c/\omega$ in the medium. Due to the dispersion in the medium each frequency component ω contained in the signal propagates at its own phase velocity and the phase of the signal is given by:

$$\phi = \frac{n\,\omega z}{c} - \omega t.$$

(2.11)

After the signal propagates a certain distance through the medium, the phase must be constant to the first order approximation in the angular frequency ω, so $d\phi/d\omega=0$:

$$\frac{d\,n(\omega)}{d\,\omega}\frac{\omega z}{c} + \frac{n\,z}{c} - t = 0.$$

(2.12)

The traveling distance z of the signal is determined as $z=v_g\,t$, where v_g is defined as

$$v_g = \frac{d\omega}{dk} = \frac{c}{n(\omega) + \omega\,dn(\omega)/d\omega} \approx v_p\left(1 - \frac{\omega}{n(\omega)}\frac{dn(\omega)}{d\omega}\right),$$

(2.13)

showing the relationship between phase velocity and group velocity. The second term depends on the dispersion characteristics of the medium and modifies the propagation velocity of the signal. It leads to the possibility to generate slow light propagation in presence of normal dispersion ($dn/d\omega > 0$) and fast light propagation in anomalous dispersion ($dn/d\omega < 0$). Figure.2.4 depicts the visual distinction between the two velocities in a dispersive medium, using a dispersion diagram. The phase velocity v_p is simply calculated as the slope of a straight line from the origin to the point **P** at an angular frequency ω_o while the group velocity v_g is determined by the slope of the line tangential to the curve at the same frequency ω_o.
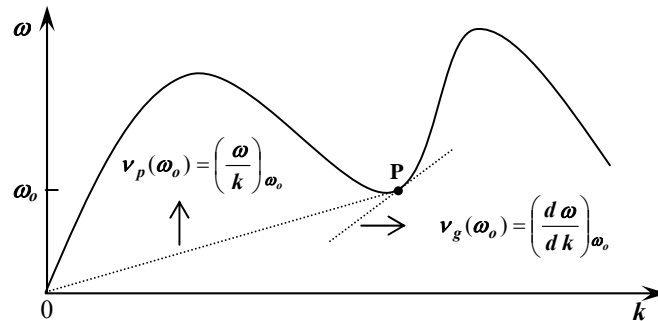
Figure 2.4: Dispersion curve of an optical medium, showing the representation of the phase velocity v_p and the group velocity v_g in the dispersion diagram.

2.1.2 Signal velocity

Einstein claimed in his theory of special relativity that *no light can travel with velocity higher-than-c*. However, looking more carefully at Eq.(2.12), one may see an apparent contradiction to the special relativity. In a medium with anomalous dispersion where $v_g > v_p$, a light signal seems to show superluminal propagation through the material or even negative velocity. Sommerfeld first pointed out this contradiction and it has then been of interest to discuss it extensively. Addressing to solve this issue, Sommerfeld and Brillouin introduced the concept of signal velocity (or information velocity) and claimed that there must be a distinction between signal velocity and group velocity. They found that in a region of small absorption or dispersion, the signal velocity doesn't differ much from the group velocity whereas in the presence of strong absorption large differences between the two velocities can appear. Unlike other velocities, it is not easy to analytically formulate the signal velocity because defining a signal is very ambiguous. Nevertheless, a signal has been defined in various ways, i.e. Brillouin stated that *a signal is a short isolated succession of wavelets, with the system at rest before the signal arrived and also after it has passed*. Eventually, one intends to impose information onto the non-zero part of a signal with an arbitrary shape.

Now let a signal proceed through a material and let us detect two instants, t_a and t_b when the non-zero part of the signal passes point *A* and point *B* (*B* being situated further along the path of propagation), respectively. Just like other velocities are defined the signal velocity is given by the ratio of the distance and the time. The definition of the signal velocity in this manner, however, raised difficulties with the principle of causality, because when considering superluminal propagation or a negative velocity the *effect* would happen before its *cause*. Since the work of Sommerfeld and Brillouin, many researches [5-16] have been done to verify whether or not the information velocity could exceed the vacuum velocity *c* and also if the group velocity could represent the signal velocity near a strong absorption. It is now widely accepted that for signals in slow light conditions signal velocity is considered as group velocity, but in ultra fast light conditions when the signal velocity is faster than *c* the information encoded in the signal does not exceed the vacuum velocity *c* and thus propagates at its own velocity that turns distinct from the group velocity [12,15]. However, this argument is still discussed openly among scientists.

2.1.3 Signal propagation in a dispersive medium

To further study the signal propagation through a dispersive medium, let us consider a Fourier transform limited Gaussian pulse for simplicity. If one defines the initial electric field

of the signal $E(0,t)$, its initial spectral distribution $\tilde{E}(0,\omega)$ is essentially related to the envelope function after performing a Fourier transform:

$$E(0,t) = E_o \exp\left[-\frac{1}{2}\left(\frac{t}{t_o}\right)^2 + i\omega_o t\right], \tag{2.14}$$

$$\tilde{E}(0,\omega) = \tilde{E}_o \exp\left[-\frac{1}{2}(\omega-\omega_o)^2 t_o^{\,2}\right]. \tag{2.15}$$

When the signal travels in a transparent medium, its spectrum is modified due to the dispersion characteristics of the material. The signal propagation can be readily predicted in the Fourier domain once the transfer function of the material is well defined, which is normally given as $T(\omega) = \exp[-ik(\omega)]$. After the signal propagates a distance z inside the optical medium, the signal spectrum in the output evolves according to the relation

$$\tilde{E}(z,\omega) = \tilde{E}(0,\omega)\exp\left[-i\,k(\omega)\,z\right], \quad k(\omega) = n\omega/c, \tag{2.16}$$

where k is the wavevector. It is convenient to expand the wavevector in a Taylor series with respect to angular frequency, for which the signal should fulfill the condition, $\Delta\omega \ll \omega_o$, ($\Delta\omega$ being the spectral width of the signal and ω_o being the center frequency). This condition results in an approximate analytical solution for the signal propagation. Substituting the Taylor expansion of the wavevector

$$k(\omega) = k_o(\omega_o) + k_1(\omega-\omega_o) + \tfrac{1}{2}k_2(\omega-\omega_o)^2 + \tfrac{1}{6}k_3(\omega-\omega_o)^3 + \cdots \tag{2.17}$$

$$k_1 = \left(\frac{d\,k(\omega)}{d\,\omega}\right)_{\omega_o}, \quad k_2 = \left(\frac{d^2\,k(\omega)}{d\,\omega^2}\right)_{\omega_o}$$

into Eq.(2.15), the signal spectrum becomes

$$\tilde{E}(z,\omega) = \exp\left[-i\,k(\omega_o)\,z - i\,k_1(\omega-\omega_o)\,z - \frac{1}{2}\left(t_o^{\,2} + i\,k_2\right)(\omega-\omega_o)^2\,z + \frac{i}{6}k_3(\omega-\omega_o)^3\,z\right]. \tag{2.18}$$

The parameters k_1 and k_2 represent the group velocity and the group velocity dispersion, respectively, and k_3 is related to the dispersion slope. If the carrier frequency is far away from the zero dispersion frequency of the medium the contribution of higher order terms for the dispersion turns negligible [17].

Neglecting the third order dispersion term k_3, the time waveform of the signal after propagation through the medium is then obtained using the inverse Fourier transform of Eq.(2.18). As a result, the time evolution of the signal is analytically derived as:

$$E(z,t) = A\exp\left[-i\omega_o\left(t - \frac{z}{v_p(\omega_o)}\right)\right]\exp\left[-2\left(t_o^{\,2} + i\,k_2 z\right)\omega_o\left(t - \frac{z}{v_g(\omega_o)}\right)^2\right]. \tag{2.19}$$

The first exponential term takes into account the phase delay of the signal with respect to the angular frequency ω_o after traveling a distance z, but it doesn't have any visible effect on the temporal distribution of the signal and doesn't carry any information since it modifies only the phase of the sinusoidal waves. The second exponential term, however, is more interesting to discuss as far as the signal propagation is concerned. The shape of the signal remains Gaussian, but it is clearly observed that the peak of the signal is delayed by an amount z/v_g depending on the group velocity v_g or group index n_g (n_g being c/v_g) after the signal has passed through the medium with a length z. Now let us consider the second order dispersion term k_2, referred to as group velocity dispersion (GVD). In general, the quadratic dependence of the refractive index on frequency gives rise to GVD, which causes normally a signal broadening if $k_2 \neq 0$ unless the signal has an initial frequency chirp with opposite sign to the value of GVD. The higher order dispersion terms in the material may also induce supplementary phase distortion if they turn non negligible when compared to k_2. Therefore, in real slow light systems, the signal experiences both time delay and distortion. It will be discussed later in detail.

2.2   Dispersion management in an optical medium

As previously mentioned, the dispersive characteristics of an optical medium are the crucial parameters to produce dynamic time delays for a light signal. All that is required to manipulate the group velocity is only the presence of spectral resonances in the material, which gives rise to a rapid change of the group index as a function of frequency. Actually, this is readily obtained within absorption or gain bands that show a complex transfer function. According to Kramers-Kronig relations the real part of the frequency-dependent refractive index n_r is related to the absorption α within the material by [18]:

$$n_r(\omega) = \frac{2}{\pi} p.v. \int_0^\infty d\omega' \frac{\omega' \alpha(\omega')}{\omega'^2 - \omega^2} \qquad (2.20)$$

$$\alpha(\omega) = -\frac{2\omega}{\pi} p.v. \int_0^\infty d\omega' \frac{n_r(\omega')}{\omega'^2 - \omega^2} , \qquad (2.21)$$

where $p.v.$ represents the Cauchy's principal value. An analysis of these relations shows that a spectrally narrow absorption tends to induce a sharp transition of the refractive index in the material, which in turn leads to a strong anomalous dispersion ($dn/d\omega \ll 0$) associated with signal advancement or fast light. On the contrary, a peak or gain band will create a strong normal dispersion ($dn/d\omega \gg 0$) in the material, resulting in signal delay or slow light. This

situation for a Lorentzian shaped absorption is graphically illustrated in Figure.2.5. The steep linear variation of the refractive index, making $dn/d\omega$ large in absolute value, induces in turn a strong change of the group index. Thereby, a large change of the relative time delay for a pulse can be observed after the pulse propagates through the material.

As a result, the key point to obtain pulse delays or advancements in slow light systems is to find some physical processes that can provide optical resonances showing the necessary spectral features, namely a narrow bandwidth and a strong amplitude.
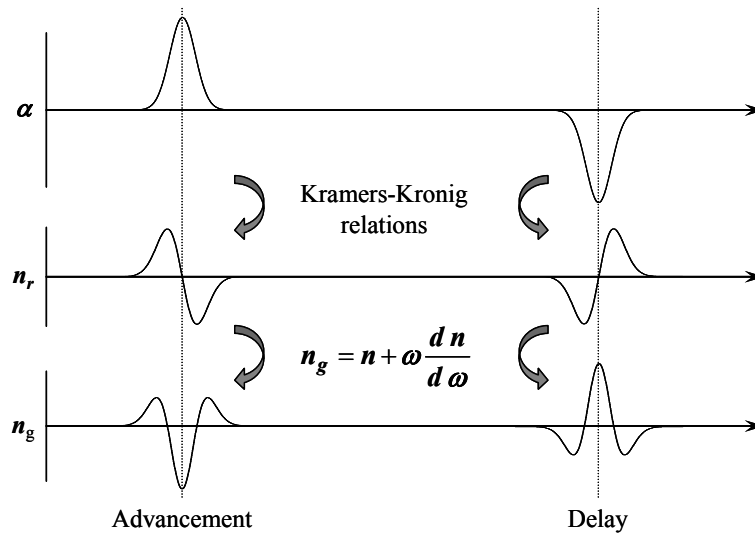
Figure 2.5: Relationship between either an absorption or a gain narrowband resonance and the refractive index, governed by the Kramers-Kronig relations. The strong dispersion in the vicinity of the absorption and gain resonances induces fast light or slow light propagation, respectively.

2.3 Optical resonances in optical fibers

A flurry of schemes for tailoring the dispersive properties of an optical medium has been actively developed in diverse materials over the last decade, in order to reduce and control the group velocity of a signal [19]. In early works, the most widely used methods to engineer the dispersion have been conducted using atomic resonances in gas atoms. However, optical fibers have recently started to stimulate this research in modern photonic systems since they show unique properties, such as low-loss transmission, flexible integration with most optical transmission systems, and operational wavelengths at telecommunication windows.

In this section, a brief overview of physical mechanisms that are responsible for creating either absorption or gain spectral resonances in optical fibers will be presented. So far, the most efficient approach is to take advantage of optical interactions accompanied with nonlinear optical phenomena. Once a strict and necessary phase matching condition in such

processes is satisfied to generate an idler wave, energy transfer occurs through the idler wave form one optical wave to another optical wave, usually referred to as pump and signal waves, respectively. If the signal wave benefits from the process of the energy transfer to experience a linear gain, the propagation speed of the signal through the medium will be reduced and will be subject to slow light. On the contrary, an optical wave which undergoes a linear loss from this process will propagate at an increased group velocity, so that fast light will be observed in transmission. Since the title of this thesis refers to Brillouin slow and fast light, both Brillouin gain and loss resonances will be discussed in detail in Chapter.3.

2.3.1 Nonlinearities in optical fibers

The predominant schemes to manage dispersion characteristics in optical fibers rely on nonlinear effects. For an intense electromagnetic field, the response of any dielectric to light becomes nonlinear. More specifically, the polarization P induced in a medium becomes nonlinear with the applied field, and thus nonlinear terms in the electric field E begin to appear in the material response. The magnitudes of the high-order dependence on the electric field are determined by the nonlinear susceptibilities χ_j [18],

$$P = \varepsilon_o \left(\chi_1 E + \chi_2 EE + \chi_3 EEE + \cdots \right)$$

$$= P_{L_1} + P_{NL_2} + P_{NL_3} + \cdots,$$

where ε_o is the vacuum permittivity. The polarization P consists of the linear susceptibility χ_1 and nonlinear susceptibilities χ_2 and χ_3. The linear susceptibility provides the dominant contribution to the polarization and its effect is included in the index of refraction n and the absorption coefficient α. On the other hand, the nonlinear parametric processes are categorized as second- or third-order processes depending on whether χ_2 and χ_3 is involved, respectively. In isotropic media at the molecule level, the second-order susceptibility χ_2 vanishes completely in the dipole approximation [18,20]. As optical fibers are constituted of amorphous silica, the second-order nonlinear interactions such as second-harmonic generation and sum-frequency generation can not be observed in fibers in a passive way [21]. However, the third-order parametric processes can occur in both isotropic and anisotropic media and is scaled by the third-order susceptibility χ_3. As a consequence, one can produce in fibers the nonlinear effects such as third-harmonic generation, four-wave mixing and parametric amplification [21].

2.3.2 Four-wave mixing

Wave mixing turns out to be one of the most important phenomena in modern nonlinear optics. When two or more waves simultaneously transmit in a nonlinear medium the interactions between the waves tend to produce new frequency components that were not present in the incident field. Due to this particular feature, four-wave mixing attracted considerable attention in wavelength division multiplexed communication systems for potential applications such as the development of tunable light source and the efficient implementation of wavelength conversion [22-25]. Actually, four-wave mixing comes from the nonlinear response of bound electrons to the applied optical field and refers to the interactions of four different waves through the third-order nonlinear polarization. In quantum mechanical terms, when the phase matching condition is satisfied, photons from one or more waves are annihilated by modulated refractive index and are then transferred at different frequencies. As a result, it leads to the generation of idler waves while energy and momentum are conserved during this process. These conditions are usually satisfied with high efficiency in the vicinity of the zero dispersion wavelength of the material as it allows the waves to propagate at similar group velocities.

For the four-wave mixing process, three distinct waves at frequencies ω_1, ω_2 and ω_3 are present in the incident field and can be coupled to give a fourth wave (signal wave). If the signal wave is created at frequency $\omega_4=\omega_1+\omega_2+\omega_3$, this nonlinear process will be referred to as third harmonic generation in the particular case: $\omega_1=\omega_2=\omega_3$, but it is rarely observed in optical fibers with high efficiencies. In practice, a signal wave generated at frequency $\omega_4=\omega_1+\omega_2-\omega_3$ is the most widely used situation to generate wavelength conversion. Once the frequency matching condition ($\omega_3+\omega_4=\omega_1+\omega_2$) and the associated phase matching condition ($k_3+k_4=k_1+k_2$) occur, photons from the incident waves are annihilated to simultaneously create photons at frequencies ω_3 and ω_4. In the particular case when only two distinct waves at
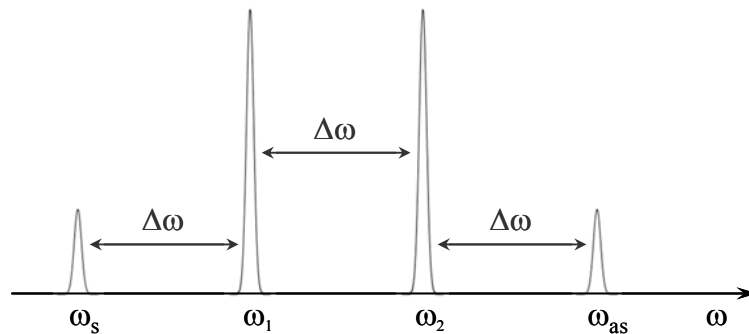
Figure 2.6: Four-wave mixing interaction in optical fibers. When the input electric field is composed of two distinct optical waves at frequencies of ω_1 and ω_2 the interaction of the two waves generates two new frequency components at frequencies ω_s and ω_{as}.

frequencies ω_1 and ω_2 ($\omega_1 < \omega_2$) are present in the incident field, it is relatively straightforward to satisfy the strict phase matching conditions. This partially degenerate case is the most relevant in optical fibers. The refractive index of the fiber is modulated by the beat frequency between the two waves, $\Delta\omega = \omega_2 - \omega_1$. As a result, new frequency components, which were not present in the incident electric field, are created at the frequency of $\omega_s = \omega_1 - \Delta\omega = 2\omega_1 - \omega_2$ (Stokes wave) and $\omega_{as} = \omega_2 + \Delta\omega = 2\omega_2 - \omega_1$ (anti-Stokes wave), as shown in Figure 2.6. The whole nonlinear interaction is described by a model coupling the three waves [22,26]. When a weak signal at frequency ω_s is simultaneously launched into the fiber the signal will be amplified, and such amplification is called parametric gain. However, it is still difficult to maintain the phase matching conditions along the fiber since microscopic fluctuations in material density such as birefringence and chromatic dispersion increase the phase mismatch. Therefore, in practice, the parametric gain using 4-wave mixing can hardly induce a sharp change of refractive index to realize slow and fast light in optical fibers.

2.3.3 Narrow band optical parametric amplification

Brillouin slow light experimentally demonstrated some impressive results on signal delays for the first time in fibers. Nevertheless, photonic community identified the narrowband feature of the Brillouin resonance as an issue and explored new schemes to increase the capacity of digital data streams. D. Dahan *et al.* [27,28] proposed the use of narrow band optical parametric amplification as optical resonances. The experimental setup made use of the combination of parametric amplification and Raman amplification in optical fibers; the coupling of two nonlinear effects offers the possibility to modify the spectral profile of resonances. Therefore, both signal delay and advancement were observed in this system with a large bandwidth at tens of Gbit/s rates for real communication applications.

The parametric gain in optical fibers has been used to generate parametric optical resonances or amplifiers. According to the theoretical prediction of the three-wave mixing model, partially degenerated four-wave mixing allows to transfer energy from a strong pump wave to a weak signal and an idler wave. The parametric gain via this process differs much if the signal and idler waves are launched into the fiber simultaneously with the pump, so that one can control the direction of the energy flow by adjusting the phase mismatching between the three waves. In particular, the signal can be either amplified or attenuated depending on the relative input phase between the incident waves. On the contrary, in the case where a signal power is relatively negligible compared to a pump power, the signal amplitude will start to be amplified. Such parametric gain is generally a linear function of the pump power and fiber length under phase matching conditions, thus this system could offer a linear all-

optical delay line. Moreover, the spectral bandwidth of parametric amplification is related to the fiber length and group velocity dispersion [20], so that this delay line can be properly designed for a required data capacity.

2.3.4   Stimulated Raman scattering

As a solution to overcome the narrow signal bandwidth of Brillouin slow light, stimulated Raman scattering in optical fibers was utilized by J. E. Sharping *et al*. to produce a large bandwidth slow light [29]. In this technique, an all-optical delay line was realized for ultra-short optical signals spectrally placed in the center of a Raman gain resonance. The group velocity of the signal was then continuously controlled by the wavelength and power of the pump wave. As a result, a signal pulse with transform-limited duration of 430 fs was temporally delayed up to 85 % of its initial pulsewidth in this experiment.

Stimulated light-scattering processes have attracted a large interest as efficient nonlinear phenomena that can provide broadband amplifiers and tunable lasers. In such processes, optical fibers play an active role as nonlinear materials since they involve molecular vibrations or acoustic phonons that are responsible for Raman and Brillouin scattering, respectively. Stimulated Raman scattering is similar to stimulated Brillouin scattering in the sense that it is an inelastic process. A fraction of pump power is rapidly transferred to vibrational modes of media and to a so-called Stokes wave whose frequency is lower than the pump frequency. Since this process accompanies the interactions between photons and optical phonons of the material structure, the energy difference between the pump and the Stokes waves is significantly large. This yields a frequency shift for the Stokes wave of about 10 THz, namely three orders of magnitude greater than Brillouin shift. Further details on Raman scattering can be found in [18,20].

2.3.5   Coherent population oscillation

Coherent population oscillation (CPO) is a quantum effect that can generate a spectrally narrow hole in the center of an absorption profile due to a wave-mixing interaction. Such a dip due to CPO was first predicted in 1967 from the interaction between two optical beams in a saturable absorber [30]. The type of spectral hole burning was for the first time experimentally observed in a ruby crystal and the spectral width of 37 Hz was measured at half width at half maximum [31]. Recently, this narrow spectral feature has been exploited for slow and fast light propagation at room temperature in semiconductor structures [32-37]
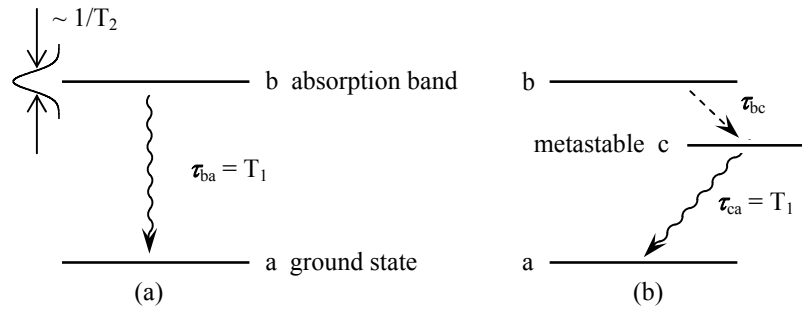
Figure 2.7: (a) CPO realized in a simple two-level system. (b) Relevant energy levels in erbium-doped optical fibers used for CPO slow and fast light. T_2 is a simple dipole moment dephasing time, which determines the spectral width of the absorption band.

such as quantum wells, quantum dots and quantum structure optical amplifiers, in solid crystals [38,39] and even in optical fibers [40-42].

The principle of CPO is in general described in a two-level system as depicted in Figure.2.7. When a strong pump wave illuminates a saturable medium, the population of the ground state is excited to the first absorption band. Then the population returns to the ground state in a few milliseconds (T_1). A weak probe wave is then launched to the medium and interferes with the pump. The induced beating signal makes the population of electron oscillate between the ground state and the excited state. Due to the long decay time T_1, the population oscillations are only appreciable under the condition that the product of δ and T_1 is ~1, where δ is a beating frequency between the pump and probe waves. When this condition is satisfied, the pump wave can efficiently scatter off the ground state population into the probe wave. As a result, a spectral hole appears at the center of the probe frequency and the spectral width of the hole is inversely proportional to the population relaxation lifetime T_2.

Recently, CPO was also observed in single-mode erbium-doped fibers (EDF) [40-42]. In practical point of view, EDF gives rise to longer interaction lengths and stronger effects for coherent population oscillations. In addition, since EDF amplifier plays the role of both an absorber and an amplifier depending on the pump power, this system opened the possibilities to realize slow and fast light and experimentally demonstrated the superluminal propagation with negative group velocity [41]. In fact, the erbium atoms in fibers are effectively a three-level system with a strong absorption band as shown in Figure.2.6, but the population of the absorption band decays very rapidly to a metastable level in a few picoseconds [20]. Thereby, such system can be regarded as a two-level system.

Bibliography

[1]   R. L. Smith, "The velocities of light," Am. J. Phys., **38**, 978 (1970).

[2]   S. C. Bloch, "Eight velocity of light," Am. J. Phys., **45**, 538 (1977).

[3]   B. E. A. Saleh and M.C. Teich, *Fundamentals of Photonics*, John Wiley & Sons, Inc., New York, 1991).

[4]   D. J. Griffiths, *Introduction to Electrodynamics*, 2nd ed., (Prentice Hall, Inc., New jersey, 1989).

[5]   L. Brillouin, *Wave propagation and group velocity*, Academic Press, New York, 1960).

[6]   P. Plesko and I. Palécz, "Experimental Observation of Sommerfeld and Brillouin Precursors in the Microwave Domain," Phys. Rev. Lett., **22**, 1201-1204 (1967).

[7]   C. G. B. Garrett and D.E. McCumber, "Propagation of a gaussian light pulse through an anomalous dispersion medium," Phys. Rev. A, **1**, 305-313 (1970).

[8]   S. Chu and S. Wong, "Linear pulse propagation in an absorbing medium," Phys. Rev. Lett., **48**, 738-741 (1982).

[9]   B. Ségard and B. Macke, "Observation of negative velocity pulse propagation," Phys. Lett., **48**, 213-216 (1985).

[10]   J. Aaviksoo, J. Kuhl, and K. Ploog, "Observation of optical precursors at pulse propagation in GaAs," Phys. Rev. A, **44**, R5353 (1991).

[11]   K. E. Oughstun and G.C. Sherman, *Electromagnetic Pulse Propagation in Causal Dielectrics*, Springer-Verlag, Berlin, 1994).

[12]   J. C. Garrison, M. W. Mitchell, R. Y. Chiao, and E.L. Bolda, "Superluminal signals: causal loop paradoxes revisited," Phys. Lett. A, **245**, 19-25 (1998).

[13]   G. Nimtz and A. Haibel, "Basics of superluminal signals," Ann. Phys, **9**, 1-5 (2000).

[14]   R. W. Boyd and D.J. Gauthier, *"Slow and Fast Light"*. 2002, Elsevier: Amsterdam. p. 497-530.

[15]   M. Centino, M. Bloemer, K. Myneni, M. Scalora, C. Sibilia, M. Bertolotti, and a.G. D'Aguanno, "Signal velocity and group velocity for an optical pulse propagation through a GaAs cavity," Phys. Rev. E, **68**, 016602 (2003).

[16]   M. D. Stenner, D. J. Gauthier, and M.A. Neifeld, "The speed of information in a fast-light optical medium," Nature, **425**, 695-698 (2003).

[17]   G. P. Agrawal, *Fiber-optic Communication System*, 3rd ed, (John Wiley & Sons, Inc., New York, 2002).

[18]   R. W. Boyd, *Nonlinear Optics*, 2nd ed., (Academic Press, New York, 2003).

[19]   J. B. Khurgin and R.S. Tucker, *Slow Light: Science and Applications*, CRS Press Boca Raton, 2009).

[20] G. P. Agrawal, *Nonlinear Fiber Optics*, 2nd ed., (Academic Press, San Diego, 1995).

[21] Y. R. Shen, *The Principles of Nonlinear Optics*, Wiley, New York, 1984).

[22] R. H. Stolen, J. E. Bjorkholm, and A. Ashkin, "Phase-matched three-wave mixing in silica fiber optical waveguides," Appl. Phys. Lett., **24**, 308 (1974).

[23] K. Inoue, "Arrangement of fiber pieces for a wide wavelength conversion range by fiber four-wave mixing," Opt. Lett., **19**, 1189-1191 (1994).

[24] S. Watanabe and T. Chikama, "Highly efficient conversion and parametric gain of nondegenerate forward four-wave mixing in a singlemode fibre," Electron. Lett., **30**, 163-164 (1994).

[25] X. Zhang and B.F. Jogersen, "Noise Characteristics and Optimum Fiber Length of Spectral Inversion Using Four-Wave Mixing in a Dispersion-Shifted Fiber," Opt. Fiber Technol., **3**, 28-43 (1997).

[26] G. Cappellini and S. Trillo, "Third-order three-wave mixing in single mode fibers," J. Opt. Soc. Am. B, **8**, 824-838 (1991).

[27] D. Dahan and G. Eisentein, "Tunable all optical delay via slow and fast light propagation in a Raman assisted fiber optical parametric amplifier: a route to all optical buffering," Opt. Express, **13**, 6234-6249 (2005).

[28] E. Shumakher, A. Willinger, R. Blit, D. Dahan, and G. Einstein, "Large tunagble delay with low distortion of 10 Gbit/s data in a slow light system based on narrow band fiber parametric amplification," Opt. Express, **14**, 8540-8545 (2006).

[29] J. E. Sharping, Y. Okawachi, and A.L. Gaeta, "Wide bandwidth slow light using a Raman fiber amplifier," Opt. Express, **13**, 6092-6098 (2005).

[30] S. E. Schwartz and T.Y. Tan, "Wave interactions in saturable absorbers," Appl. Phys. Lett., **10**, 4-7 (1967).

[31] L. W. Hillman, R. W. Boyd, J. Krasinski, and C.R.S. Jr., "Observation of a spectral hole due to population oscillations in a homogeneously broadened optical absorption line," Opt. Commun., **45**, 416-419 (1983).

[32] P. C. Ku, F. Sedgwick, C. J. Chang-Hasnain, P. Palinginis, T. Li, H. Wang, S. W. Chang, and S.L. Chuang, "Slow light in semiconductor quantum wells," Opt. Lett., **29**, 2291-2293 (2004).

[33] J. Mork, R. kjaer, M. Van der Poel, and K. Yvind, "Slow light in a semiconductor waveguide at gigahertz frequencies," Opt. Express, **13**, 8136-8145 (2005).

[34] P. Palinginis, S. Crankshaw, F. Sedgwick, E. T. Kim, M. Moewe, C. J. Chang-Hasnain, H. L. Wang, and S.L. Chuang, "Ultraslow light (<200m/s) propagation in a semiconductor nanostructure," Appl. Phys. Lett., **87**, 171102 (2005).

[35] F. Ohman, K. Yvind, and J. Mork, "Voltage-controlled slow light in an integrated semiconductor structure with net gain," Opt. Express, **14**, 9955-9962 (2006).

[36] H. Su and S.L. Chuang, "Room temperature slow and fast light in quantum-dot semiconductor optical amplifier," Appl. Phys. Lett., **88**, 061102 (2006).

[37] P. K. Koondratko, S. W. Chang, H. Su, and S.L. Chuang, "Optical and electrical control of slow light p-doped and intrinsic quantum-dot electroabsorbers," Appl. Phys. Lett., **90**, 251108 (2007).

[38] M. S. Bigelow, N. N. Lepeshkin, and R.W. Boyd, "Superluminal and slow light propagation in a room temperature solid," Science, **301**, 200-202 (2003).

[39] M. S. Bigelow, N. N. Lepeshkin, and R.W. Boyd, "Observation of ultraslow light propagation in a ruby crystal at room temperature," Phys. Rev. Lett., **90**, 113903 (2003).

[40] A. Schweinsberg, N. N. Lepeshkin, M. S. Bigelow, R. W. Boyd, and S. Jarabo, "Observation of superluminal and slow light propagation in erbium-doped optical fiber," Europhys. Lett., **73**, 218-224 (2006).

[41] G. M. Gehring, A. Schweisberg, C. Barsi, N. Kostinski, and R.W. Boyd, "Observation of backwards pulse propagation through a medium with a negative group velocity," Science **312**, 895-897 (2006).

[42] H. Shin, A. Schweinsberg, C. Barsi, N. Kostinski, H. J. Chang, R. W. Boyd, Q.-H. Park, and D.J. Gauthier, "Reducing pulse distortion in fast-light pulse propagation through an erbium-doped fiber amplifier," Opt. Lett., **32**, 906-908 (2007).

Chapter 3

Brillouin Scattering

Since the invention of the laser in the early 1960's, the optical response of a transparent medium to light has started to be considered as nonlinear. When the optical intensity of the incident light increases to reach a critical level the light-matter interaction in the medium starts to build up nonlinear effects during the light propagation [1,2]. In optical fibers, nonlinear effects manifest through some parametric processes such as four-wave mixing, self-phase modulation and cross-phase modulation. In these nonlinear phenomena, the refractive index of the fiber is modulated with respect to the light intensity and the induced index grating scatters photons from the incident lights. Light scattering such as stimulated Raman and Brillouin scattering can also occur in fibers as a result of parametric interaction of light waves through optical or acoustic phonons (molecular vibrations). Due to the active participation of the nonlinear medium in these processes, a strict phase matching condition can be straightforwardly satisfied. Once the linear dispersion relations between light and phonons are matched, the incident light is strongly scattered and the scattered light is frequency-shifted. In this chapter, Brillouin scattering in silica will be discussed in detail, in terms of both spontaneous and stimulated processes.

3.1   Linear light scattering

3.1.1   Generalities

Light scattering is known as a general physical process in an optical medium. When one or more localized non-uniformities are present in the medium, light intends to be forced to deviate from a straight trajectory while being transmitted through the medium. In other words, light scattering occurs as a consequence of fluctuations in the optical properties of the medium. Nevertheless, light can be scattered under conditions such that the optical properties of the medium are not modified by the incident light. This scattering is referred to as spontaneous or linear scattering. In optical fibers, the type of spontaneous scattering is more concretely identified in terms of spectral components of the scattered light. It is separated in two main categories: *elastic* scattering or *inelastic* scattering. However, the universal principles of energy and momentum conservations are preserved in all cases.

- In *elastic* scattering, the induced light from a scattering process has an identical spectral profile to the incident light.
- In *inelastic* scattering, energy exchange occurs between light and the dielectric medium, which leads to a frequency shift between incident and scattered lights.

Under most general circumstances, the scattered light shows spectral distributions as depicted in Figure.3.1, where Brillouin, Rayleigh, Rayleigh-wing and Raman features are depicted [1]. Note that the peak amplitude and the spectral width of the scattered light are not correctly scaled, but Table 3.1 provides some physical parameters for those processes. By definition, the down-shifted frequency components are referred to as Stokes components while the up-shifted components are called anti-Stokes waves. Different spectral characteristics of the scattered light are observed for different scattering processes since distinct types of interaction between the radiation and the media are respectively involved. The four different scattering phenomena can be briefly described as [1]:

- ***Brillouin scattering*** is an inelastic process. Light is scattered by a traveling density perturbation associated with propagating pressure waves in the medium. Formally, it is considered as light scattering by the interaction of photons with acoustic phonons in the medium. The frequency of the acoustic mode is relatively low, so the induced frequency shift is ranged in the order of 10^{10} Hz below the incident frequency.
- ***Rayleigh scattering*** is a quasielastic process, which originates from non-propagating density fluctuations. Formally, it can be described as light scattering resulting from

fluctuation of material entropy, i.e. the degree of molecular organization states. This effect doesn't occur in mono-crystal structure, but in amorphous media such as optical fibers it turns to be an important phenomenon.

- *Rayleigh-wing scattering* is scattering in the wings of the Rayleigh line. In general, it results from fluctuations in the orientation of asymmetric molecules. Since the molecular reorientation process is very rapid, the wings spread over a very large spectral width.

- *Raman scattering* is a highly inelastic process. The interaction between light and the vibrational modes of molecules in the media scatters the light. In particular, optical phonons of the material structure diffract photons from the light. The scattered photons are then transferred at frequency, which is largely shifted from the incident light frequency by some 10^{13} Hz.
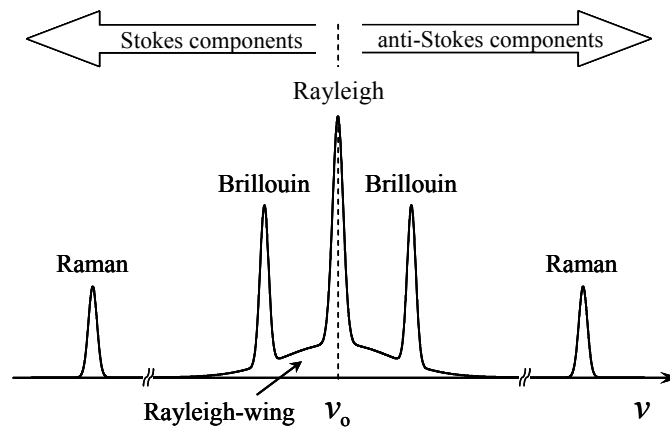
Figure 3.1: Typical spectral components of spontaneous scattering in an inhomogeneous medium.

Process	Shift [cm^{-1}]	Linewidth [cm^{-1}]	Relaxation time [s]	Gain [m/W]
Brillouin	1	$5 \cdot 10^{-3}$	10^{-9}	$2 \cdot 10^{-13}$
Rayleigh	0	$5 \cdot 10^{-4}$	10^{-8}	
Rayleigh-wing	0	5	10^{-12}	
Raman	1000	5	10^{-12}	$5 \cdot 10^{-11}$

Table 3.1: Typical characteristics describing several light scattering processes in liquids. The gain concerns the stimulated version of the processes in silica.

Since the last two processes are not directly relevant to the content of this thesis, a full description of these scattering processes will be devoted to References [1-4], but only the scattering processes related to static and propagating density fluctuations are discussed in the next sections.

3.1.1.1 Perturbed wave equation

When light propagates in optical media, the wave equation (2.5) has to take into account the polarization field P in order to describe the material response to the light and is modified as:

$$\nabla^2 E - \frac{1}{c^2}\frac{\partial^2 E}{\partial t^2} = \mu_o \frac{\partial^2 P}{\partial t^2}, \tag{3.1}$$

For homogeneous and isotropic media, the polarization field is proportional to the applied electric field E and to the associated dielectric susceptibility of the media χ: $P = \varepsilon_o \chi E$. Substituting this linear dependence into Eq.(3.1), the wave equation is expressed as:

$$\nabla^2 E - \frac{n^2}{c^2}\frac{\partial^2 E}{\partial t^2} = 0, \tag{3.2}$$

where $n = \sqrt{1+\chi} = \sqrt{\varepsilon/\varepsilon_o}$ presents the refractive index, ε being the dielectric constant. The wave equation (3.2) in an optical medium is identical to Eq.(2.5), excepted the propagation velocity of light: in the medium, the vacuum velocity c is replaced by $v=c/n$. Nevertheless, at the scale of 10^{-10} m (~atomic radius), a real optical medium can no longer be considered homogeneous since microscopic variations of density along the media will give rise to inhomogeneities along the direction of light propagation. Therefore, the constant scalar dielectric susceptibility χ can be conveniently replaced by a tensor $\chi + \Delta\chi(r,t)$ [5], so that after substituting $P = \varepsilon_o \chi E + \varepsilon_o \Delta\chi E = \varepsilon_o \chi E + \Delta\varepsilon E$, Eq.(3.2) becomes

$$\nabla^2 E - \frac{n^2}{c^2}\frac{\partial^2 E}{\partial t^2} = \mu_o \frac{\partial^2}{\partial t^2}(\Delta\varepsilon\, E). \tag{3.3}$$

The right hand side of this perturbed wave equation is responsible for the mechanism of light scattering. The perturbation term $\Delta\varepsilon$ can be decomposed into scalar and tensorial distributions as follows: $\Delta\varepsilon(r,t) = \Delta\varepsilon_s(r,t) + \Delta\varepsilon_t(r,t)$. The diagonal scalar term $\Delta\varepsilon_s$ describes the fluctuations in thermodynamic quantities such as density, temperature, entropy or pressure. Formally, such fluctuations give rise to light scattering such as Brillouin and Rayleigh scattering. On the contrary, the purely off-diagonal term $\Delta\varepsilon_t$ can be further decoupled in symmetric and asymmetric contributions, both statistically independent and intrinsically related to the optical polarisability of the medium [4]. The symmetric part leads to Rayleigh-wing scattering while the asymmetric one gives Raman scattering.

3.1.2 Rayleigh scattering

In the perturbed wave equation (3.3), the dielectric constant $\Delta\varepsilon$ taken as a scalar quantity is considered mainly as a function of material density. In linear regime, the presence of light in

the medium causes an extremely weak heating while interacting with the material [3], so that the temperature dependence can be ignored. Thus one can write:

$$\Delta\varepsilon = \frac{\partial\varepsilon}{\partial\rho}\Delta\rho. \tag{3.4}$$

The fluctuations of the material density $\Delta\rho$ can also be expanded as a function of two independent quantities, pressure p and entropy s, so that:

$$\Delta\rho = \frac{\partial\rho}{\partial p}\bigg|_s \Delta p + \frac{\partial\rho}{\partial s}\bigg|_p \Delta s. \tag{3.5}$$

The first term describes adiabatic density fluctuations (i.e. acoustic wave) and gives rise to Brillouin scattering. The second term corresponds to isobaric density fluctuations (i.e. temperature or entropy variations at a constant pressure) and is responsible for Rayleigh scattering. Entropy variations are usually described by a diffusion equation, given as:

$$\rho\, c_p \frac{\partial\Delta s}{\partial t} - \kappa\nabla^2\Delta s = 0, \tag{3.6}$$

where c_p and κ present the specific heat at a constant pressure and the thermal conductivity, respectively. The general solution of Eq.(3.6) is:

$$\Delta s(r,t) = \Delta s_o \exp[-\delta\, t]\exp[-i(q\cdot r)], \tag{3.7}$$

where q is the wavevector of the scattered light. This fluctuations are damped at a rate of $\delta=\kappa q^2/\rho c_p$. Here, one can see that the entropy wave does not propagate along the media. Now, let us replace Δs in Eq.(3.5) by the general expression from Eq.(3.7) while discarding the first term of Eq.(3.5). This shows that the term of the induced polarization has only the same frequency component ω as the incident light frequency; thereby the scattered light remains spectrally unchanged.

3.1.3   Spontaneous Brillouin scattering

The equation of motion for pressure fluctuations Δp, which is the first term in Eq.(3.5), is usually described as an acoustic wave. In general, the induced acoustic wave is governed by the following equation [1,3]:

$$\frac{\partial^2\Delta p}{\partial t^2} - \Gamma\nabla^2\frac{\partial\Delta p}{\partial t} - v_a{}^2\nabla^2\Delta p = 0, \tag{3.8}$$

where Γ is the acoustic damping coefficient, related to the shear and bulk viscosity coefficients in the medium. Moreover, the sound velocity in the medium v_a can be expressed as a function of thermodynamic properties as:

$$v_a = \sqrt{\frac{K}{\rho}} = \sqrt{\frac{1}{C_s \rho}},$$ (3.9)

where K and C_s denote the bulk modulus and the adiabatic compressibility, respectively. The general solution of Eq.(3.8) can be found as a propagation wave:

$$\Delta p(r,t) = \Delta p_o \exp[i(q \cdot r - \Omega t)],$$ (3.10)

and here the phonon dispersion relation, $\Omega = |q|v_a$ must be satisfied to give rise to an acoustic wave. Inserting Eq.(3.10) into the perturbed term of Eq.(3.3), the wave equation for the scattered light is obtained as:

$$\nabla^2 E - \frac{n^2}{c^2}\frac{\partial^2 E}{\partial t^2} = \frac{\gamma_e C_s}{c^2}\Delta p_o E_o[(\omega-\Omega)^2 \exp[i(k-q) \cdot r - i(\omega-\Omega)t]$$ (3.11)

$$+(\omega-\Omega)^2 \exp[i(k+q) \cdot r - i(\omega+\Omega)t],$$

where γ_e is an electrostrictive constant, defined as $\gamma_e = \rho_o(\partial \varepsilon / \partial \rho)$.

Spontaneous Brillouin Stokes scattering

The first term in the right part of Eq.(3.11) represents a Stokes wave in Brillouin scattering as an oscillating component. To satisfy energy and momentum conservations, the Stokes wave must have a wavevector of $k'=k-q$ and an angular frequency of $\omega'=\omega-\Omega$. Indeed, three waves are involved in this scattering interaction: the incident wave at frequency ω, the scattered wave (Stokes wave) at frequency ω' and the acoustic wave at frequency Ω. In principle, the three waves are entirely coupled together by means of dispersion relations, $\omega=|k|c/n$, $\omega'=|k'|c/n$ and $\Omega=|q|v_a$. Since the frequency of the sound wave Ω is much smaller than the optical frequencies ω and ω', one can assume that $|q|=2|k|\sin(\theta/2)$ with the approximation that $|k|\approx|k'|$, as illustrated in Figure.3.2. Using the dispersion relations, the frequency of the acoustic wave can be expressed by:

$$\Omega = 2|k|v_a \sin(\theta/2) = 2n\omega\frac{v_a}{c}\sin(\theta/2).$$ (3.12)

In this equation, it is clearly observed that the Stokes frequency shift engendered by Brillouin scattering is highly dependent on the scattering angle θ. In practice, the frequency shift is maximum in the backward direction (when $\theta=\pi$) and is equal to zero in the forward direction (when $\theta=0$). For this reason, the Stokes wave is usually generated by a receding acoustic wave (co-propagating with the incident wave). Therefore, the Brillouin Stokes wave propagates in the opposite direction to the incident light and the Brillouin frequency shift is given by:

$$v_B = \frac{\Omega}{2\pi} = \frac{2nv_a}{\lambda}.$$ (3.13)

In a quantum point of view, this process can be represented as photons from the incident light that are annihilated by the acoustic wave and scattered photons that are created at frequency $-\nu_B$ below the incident frequency.
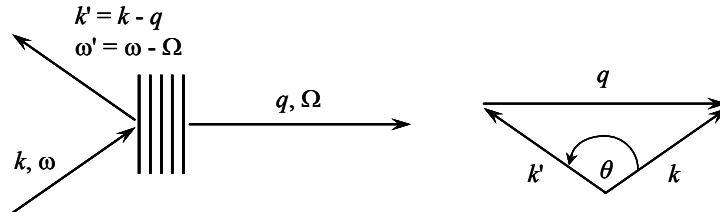
Figure 3.2: Illustration of Stokes scattering in terms of dispersion relations.

Spontaneous Brillouin anti-Stokes scattering

An analogous analysis to the Stokes wave can be developed for the second term in the right part of Eq.(3.11). This process is responsible for the generation of an anti-Stokes wave. In the same manner, the anti-Stokes wave has a wavevector of $k'=k+q$ and an angular frequency of $\omega'=\omega+\Omega$. As illustrated in Figure.3.3, this wave is visualized as light scattered from an oncoming acoustic wave (counter-propagating with the incident wave). Quantum-mechanically, Brillouin anti-Stokes is described as simultaneous absorption of both incident photons and acoustic phonons, followed by the emission of photons at a frequency $+\nu_B$ above the incident frequency.
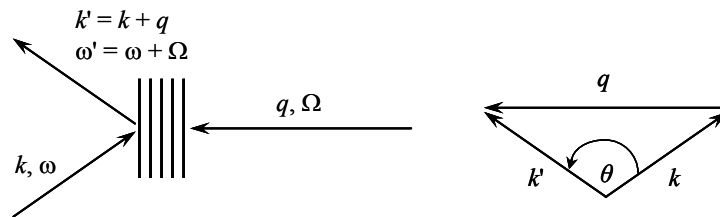
Figure 3.3: Illustration of anti-Stokes scattering in terms of dispersion relations.

Figure.3.4 depicts the measured spectrum of spontaneous Brillouin scattering in optical fibers, where the center peak represents the pump wave. It is clearly shown that the spontaneous Stokes and anti-Stokes waves are equally shifted from the pump frequency with identical amplitude.
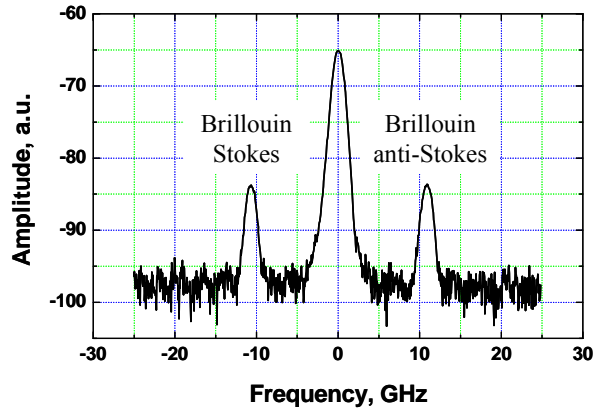
Figure 3.4: Measured spectral profile of spontaneously scattered Brillouin Stokes and anti-Stokes waves in optical fibers. A fraction of the pump wave was also simultaneously detected for a clear demonstration of frequency shifts of the scattered waves.

The damping parameter Γ in eq. (3.8) for the acoustic wave has been ignored so far. If this term is inserted in the complete analysis of Brillouin scattering, a spectral distribution obviously appears for the light scattered into direction θ. The spectral width of Brillouin scattering at full width at half maximum (FWHM) is given by:

$$\delta\omega = \Gamma|q|^2 = 4\Gamma n^2 \frac{\omega^2}{c^2}\sin(\theta/2). \tag{3.14}$$

Due to the damping characteristics, the acoustic wave only propagates over several cycles of the incident light and its intensity undergoes an exponential decrease as:

$$|\Delta p(t)|^2 = |\Delta p(0)|^2 \exp[-t/\tau_p], \tag{3.15}$$

where $\tau_p = (\Gamma/|q|^2)^{-1}$ is the average life time of acoustic phonons in media, inversely depending on the acoustic damping coefficient. In the Fourier domain, the backscattered light has a spectral profile with a Lorentzian line shape with a FWHM of:

$$\frac{\delta\omega}{2\pi} = \frac{1}{\pi\tau_p}. \tag{3.16}$$

The phonon life time varies substantially with the frequency of the acoustic wave, and thus with the frequency of the incident light [2]. Table 3.1 represents some spectral characteristics of Brillouin scattering in silica with respect to the incident wavelength. The velocity of acoustic wave in standard single-mode fibers is estimated to be v_a=5775 m/s in this table.

Wavelength [nm]	Brillouin shift [GHz]	Brillouin linewidth [MHz]
514	34.0	100
832	21.6	70
1320	12.8	35
1550	10.8	29

Table 3.2: Characteristics of the Brillouin spectrum at different pump wavelengths. In all situations, the acoustic velocity in silica was considered as a constant, v_a=5775 m/s.

3.2 Stimulated Brillouin scattering

Spontaneous Brillouin scattering was discovered in 1922 by Leon Brillouin [6] as light is scattered by the thermally fluctuating density in a medium. However, the advent of the laser in the early 60's changed the physical view on Brillouin scattering since the intense coherent optical wave significantly enhanced the scattering process. Consequently, more photons from the laser beam are annihilated whereas the Stokes wave experiences an exponential growth due to the amplitude growth of the acoustic wave. This regime corresponds to the phenomenon referred to as stimulated Brillouin scattering (SBS). SBS as a nonlinear scattering was first observed in 1964 by Chiao *et al.* in quartz and sapphire [7].

3.2.1 Electrostriction

Electrostriction is basically described as the tendency of a material to become compressed in the presence of an electric field. As a consequence of the maximization of the potential energy, molecules in a medium tend to be attracted into the regions where an intense electric field is localized. The potential energy density of media u is proportional to the dielectric constant as:

$$u = \frac{\varepsilon}{8\pi} E^2.$$ (3.17)

When the material density is perturbed by an amount $\Delta\rho$, the associated dielectric constant also changes from the origin value ε_o to the value $\varepsilon_o+\Delta\varepsilon$, where

$$\Delta\varepsilon = \frac{\partial\varepsilon}{\partial\rho}\Delta\rho.$$ (3.18)

Therefore, the energy density Δu can be expressed according to the variation of the dielectric constant:

$$\Delta u = \frac{E^2}{8\pi}\Delta\varepsilon = \frac{E^2}{8\pi}\left(\frac{\partial\varepsilon}{\partial\rho}\right)\Delta\rho.$$ (3.19)

According to the first law of thermodynamics, the change in energy Δu must be equal to the work Δw, which is performed to compress the media:

$$\Delta w = p_{st}\frac{\Delta V}{V} = -p_{st}\frac{\Delta \rho}{\rho}. \tag{3.20}$$

The electrostrictive pressure p_{st} represents the contribution of the electric field to the pressure in media. Since $\Delta u = \Delta w$, by equating Eq.(3.19) and Eq(3.20), the electrostrictive pressure can be derived as:

$$p_{st} = -\rho\left(\frac{\partial \varepsilon}{\partial \rho}\right)\frac{E^2}{8\pi} = -\gamma_e\frac{E^2}{8\pi}, \tag{3.21}$$

where $\gamma_e = \rho_o(\partial \varepsilon/\partial \rho)$ was already defined as the electrostrictive constant in section 3.1.1. Since p_{st} has a negative value, the net pressure turns to be reduced in the regions where the electric field is intense. As a result, the molecules will be naturally pulled into those regions within the medium, so that the material density will be locally compressed in the medium. In general, the molecule displacement is very slowly processed compared to the frequency of the optical waves, so that the effect on the material must be characterized by the time averaged value $<E^2>$ instead of the instantaneous field E^2 in Eq.(3.21).

3.2.2 Stimulated scattering process

The process of SBS is classically described as a nonlinear interaction between a pump wave at frequency ν_p and a Stokes wave at frequency ν_S. The two waves are coupled by nonlinear polarizations. It must be pointed out that the higher order polarization associated to SBS is not caused by the nonlinear susceptibilities induced by a parametric process, but by a sound wave induced by mean of electrostriction. Therefore, the description of SBS starts from the propagation of the three interacting waves using the following equations:

$$\nabla^2 E_p - \frac{n^2}{c^2}\frac{\partial^2 E_p}{\partial t^2} = \mu_o\frac{\partial^2 P_p^{NL}}{\partial t^2} \tag{3.22a}$$

$$\nabla^2 E_S - \frac{n^2}{c^2}\frac{\partial^2 E_S}{\partial t^2} = \mu_o\frac{\partial^2 P_S^{NL}}{\partial t^2} \tag{3.22b}$$

$$\frac{\partial^2 \Delta\rho}{\partial t^2} + \Gamma\nabla^2\frac{\partial \Delta\rho}{\partial t} - v_a\nabla^2\rho = -\nabla\cdot f, \tag{3.22c}$$

where E_p and E_S are the amplitudes of the electric fields (pump and Stokes waves), respectively. Notice that, here, $\Delta\rho$ denotes the density variation rather than the pressure variation to describe the acoustic wave. The equations (3.22) can in turn be all coupled through the electrostrictive force f using the material constitutive relations given by:

$$P^{NL}(r,t) = \Delta\varepsilon\, E(r,t) = \frac{\gamma_e}{\rho_o}\Delta\rho\, E(r,t) \tag{3.23a}$$

$$\Delta \cdot f(r,t) = \frac{1}{2}\gamma_e \nabla^2 \left\langle \left| E_p(r,t) + E_S(r,t) \right|^2 \right\rangle . \tag{3.23b}$$

To simplify the coupled equations involved in SBS, one can assume that:

- The state of polarization (SOP) of the pump wave is parallel to the SOP of the Stokes wave, designated by the unit polarization vector e.

- The fiber attenuation α is considered negligible while the acoustic damping coefficient Γ is maintained in the expressions.

- The system is in steady-state conditions, where the life time of acoustic wave is so short that it can be neglected when compared to that of the pump wave.

- The pump wave is not depleted during the SBS process.

These simplifications will be discussed later in detail.

3.2.2.1 SBS-induced gain resonance

Stimulated Stokes scattering can be observed under the conditions that the dispersion relations fulfill $k_p = k_S + \Omega$. The conditions indicate that the acoustic wave co-propagates with the pump in the direction of $+z$. In unperturbed situations (when $f = 0$), the three waves propagate in the optical medium as independent plane waves represented by the exponential terms in Eq.(3.24). On the contrary, the presence of the force term f (the so-called electrostriction) will modify the amplitudes of the waves (E_p, E_S and A) through coupling effects. In such circumstance, the slowly-varying envelope approximation can be applied to the propagation equations for the waves, resulting in:

$$E_p = e\, E_p(z,t)\exp[i(\omega_p t - k_p z)] \tag{3.24a}$$

$$E_S = e\, E_S(z,t)\exp[i(\omega_S t + k_S z)] \tag{3.24c}$$

$$\Delta\rho = A(z,t)\exp[i(\Omega t - q z)]. \tag{3.24b}$$

Let us substitute Equations (3.24) into Equations (3.23). By retaining only the resonant terms for each wave, one can obtain:

$$P_p^{NL} = e\frac{\gamma_e}{2\rho_o} A(z,t) E_S(z,t)\exp[i(\omega_p t - k_p z)] \tag{3.25a}$$

$$P_S^{NL} = e\frac{\gamma_e}{2\rho_o} A^*(z,t) E_p(z,t)\exp[i(\omega_S t + k_S z)] \tag{3.25b}$$

$$\nabla \cdot f = \frac{\gamma_e q^2}{2}[E_p(z,t)\, E_S^*(z,t)]\exp[i(\Omega t - q z)]. \tag{3.25c}$$

In turn, substituting Equations (3.24) and (3.25) into Equations (3.22) results in three coupled equations responsible for the description of stimulated Brillouin scattering. Due to the slowly-varying envelope approximation, a simplified form to the coupled equations can be found:

$$\left[\frac{\partial}{\partial z}+\frac{n}{c}\frac{\partial}{\partial t}\right]E_p = i\frac{k_p\gamma_e}{4\varepsilon\rho_o}AE_S \tag{3.26a}$$

$$\left[-\frac{\partial}{\partial z}+\frac{n}{c}\frac{\partial}{\partial t}\right]E_S = i\frac{k_S\gamma_e}{4\varepsilon\rho_o}A^*E_p \tag{3.26b}$$

$$\left[\frac{\partial}{\partial z}+\frac{2\Omega-i\Gamma q^2}{2\Omega v_a}\frac{\partial}{\partial t}+\frac{\Gamma q^2}{2v_a}\right]A = i\frac{q\gamma_e}{4v_a^2}E_p E_S^*. \tag{3.26c}$$

Since the acoustic wave is rapidly damped, the mean free path of acoustic phonons is typically very small ($\sim 10^{-4}$ m) compared to the distance over which optical fields vary significantly. Therefore, the spatial derivative term in Eq.(3.26c) can be conventionally dropped. The time derivative term can also vanish as assuming the steady-state conditions. As a result, Eq.(3.26c) can be substantially simplified and the amplitude of the acoustic wave is in turn given by:

$$A = i\frac{q\gamma_e}{2\Gamma_B v_a}E_p E_S^*, \tag{3.27}$$

where $\Gamma_B=\Gamma q^2$ denotes the bandwidth of Brillouin scattering. Inserting this value into the equations (3.26) leads to two coupled equations relating the pump and Stokes waves:

$$\frac{\partial E_p}{\partial z} = -\frac{q k_p \gamma_e^2}{8\varepsilon\rho_o\Gamma_B v_a}\frac{|E_S|^2 E_p}{1-i(2\Delta v/\Delta v_B)} \tag{3.28a}$$

$$\frac{\partial E_S}{\partial z} = -\frac{q k_S \gamma_e^2}{8\varepsilon\rho_o\Gamma_B v_a}\frac{|E_p|^2 E_S}{1-i(2\Delta v/\Delta v_B)}, \tag{3.28b}$$

Analyzing the form of these equations, one can see two main phenomena occurring to the optical waves during the SBS process: energy transfer and nonlinear phase between the pump and Stokes waves can be predicted according to the real and imaginary part of the equations, respectively. This system can be further simplified by introducing the intensities of the optical waves in the coupled equations while defining $I = \frac{1}{2}n\varepsilon_0 c|E|^2$:

$$\frac{\partial I_p}{\partial z} = -g_B(v)I_p I_S \tag{3.29a}$$

$$\frac{\partial I_S}{\partial z} = -g_B(v)I_S I_P, \tag{3.29b}$$

where $g_B(v)$ represents the Brillouin gain spectrum. It is defined as:

$$g_B(\nu) = g_B \frac{(\Delta \nu_B / 2)^2}{(\nu - \Delta \nu)^2 + (\Delta \nu_B / 2)^2},$$ (3.30)

where g_B is the Brillouin gain coefficient. Equivalent expressions of g_B in terms of the constitutive parameters are shown in literatures

$$g_B = \frac{q k_p^2 \gamma_e^2}{8 \varepsilon \rho_o \Gamma_B \nu_a} \frac{1}{n \varepsilon_o c} = \frac{2 \pi n^7 p_{12}^2}{c \lambda_p^2 \rho \Delta \nu_B \nu_a},$$ (3.31)

where λ_p denotes the pump wavelength and p_{12} is the longitudinal elasto-optic coefficient. In bulk silica, the measurable value of g_B is approximately $5 \cdot 10^{-11}$ m/W. The SBS process scatters photons off the pump wave so as to create the amplification at the Stokes wave. The gain spectrum has inherently a Lorentzian distribution centered at the Stokes shift and a spectral width $\Delta \nu_B$ at full width at half maximum, as depicted in Figure.3.5.
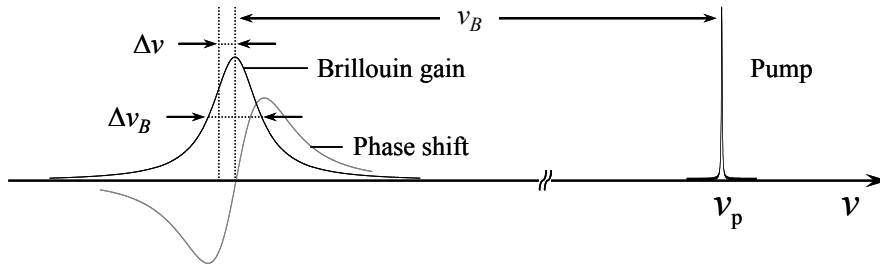
Figure 3.5: The Brillouin gain resonance with a Lorentzian shape and the associated phase shift.

The equations (3.29) describe the spatial evolution of the two waves, resulting in an analytical solution for Stokes wave [8,9] as:

$$I_S(z) = I_S(L) \exp[g_B I_p(0)(L-z)],$$ (3.32)

where the Stokes wave is launched into the material at $z=L$. It is clearly seen that the Stokes wave experiences an exponential growth as a function of the pump intensity while propagating in the opposite direction to the pump wave.

It is also interesting to discuss the transition of the phase shift associated to the amplification through SBS. By taking into account the imaginary parts of equations (3.28), the SBS-induced phase shifts for the two waves can be expressed as:

$$\frac{\partial \Phi_p^{SBS}}{\partial z} = -\frac{1}{2} g_B I_S \frac{(2 \Delta \nu / \Delta \nu_B)}{1 + (2 \Delta \nu / \Delta \nu_B)^2}$$ (3.33a)

$$\frac{\partial \Phi_S^{SBS}}{\partial z} = -\frac{1}{2} g_B I_p \frac{(2 \Delta \nu / \Delta \nu_B)}{1 + (2 \Delta \nu / \Delta \nu_B)^2}.$$ (3.33b)

The phase shift is usually defined in the manner that a positive Φ^{SBS} causes an additional positive delay. As a result, positive Δv makes optical waves retarded while the waves are advanced with negative Δv.

3.2.2.2 SBS-induced loss resonance

SBS-induced loss resonance is mathematically described in the same manner as the Stokes scattering. The only difference is that the sign of Brillouin gain is negative and the frequencies of the two waves are swapped ($v_{AS} > v_p$). The interaction between two counter-propagating waves, pump and anti-Stokes, fulfills the following equations:

$$\frac{\partial I_p}{\partial z} = -g_B(v)I_p I_{AS} \qquad\qquad (3.34a)$$

$$\frac{\partial I_{AS}}{\partial z} = +g_B(v)I_{AS}I_P , \qquad\qquad (3.34b)$$

which are formally similar to the equations (3.29). Nevertheless, the change of sign in Eq.(3.34b) implies that the anti-Stokes signal undergoes an attenuation while propagating in the fibers. The spectrum of Brillouin absorption is identical to that of Brillouin gain as a Lorentzian distribution and its characteristics are depicted in Figure.3.6.
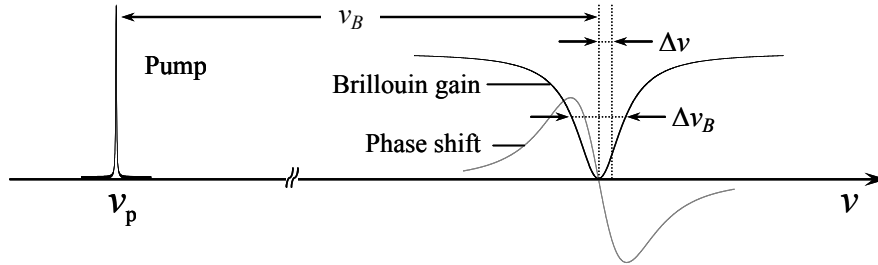
Figure 3.6: The Brillouin loss resonance with a Lorentzian shape and the associated phase shift.

3.2.2.3 Usual simplifications in the description of the SBS process

Parallel polarizations

If the states of polarization (SOP) of the pump and Stokes waves are not parallel, the efficiency of SBS tends to significantly decrease. The scalar product of the polarization vectors $|e_p \cdot e_S|$ is no longer equal to unity, so that Eq.(3.27) has to be replaced by:

$$A = -i\left|e_p \cdot e_S\right| \frac{q\gamma_e}{2\Gamma_B v_a} \frac{E_p E_S^*}{1-i(2\Delta v / \Delta v_B)} . \qquad\qquad (3.35)$$

Therefore, the polarization mixing efficiency $\eta_p = |e_p \cdot e_S|^2$ manifests the efficiency of Brillouin gain in Eq.(3.30) as it is added in the equation:

$$g_B(\nu) = \eta_p\, g_B \frac{\left(\Delta\nu_B/2\right)^2}{\left(\nu - \Delta\nu_B\right)^2 + \left(\Delta\nu_B/2\right)^2}. \tag{3.36}$$

The effect of η_p is so significant that it can completely suppress the SBS phenomenon when the SOPs of the two waves are relatively orthogonal.

No fiber attenuation

The most distinguished feature of the optical fibers is the close-to-transparent characteristics. However, a light wave experiences some linear attenuation during propagation in fibers. The fiber attenuation is mainly due to Rayleigh scattering and in standard single-mode fibers the attenuation α is approximately 0.18 dB/km at 1550 nm. When considering this parameter, the equations (3.29) has to be modified as:

$$\frac{\partial I_p}{\partial z} = -g_B(\nu) I_p I_S - \alpha I_p \tag{3.37a}$$

$$\frac{\partial I_S}{\partial z} = -g_B(\nu) I_S I_P + \alpha I_S. \tag{3.37b}$$

Unfortunately, exact analytical solutions for these coupled equations are not possible [10], but numerical implementations for the equations (3.26) while neglecting the fiber attenuation show good agreement with the experimental results.

Steady-state conditions

The amplitude of the acoustic wave A in Eq.(3.27) was calculated under steady-state conditions. In such conditions, the optical waves must consist of essentially DC components, thereby the life time of phonons t_{phonon} can be neglected. However, when the waves are intensity-modulated, i.e. pulse operations, the Brillouin gain turns to be time dependent. If duration of the pulse t_{pulse} is significantly longer than t_{phonon}, which represents a quasi-DC regime, these conditions are still valid. On the contrary, if $t_{pulse} < t_{phonon}$, one must take into account the dynamics of the acoustic wave.

Non-depleted pump

In the assumption in which the intensity of the pump in Eq.(3.29) wave remains constant while transmitting in optical fibers, namely non-depleted pump, the Stokes wave takes benefits from energy transfer in the SBS process and undergoes an exponential growth in Eq.(3.32). The SBS gain shows then a logarithmic dependence on the pump intensity, so that as far as the signal gain is concerned this system can be regarded as a linear system. However, if the Stokes wave grows to a critical intensity comparable to that of the pump wave, the pump must start to be significantly depleted and this system turns to be a nonlinear system.

3.2.3 Graphical illustration of stimulated Brillouin scattering

Figure.3.7 depicts the schematic illustration of stimulated Brillouin scattering (SBS) as a parametric process of two counter-propagating optical waves and acoustic wave in optical fibers. Here, the signal wave at frequency ν_s propagates in the opposite direction to the pump wave at frequency ν_p. Once the frequency separation between two waves is equal to the Brillouin frequency of the fiber or the frequency of acoustic wave, namely phase matching conditions ($\nu_p = \nu_s + \nu_B$), the interference between the pump and signal waves generates an optical beating resonant at frequency ν_B so as to reinforce the acoustic wave. In addition, due to the phenomenon of electrostriction, the material density is strongly fluctuated along the fiber and the refractive index turns to be modulated along the fiber core. Then this nonlinear interaction induces a dynamic Bragg-type grating in the fiber core, which co-propagates with the pump wave and this grating in turn diffracts photons from the pump to the signal, thereby resulting in the signal amplification. The whole process is self-sustained in a complete feedback loop and enhances the Brillouin scattering process: it is referred as stimulated Brillouin scattering.
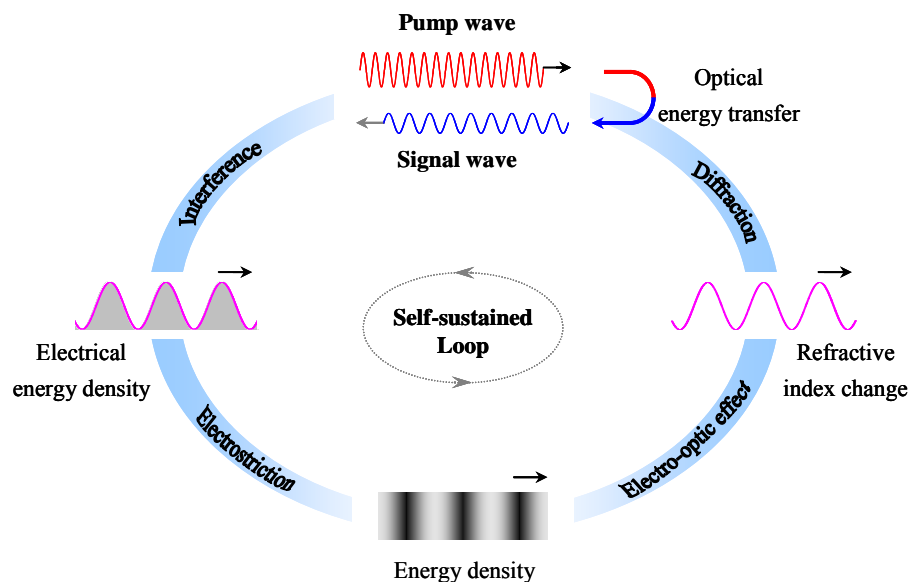
Figure 3.7: Schematic representation of the four different effects involved in SBS as a parametric process. The successive realization of this feedback loop reinforces the energy transfer (counterclockwise succession).

Bibliography

[1]   R. W. Boyd, *Nonlinear Optics*, 2nd ed. (Academic Press, New York, 2003).

[2]   G. P. Agrawal, *Nonlinear Fiber Optics*, 3rd ed. (Academic Press, San Diego, 1995).

[3]   I. L. Fabelinskii, *Molecular Scattering of Light* (Plenum Press, New York, 1968).

[4]   Y. R. Shen, *The principle of nonlinear optics* (Wiley, New York, 1984).

[5]   L. D. landau and E. M. Lifshitz, *Statistical physics*, 3rd ed. (Butterworth-Heinemann, 1984).

[6]   L. Brillouin, "Diffusion of light and X-rays by a transparent homogeneous body. The influence of thermal agitation," Ann. phys. **17**, 88-122 (1922).

[7]   R. Y. Chiao, C. H. Townes and B. P. Stoicheff, "Stimulated Brillouin scattering and coherent generation of intense hypersonic waves," Phys. Rev. Lett. **12**, 592-596 (1964).

[8]   R. H. Enns and I. P. Batra, "Saturation and depletion in stimulated light scattering," Phys. Lett. A, **28**, 591-592 (1969).

[9]   C. L. Tang, "Saturation and spectral characteristics of the Stokes emission in the stimulated Brillouin process," J. Appl. Phys. **37**, 2945-2955 (1966).

[10] L. Chen and X. Bao, "Analytical and numerical solutions for steady state stimulated Brillouin scattering in a single-mode fiber," Opt. Commun. **152**, 65-70 (1998).

Chapter 4

Brillouin slow & fast light in optical fibers

Slow & fast light based on stimulated Brillouin scattering (SBS) in optical fibers has been experimentally and efficiently demonstrated at EPFL, Switzerland [1,2] in 2004, and independently a few months later at Cornell University. Unlike the experimental conditions and the operational characteristics of the former slow and fast light systems [3-7], Brillouin slow light was readily realized in standard optical fibers with a simple benchtop configuration. Moreover, its room-temperature operation at any wavelength has received tremendous interest from the optical communication society for fascinating potential applications such as all-optical delay lines, optical buffers and signal synchronizations. To date, Brillouin slow light has already shown the possibilities to manipulate the group velocity of a light signal from as slow as v_g=71000 km/s to superluminal propagation, even reaching negative velocities [2]. However, Brillouin slow light is not widely exploited in a continuous data stream for communication applications due to some inherent features of this system: narrow signal bandwidth, strong change of signal amplitude and significant signal distortion. So far, these limitations have been extensively investigated to improve the Brillouin slow light system, as optimizing the gain spectral profile and the induced dispersion in the material. This thesis work was also aimed at proposing an adequate solution for each issue to make Brillouin slow light a completely operating all-optical delaying system.

4.1 Basic Brillouin slow light system

4.1.1 Analytical model of Brillouin slow light

4.1.1.1 Signal delay via stimulated Brillouin scattering

As mentioned in the previous chapter, stimulated Brillouin scattering in optical fibers is usually described as a nonlinear interaction between two counter-propagating waves, a strong pump at frequency ν_p and a weak probe at frequency ν_s. Under particular phase matching conditions, the two waves are coupled by means of an acoustic wave induced by the phenomenon of electrostriction. Using the slowly varying envelope approximation, the SBS interaction is fully described by three coupled amplitude equations [8,9]:

$$\frac{\partial E_p}{\partial z} + \frac{n}{c}\frac{\partial E_p}{\partial t} = i\, g_1\, E_S\, A \tag{4.1a}$$

$$-\frac{\partial E_S}{\partial z} + \frac{n}{c}\frac{\partial E_S}{\partial t} = i\, g_1\, E_p\, A^* \tag{4.1b}$$

$$\frac{\partial A}{\partial t} + \left(\frac{\Gamma_B}{2} - i\,\delta\omega\right)A = i\, g_2 E_p E_S^*, \tag{4.1c}$$

where the fiber loss α is neglected. E_p, E_s and A are the field amplitudes of the pump, the probe and the acoustic waves, respectively; n is the refractive index of the fiber; $\Gamma_B/2\pi$ represents the bandwidth of the Brillouin resonance at full width at half maximum; $\delta\omega$ is the detuning of the probe frequency from the center frequency of the Brillouin gain resonance, $\delta\omega=\omega_s-\omega_p+\Omega_B$; Ω_B is the Brillouin frequency shift of the optical fiber; $g_1 = \omega_p\gamma_e/(4cn\rho_0)$ and $g_2=\gamma_e\Omega_B/(2cnv_a^2)$. To derive analytical solutions of Equations (4.1), let us consider a weak interaction regime, so that the continuous-wave pump remains undepleted during the SBS process. Moreover, assuming steady state conditions, the equations can be simplified as:

$$-\frac{\partial E_s}{\partial z} + \frac{n}{c}\frac{\partial E_s}{\partial t} = i\, g_1\, E_p\, A^* \tag{4.2a}$$

$$A^* = \frac{-i\, g_2 E_p^* E_s}{\Gamma_B/2 + i\,\delta\omega}. \tag{4.2b}$$

After substituting Eq.(4.2b) into Eq.(4.2a), the spatial amplitude evolution of the probe wave is obtained as:

$$\frac{\partial E_s}{\partial z} = \left(i\frac{n\omega}{c} - \frac{g_1 g_2 I_p}{\Gamma_B/2 + i\delta\omega}\right)E_s. \tag{4.3}$$

By simply integrating Eq.(4.3) with respect to space, the dispersion $k_s(\omega)$ induced by the stimulated Brillouin scattering process can be expressed as:

$$k_s(\omega) = n\frac{\omega}{c} - \frac{i}{2}\left(\frac{g_o I_p}{1 + i\,2\delta\omega/\Gamma_B}\right) \equiv \frac{\omega}{c}n'_s.$$

(4.4)

From the form of Eq.(4.4) as a complex response function, it is clearly seen that the SBS process generates a pure gain resonance with a Lorentzian shape, centered at the probe frequency. The effective complex index n'_s is given by:

$$n'_s = n - i\frac{c}{2\omega}\left(\frac{g_o I_p}{1 + i\,2\delta\omega/\Gamma_B}\right),$$

(4.5)

and the gain coefficient $g_s(\omega)$, the refractive index $n_s(\omega)$ and group index $n_g(\omega)$ can be expressed as a function of frequency deviation, respectively:

$$g_s(\omega) = -\left(\frac{2\omega}{c}\right)\mathrm{Im}(n'_s) = \frac{g_o I_p}{1 + 4\delta\omega^2/\Gamma_B^2}$$

(4.6)

$$n_s(\omega) = \mathrm{Re}\{n'_s\} = n + \frac{c\,g_o I_p}{\omega}\frac{\delta\omega/\Gamma_B}{1 + 4\delta\omega^2/\Gamma_B^2}$$

(4.7)

$$n_g(\omega) = n_s + \omega\frac{dn_s}{d\omega} = n + \frac{c\,g_o I_p}{\Gamma_B}\frac{1 - 4\delta\omega^2/\Gamma_B^2}{\left(1 + 4\delta\omega^2/\Gamma_B^2\right)^2}$$

(4.8)

Figure 4.1.1 represents the schematic illustrations, showing the modification of the group velocity in a material, using stimulated Brillouin scattering in optical fibers. When a monochromatic pump wave at frequency ν_p propagates through the fiber, an efficient narrowband amplification or attenuation can be created by the SBS process, as shown in Figure 4.1.1a. In a standard optical fiber the Brillouin gain resonance g_s with a Lorentzian shape is spectrally centered at frequency $-\nu_B$ (~11 GHz) below the pump frequency and has a spectral FWHM width 30 MHz [10]. According to Kramers-Kronig relations, a sharp transition in the effective refractive index n_s is accompanied in the vicinity of the gain resonance, as shown in Figure.4.1.1b. Then the large normal dispersion ($dn_s/d\omega > 0$) induced by SBS gives rise to a strong change in the group index n_g, resulting in an increase in group index, as shown in Figure.4.1.1c. As a result, the group velocity $v_g = c/n_g$ at which a signal travels through the fiber decreases, leading to the generation of slow light and signal delay. Fast light and signal advancement can also be produced using SBS, simply by swapping the frequencies of the pump and signal waves. As depicted in the right side of Figure.4.1.1, SBS can generate a narrowband loss resonance at frequency $+\nu_B$ above the pump frequency and a large anomalous dispersion across the loss band. Therefore, the group index in the center of
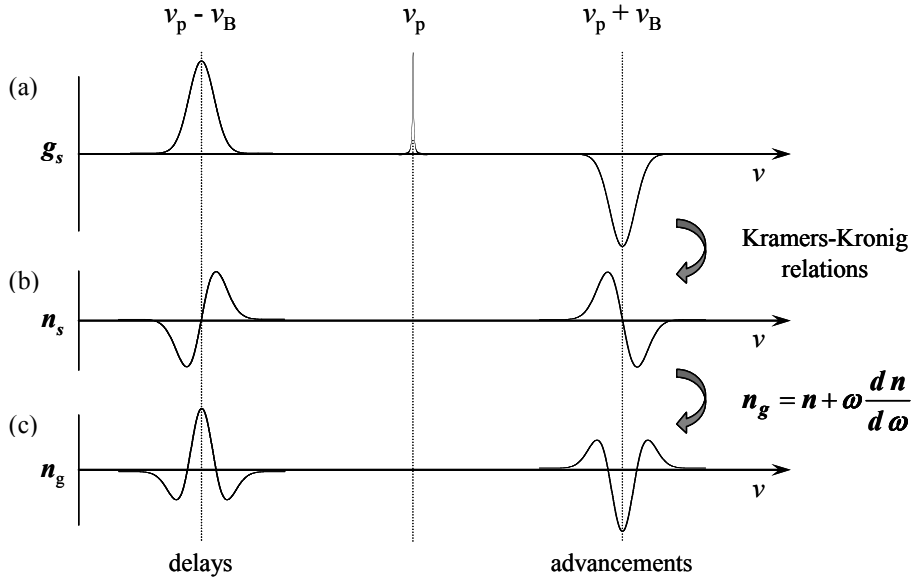
Figure 4.1.1: Schematic illustrations of the principle of group velocity control using stimulated Brillouin scattering in optical fibers. On left, SBS gain resonance at frequency $-\nu_B$ below the pump frequency induces a large normal dispersion across the gain band, which is responsible for signal delay. On the contrary, on right, the generation of signal advancements in the vicinity of a SBS loss resonance is depicted.

the absorption is significantly reduced, and thus it allows a signal to propagate in optical fibers with an increased group velocity.

To estimate the amount of delay that a signal will experience in a Brillouin delay line, let us consider a standard single-mode fiber with a length L as a Brillouin gain medium, over which a signal propagates. After passing through the fiber, the signal arrives at the end of the fiber with a transit time $T=L/\nu_g$. Due to the dependence of the group index on the induced dispersion in Eq.(4.7), the relative transit time of the signal through the fiber can be varied through the group index change, and thus the group velocity change. In consequence, the relative signal delay ΔT_d between situations with and without the pumping is given by:

$$\Delta T_d = \frac{L}{c}\Delta n_g = \frac{G}{\Gamma_B}\frac{1-4\delta\omega^2/\Gamma_B^2}{\left(1+4\delta\omega^2/\Gamma_B^2\right)^2} \tag{4.9}$$

$$\simeq \frac{G}{\Gamma_B}\left(1-12\delta\omega^2/\Gamma_B^2\right) \quad \text{when } 4\delta\omega^2/\Gamma_B^2 \ll 1,$$

where $G=g_o I_p L$ is relevant to the Brillouin gain, I_p is the pump intensity and L is the fiber length. In the exact center of the resonance ($\delta\omega=0$), the relative signal delay achievable in Brillouin slow light is then simplified as:

$$\Delta T_d \simeq \frac{G}{\Gamma_B}. \tag{4.10}$$

It is clearly shown that the relative signal delay ΔT_d via a Brillouin fiber delay line has a logarithmic dependence on the net signal gain in most implementations, since the G exponentiated represents the net signal gain. On the other hand, it is inversely proportional to the bandwidth of a given Brillouin resonance, so that a narrower gain resonance will result in a larger signal delay. Nevertheless, using the SBS process a dynamic control of the speed of a light signal can be all-optically produced in optical fibers, since a signal can actually be linearly delayed or accelerated using the Brillouin interaction by simply and proportionally varying the pump intensity I_p.

4.1.1.2 Signal distortion in Brillouin slow light

In absence of gain saturation or pump depletion a Brillouin fiber delay line is usually described as a stationary linear system as far as the signal transformation is concerned. The transfer function of the Brillouin slow light system $T(\omega)$ can be expressed as:

$$T(\omega) = \exp\left[i\,k_s(\omega)\,L\right] = \exp\left[\frac{G}{2}\left(\frac{1}{1+\left(2\omega/\Gamma_B\right)^2}\right) - i\,\frac{2\omega/\Gamma_B}{1+\left(2\omega/\Gamma_B\right)^2}\right] \qquad (4.11)$$

$$= \exp\left[G(\omega) + i\,\Phi(\omega)\right],$$

where L is the effective length of the fiber used as a Brillouin gain medium. Since the Brillouin resonance has a complex response, the amplitude and the phase of the signal is transformed by the real and the imaginary parts of $T(\omega)$, respectively. When $(2\omega/\Gamma_B)^2 \ll 1$, the real and imaginary parts of the transfer function of the delaying system can be further explicitly expressed as:

$$G(\omega) = \frac{G}{2}\left(1 - \left(2/\Gamma_B\right)^2\omega^2 + \left(2/\Gamma_B\right)^4\omega^4 + \left(2/\Gamma_B\right)^6\omega^6 + \cdots\right) \qquad (4.12a)$$

$$\Phi(\omega) = -\left(\left(2/\Gamma_B\right)\omega - \left(2/\Gamma_B\right)^3\omega^3 + \left(2/\Gamma_B\right)^5\omega^5 + \cdots\right). \qquad (4.12b)$$

The frequency dependence of the signal gain is responsible for a spectral filtering effect (low-pass filter) and distorts the signal shape. Therefore, a temporal broadening of signal is essentially observed when a signal emerges from the Brillouin delay line. This is referred to as gain broadening, B_G. On the other hand, due to the large induced dispersion associated to the imaginary part of $T(\omega)$, the higher order dispersion terms (except the first term, which is directly responsible for the signal delaying) inherently produces an additional phase distortion, referred to as dispersion broadening, B_D. Therefore, the total pulse broadening, B_{total} must be calculated by the geometrical sum of the two broadening factors: $B^2_{total} = B^2_G + B^2_D$. It is clearly shown that the amplitude response $G(\omega)$ contains only even

terms in its polynomial expansion with respect to angular frequency while the phase response $\Phi(\omega)$ is anti-symmetric and contains only odd terms. In other words, these two broadening effects can not mutually cancel to compensate the signal distortion. Moreover, since there is no quadratic dependence in the phase response, the introduction of ordinary chromatic dispersion into the Brillouin slow light system can only bring further distortion. Signal distortion essentially accompanies signal delay in any kind of linear slow light systems.

Let us launch a transform-limited Gaussian pulse as a light signal into a Brillouin slow light system. The amplitude of the initial electric field is defined as:

$$E(t) = \exp\left[-\frac{1}{2}\left(\frac{t}{t_o}\right)^2\right],\tag{4.13}$$

where t_o is related to the pulse duration. The pulse duration at full width at half maximum (FWHM) is given by $t_{in} = 2t_o\sqrt{\ln 2}$. The spectrum of the pulse can be simply obtained by the Fourier transform of the envelope function:

$$\tilde{E}(\omega) = \sqrt{2\pi t_o^2}\,\exp\left[-\frac{\omega^2 t_o^2}{2}\right].\tag{4.14}$$

The spectral width (FWHM) of the initial pulse is given by $\Delta\omega_{in} = 2\sqrt{\ln 2}\,/\,t_o$. The propagation of the different frequency components forming the signal pulse depends on the dispersive properties in the fiber modified by SBS amplification, so that the spectrum of the pulse exiting from the slow light medium is given as:

$$\tilde{E}_{out}(\omega) = T(\omega)\cdot\tilde{E}_{in}(\omega) = \exp\left[G(\omega)\right]\cdot\exp\left[i\,\Phi(\omega)\right]\cdot\tilde{E}_{in}(\omega)\tag{4.15}$$

$$= \exp\left[G\right]\exp\left[-\left(\frac{1}{2}t_o^2 + \frac{2G}{\Gamma_B^2}\right)\omega^2 - i\left(\frac{2}{\Gamma_B}\omega - \frac{8}{\Gamma_B^3}\omega^3\right)\right].$$

Figure 4.1.2 depicts a simple sketch of the pulse propagation in the Brillouin slow light system. Unfortunately, the electric field of the output pulse can not be analytically expressed by performing the inverse Fourier transform of Eq.(4.15). However, if it is assumed that the output pulse maintains its Gaussian shape, the FWHM width of the output pulse can be
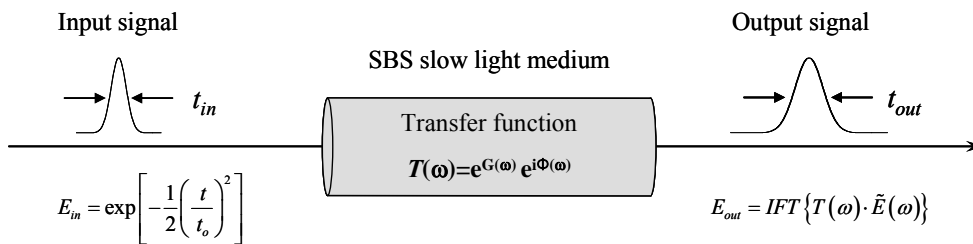
Figure 4.1.2: Transformation of signal after propagating through a Brillouin slow light medium, where $T(\omega)$ represents the transfer function of Brillouin slow light. *IFT*; inverse Fourier transform.

approximated by a general Heisenberg's uncertainty relation. According to this relation, the product of the spectral and temporal widths for chirped-free Gaussian pulse is 0.441 [11]. The power spectrum of the output pulse is represented by the modulus of Eq.(4.15) and results in the spectral width (FWHM):

$$\Delta\omega_{out} = 2\sqrt{\frac{\ln 2}{t_o^2 + 4G/\Gamma_B^2}}.$$ (4.16)

As a consequence, the pulse-broadening factor B is found as:

$$B = \frac{t_{in}}{t_{out}} = \frac{\Delta\omega_{out}}{\Delta\omega_{in}} = \sqrt{1 + \frac{4}{t_o^2\,\Gamma_B^2}G} = \sqrt{1 + \frac{16\ln 2}{t_{in}^2\,\Gamma_B^2}G} = \sqrt{1 + \frac{16\ln 2}{t_{in}^2\,\Gamma_B}(\Delta T_d)}.$$ (4.17)

It must be noticed that this broadening factor takes into account only gain broadening caused by the non-flat spectral amplification. For this reason, it can be predicted that a short pulse whose spectral width is considerably broader than the bandwidth of a given SBS resonance can not be delayed or advanced without a significant distortion.

4.1.2   Principle of Brillouin slow light

Figure.4.1.3 depicts the schematic principle to generate slow and fast light using stimulated Brillouin scattering in optical fibers. A basic Brillouin slow light system consists of a very simple configuration, in which a continuous-wave (CW) pump is launched into one end of an optical fiber with Brillouin shift ν_B via a fiber circulator and a signal is simultaneously introduced into the other end of the fiber. When the pump propagates through the fiber, acoustic phonons are thermally excited and scatter off photons from the pump light to produce a SBS gain resonance at frequency $-\nu_B$ below the pump frequency. The spectral FWHM width of Brillouin scattering is typically ~30 MHz for a standard single-mode fiber.
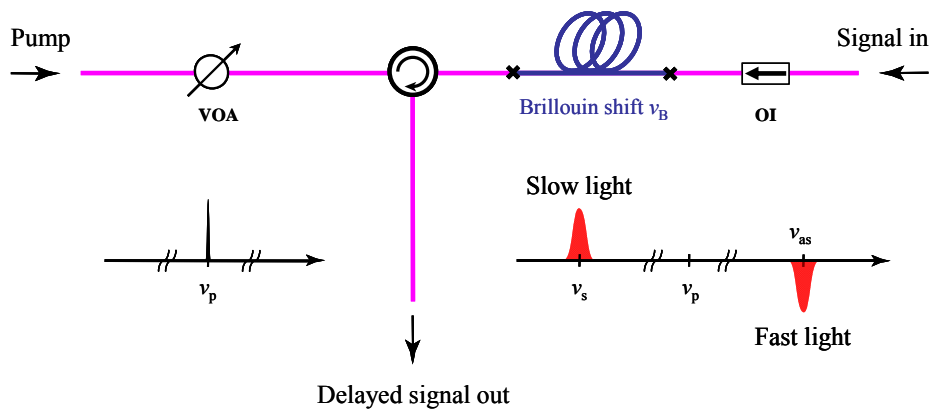
Figure 4.1.3: Schematic diagram to generate Brillouin slow and fast light in optical fibers. VOA; variable optical attenuator, OI; optical isolator.

Besides the gain band, the pump creates a SBS loss resonance with an identical bandwidth at frequency $+\nu_B$ above the pump frequency. When the signal pulse is spectrally placed at center of the gain or absorption (particular phase matching conditions) the group velocity of the signal is efficiently reduced or increased, respectively. Since the amplitudes of the resonances can be controlled with the pump power, the amount of signal delay can be precisely determined, simply by varying the pump power using an optical variable attenuator before it enters into the fiber.

Maximum time delay due to pump depletion

In a small signal regime, Brillouin slow light is usually regarded as a linear delay line, showing a linear dependence of time delay on logarithmic signal gain, as expressed in Eq.(4.10). However, the maximum time delay achievable through the delay line is in principle limited by pump depletion. When the Brillouin system undergoes the pump depletion the signal gain starts to be saturated, and it may occur that the significantly amplified signal generates another Stokes wave by self-depletion [8,9,12]. Consequently, the signal delay turns to be decoupled from the signal gain. Figure.4.1.4 demonstrates experimentally the effect of pump depletion on Brillouin slow light. To accurately determine the amount of the achieved time delay, a sinusoidally modulated wave at 1 MHz was used as a signal. The phase of the sine wave after propagating through the Brillouin gain medium was measured as a function of the pump power. According to the phase difference obtained with and without pumping, the signal delays that the signal experienced through the Brillouin
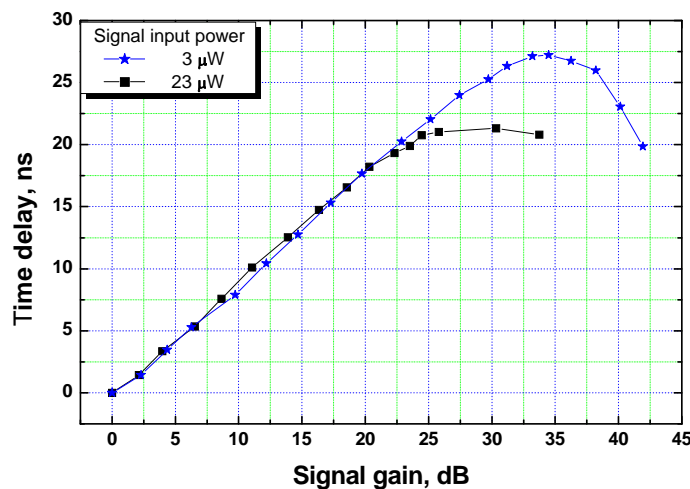
Figure 4.1.4: Measured time delays for a 1 MHz sine modulated signal as a function of the signal gain. The experiment was repeated for different signal input powers at 3 μW and 23 μW with star and square symbols, respectively.

delay line were obtained and plotted as a function of signal gain in Figure.4.1.4. This experiment was performed with two different levels of signal input power at 3 µW and 23 µW while preserving the same environmental conditions. In both cases, the signals are clearly delayed in a proportional manner with the signal gain in a small gain regime, showing good agreements with the theoretical results, and proving the linearity of the system. However, in a large gain regime, the signal delay tends to saturate with the signal gain and to even decrease for larger gains. The time delay is totally decoupled from the signal gain when the signal is so amplified that it can generate another Brillouin Stokes wave at frequency -ν_B below the signal frequency. For this reason, the maximum time delays achieved in this experiment were different for the two signals with different input powers. In consequence, for a given Brillouin slow light system, the maximum time delay can be simply extended by decreasing the signal input power. However, the maximum Brillouin gain for a signal is strictly limited, on account of amplified spontaneous Brillouin scattering. If the pump power increases so much to reach a critical level, thermally excited acoustic phonons scatter photons in the pump at the entrance of the fiber. In turn, this spontaneous Stokes wave is significantly amplified and depletes the pump, saturating energy transfer from the pump to the signal.

4.2   Broadband Brillouin slow light

To date, Brillouin slow light has been considered as a promising technique to provide all-optical buffers for future optical routers. However, the inherently narrow bandwidth of stimulated Brillouin scattering in optical fibers limits the full implementation of this system in practical applications. Actually, the bandwidth of SBS in fibers can be passively broadened by changing the intrinsic properties of the fiber such as doping concentration on the fiber core, but to an inefficient extent. The natural linewidth of SBS in a standard optical fiber is as narrow as 30 MHz due to the slow decaying feature of acoustic phonons and it limits the data rates in delay lines up to ~50 Mbit/s.

4.2.1   Arbitrary bandwidth by pump modulation

SBS gain resonance has a linear dependence on the pump frequency. It means that if a polychromatic pump wave is involved in the SBS process, each monochromatic wave of the pump can generate its own gain resonance at different frequency, corresponding to frequency matching conditions for stimulated Brillouin scattering [13,14]. The combination of each gain spectrum represents the effective Brillouin gain spectrum, so that the spectral distribution of SBS gain can be drastically engineered and shaped by simply modifying the pump power spectrum. Consequently, the effective power spectrum of SBS gain $g_{\text{eff}}(\nu)$ is expressed by the convolution of the pump power spectrum and the intrinsic Brillouin gain spectrum $g_{\text{B}}(\nu)$ [15,16]:

$$g\left(\nu_{eff}\right) = P\left(\nu\right) \otimes g_{B}\left(\nu\right), \tag{4.18}$$

where $\otimes$ denotes convolution and $P(\nu)$ is the normalized pump power spectral density (integral over spectrum is unity). For a Lorentzian shape of the pump spectrum, the effective gain curve remains Lorentzian, and its width is given by the sum of the two spectral widths $\Delta\nu_B + \Delta\nu_p$, $\Delta\nu_B$ being the spectral width of natural Brillouin gain given by Eq.(4.6) and $\Delta\nu_p$ being that of the pump power spectrum. Figure 4.2.1 depicts the spectral distribution of the effective Brillouin gain g_{eff} as a result of the convolution, showing the smoothed power

$$P(\nu) \qquad\qquad g_{\text{B}}(\nu) \qquad\qquad g_{\text{eff}}(\nu)$$
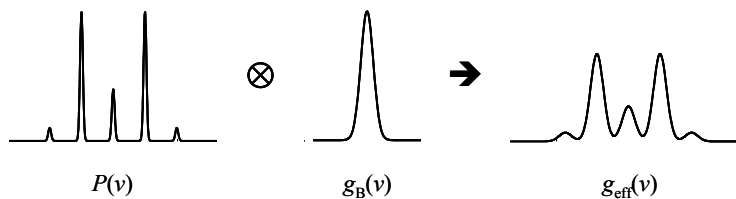
Figure 4.2.1: The effective Brillouin gain spectrum $g_{\text{eff}}(\nu)$, resulting from the convolution of the pump power spectrum and the intrinsic Brillouin gain spectrum.

spectrum of the pump. Therefore, when the pump wave is adequately modulated to broaden the pump spectrum and its spectral width is much broader than that of the natural Brillouin resonance ($\Delta v_B << \Delta v_P$), the spectral shape of the effective Brillouin gain is essentially given by the pump power spectrum.

Actually, the extension of the effective SBS bandwidth led to a tremendous improvement on signal bandwidth for Brillouin slow light, and thus Brillouin slow light turns out to be a suitable solution as a delay line in a multi-Gbits/s transmission. However, it must be pointed out that the bandwidth extension requires an increase of the pump power to maintain an equivalent delay. This comes from two facts: first, the peak level of the effective Brillouin gain is decreased proportionally to the relative spectral broadening as a result of the convolution. Second, as shown in Eq.(4.10) the amount of delay is inversely proportional to the bandwidth of the Brillouin resonance.

Broadband SBS slow light was, for the first time, experimentally demonstrated by Gonzalez-Herráez *et al.* using a randomly modulated pump source [16], as shown in
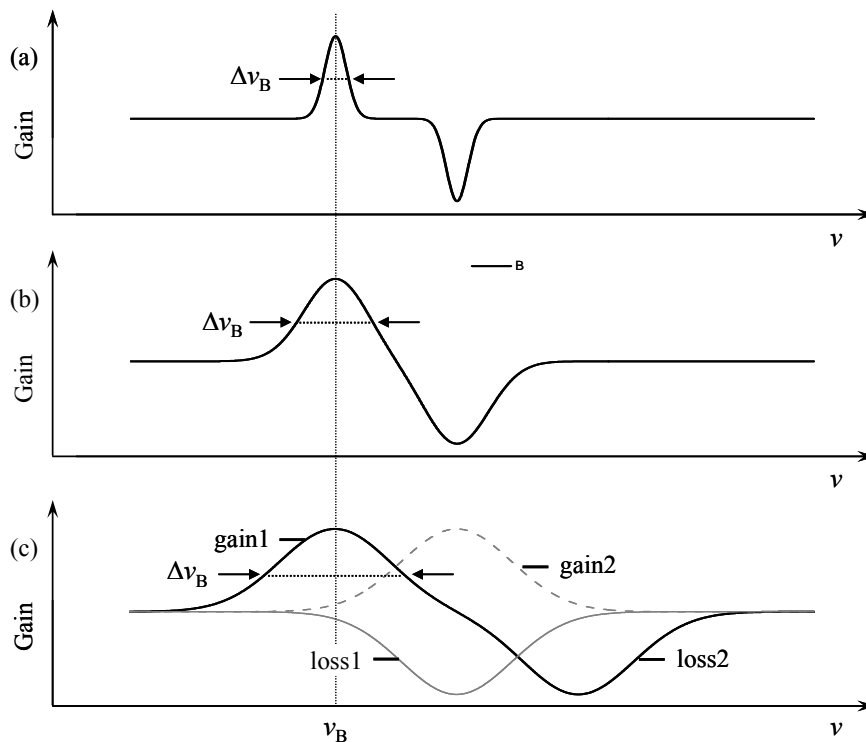
Figure 4.2.2: Effective SBS gain spectra induced by a randomly modulated pump source. (a) The first experimental demonstration of the broadband Brillouin gain resonance, and (b) the maximum achievable SBS bandwidth limited by the overlap of the SBS loss resonance. The right wing of the gain is canceled out by the identical left wing of the loss, resulting in the maximum bandwidth $\Delta v_B \approx v_B$. (c) However, when introducing another pump (pump2) the SBS gain2 generated by the pump2 compensates the SBS loss1, which allows the further extension of the effective bandwidth of the SBS gain1.

Figure.4.2.2a. By directly modulating the current of the pump laser diode, the Brillouin bandwidth was effectively enlarged up to 325 MHz at FWHM and produced successful signal delays up to 1.1-bit delays for 2.7 ns pulse through the Brillouin slow light medium. The realization of broadband signal delay in Brillouin slow light was thoroughly studied by *Zhu et al.*, showing the fundamental limitation of the maximum achievable bandwidth [17]. It is mainly due to the presence of the SBS loss resonance, as shown in Figure.4.2.2b. Simultaneous growth of the Brillouin loss resonance restricts the Brillouin gain to spread over in frequency, resulting in the maximum bandwidth up to 14 GHz. However, Song *et al*. proposed a solution to open unlimited-bandwidth Brillouin slow light by introducing another pump (pump2) positioned at frequency $+2\nu_B$ above the pump1 frequency [18]. As in a typical SBS process, two distinct pumps generate the Brillouin gains and losses at $\pm\nu_B$ with respect to the frequencies of the pumps. Here, it must be pointed out that the spectral characteristics of the loss1 and gain2 are identical in terms of the bandwidth, the peak amplitude and the center frequency except the opposite signs as shown in Figure.4.2.2c. In consequence, these two resonances completely overlap and mutually neutralize, so that it offers the possibility to overcome the fundamental limitation and to lead to further extension of SBS bandwidth. This way 25 GHz bandwidth SBS slow light was experimentally demonstrated.

4.2.2 Gain-doublet by a bichromatic pump

As discussed in the previous section, a double-frequency pump generates two separate SBS gain bands with identical spectra [19-21]. In between the resonances a spectral region with anomalous dispersion appears with a broad window, as shown in Figure.4.2.3. Therefore, a broadband fast light can be realized when the signal pulse is spectrally set in the valley between the two peaks. Moreover, the pump laser can be directly modulated by a noise
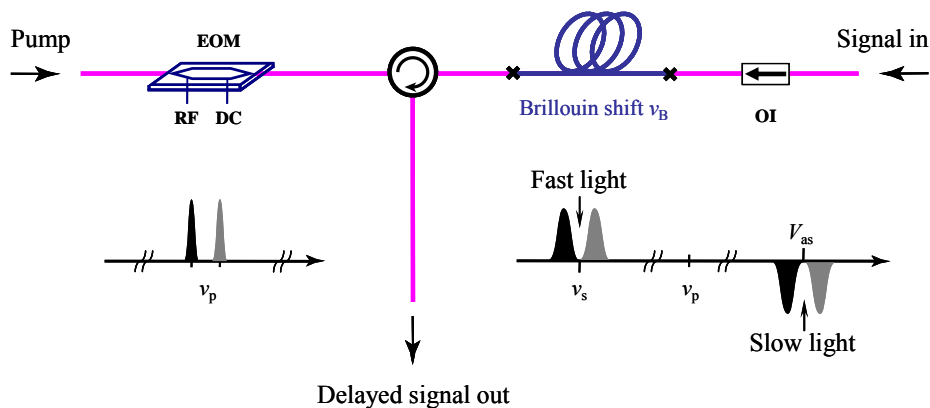
Figure 4.2.3: Schematic diagram to produce a Brillouin gain/loss doublet using a two-tone pump generated by external modulation. EOM; electro-optic modulator, OI; optical isolator.

generator to broaden its spectrum [16], so that the effective spectral profile of the Brillouin gain doublet can be modified. This way the spectral shape of the gain is precisely chosen so as to optimize the delay/distortion characteristics of the medium, which gives rise to maximum pulse advancement with low distortion and small power variation.

A conventional single mode optical fiber with a length of 2 km is used as the SBS gain medium. The Brillouin characteristics of this fiber were measured, showing a Brillouin shift of 10.8 GHz and an SBS gain bandwidth of 27 MHz. A commercial DFB laser emitting at 1532 nm is used to generate the double-frequency pump beam. The laser light is modulated by means of a Mach-Zehnder electro-optic modulator (EOM) driven with a 100 MHz tone. The DC bias voltage on the modulator is accurately adjusted, so that a full extinction of the carrier is achieved. As a consequence, the optical spectrum at the output of the modulator contains only two sidebands that create two close SBS gain resonances with identical spectra, showing a separation between central frequencies of 200 MHz with perfect inherent stability. Moreover, a direct modulation was applied to the pump laser in order to broaden its spectrum. This way an optimized spectral shape could maximize the pulse advancement with low distortion in this Brillouin slow light system. The laser current is directly modulated by use of a noise generator and its spectral width is slightly broadened to 44 MHz. This way a wideband quasi parabolic spectral distribution was obtained with a width of FWHM 160 MHz across the two peaks. The signal pulse train is produced from a distinct DFB laser operating at the same wavelength of 1532 nm. The temperature and bias current of the laser are precisely adjusted to ensure propagation in the dip between the two gain resonances. The laser is then fast-optically gated using another EOM to generate a pulse train. This pulse in turn enters into the fiber and counter-propagates with the pump.

A gain doublet is generated after propagating through the 2 km optical fiber as shown in Figure.4.2.4a. It must be pointed out that the Brillouin spectrum in the case of modulation is much smoother than in the unmodulated case. The overlapping of the two gain distributions obtained using the modulated pump gives rise to a perfect linear transition in the effective refractive index that results in fast light propagation with minimal distortion. Positioning spectrally the signal in the dip between the two gain peaks offers the further advantage to give a minimal amplification while fully maintaining the delaying effect. The FWHM pulse width used in this experiment is 6.6 ns and Figure.4.2.4b shows the non-normalized time waveforms of the pulse after passing through the fiber. The pulses are clearly advanced with respect to the pump power.

The scheme is very flexible and can match any signal bandwidth up to several GHz by simply increasing the frequency doublet separation and the spectral broadening. It makes possible a fine optimization of the distortion and the advancement by properly setting the
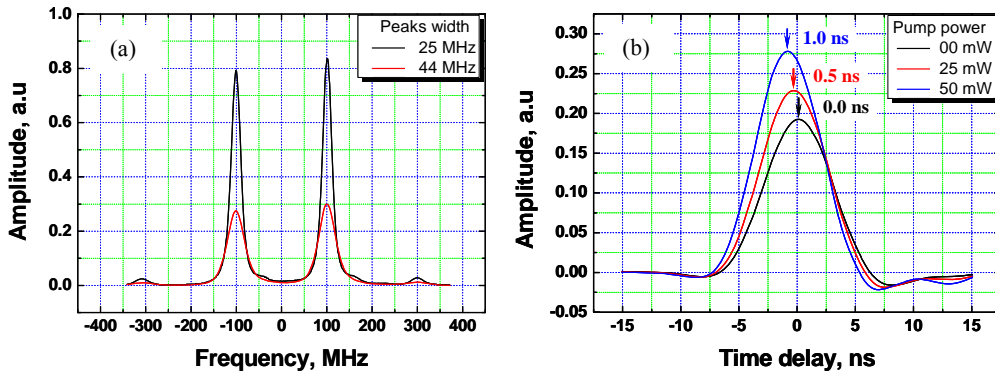
Figure 4.2.4: (a) The SBS doublet generated by the spectrally broadened bichromatic pump source. (b) The time waveforms of the signal pulses after propagating through the fiber for different pump powers, showing clear signal advancement.

amount of broadening with respect to the doublet separation. The scheme can also be applied for slow light generation in the middle of the loss doublet induced by anti-Stokes. This scheme offers an advantage that signal delays can be produced with a reduced signal amplitude change. However, a presumable limitation of maximum achievable time delay can be discussed. As the pump power increases the Brillouin gains in the two resonance peaks starts to be so large that amplified spontaneous emission present in these peaks leads rapidly to pump saturation. Consequently, the maximum pump power to generate the delays remains limited.

4.2.3   Gain-doublet by a concatenated fiber

In general, a double Brillouin gain peak can be created when the pump beam is externally modulated, and the spectral separation between the two gain/loss resonances is controlled by the modulation frequency. However, such a double resonance in optical fibers can be achieved in a passive way with a very simple experimental configuration. This system is conceptually similar to those developed previously in [19-21], but it has two crucial advantages: first, it eliminates the need of an external electro-optic modulator, drastically simplifying and optimizing the operation; second, it makes the operation in the optimum delay-bandwidth product conditions easily possible. The setup proposed here simply consists of two appended fiber segments with different Brillouin shifts [22]. This causes naturally and passively the generation of two spectrally close Brillouin gain resonances using a single pump and with no need to insert any kind of modulator, as far as the total gain after propagation through the 2 segments is considered. To optimize the delay-bandwidth product, a definite pump broadening is introduced by direct current modulation of the pump laser. The

width of the gain resonances can be adjusted this way to closely match the optimum value relating the separation of the resonances and their widths.

4.2.3.1   Direct consequence of the linearity of Brillouin amplification

The Brillouin shift is given by $v_B=2nv_a/\lambda$ where n is the refractive index, λ is the wavelength of the pump in vacuum and v_a is the acoustic velocity within the fiber. Since the Brillouin shift v_B is determined by the velocity of the acoustic grating along the fiber, it can be readily influenced by changing the mechanical properties of the fiber such as the applied strain or the ambient temperature [10,23]. In addition, the frequency shift is also affected by the doping concentrations in the core and cladding of the fiber [10]. Let us now consider two spliced segments of optical fibers with similar length but different core doping concentrations (and hence different Brillouin shifts) as shown in Figure 4.2.5. From a qualitative point of view, it can be seen that each fiber segment will have the Brillouin gain curve tuned at a different position, and hence two gain resonances will appear in the spectrum of the full system. In these conditions, anomalous dispersion appears in the middle of the gain doublet, thus signal advancement and fast light can be realized when the signal is spectrally positioned in the valley between the two peaks.
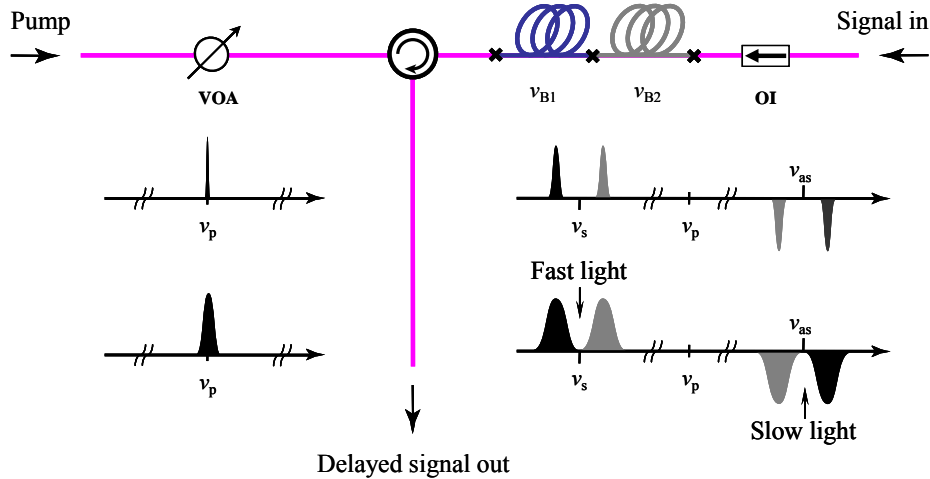
Figure 4.2.5: Principle of the single-pumped passive configuration to generate a SBS gain or loss doublet. A partial overlap of the gain spectra can be created by using a spectrally broadened pump, as shown on the bottom situation.

The evolution of the probe wave intensity along the fibers will be given by the following equation:

$$\frac{dI_s}{dz} = g_B(z, \nu) I_p I_s - \alpha I_s, \qquad (4.19)$$

where I_p and I_s are, respectively, the pump and probe intensities, α is the attenuation coefficient of the fiber and $g_B(z, \nu)$ is the natural Brillouin gain curve at each position, given by the usual Lorentzian shape:

$$g_B(z, \nu) = g_B \frac{1}{1 - 2j\left[(\nu - \nu_B(z))/\Delta \nu_B(z)\right]}, \qquad (4.20)$$

where ν is the frequency different between the pump and probe waves and $\Delta \nu_B$ is the FWHM width of the Brillouin gain spectrum. Assuming negligible pump depletion, the evolution of the counter-propagating pump intensity can be written as:

$$I_p(z) = I_o \exp(-(L - \alpha)z), \qquad (4.21)$$

where I_o is the pump intensity launched into the far end of the fiber and L the fiber length. Inserting Eq.(4.21) into Eq.(4.19), the following explicit expression is obtained for I_s at the output:

$$I_s(L) = I_s(0) \exp\left(I_0 \int_0^L \left[g_B(z, \nu) \exp(-\alpha z) - \alpha\right] dz\right). \qquad (4.22)$$

In the case depicted in Figure 4.2.4 and assuming that the Brillouin linear gain g_B is position-independent in each fiber segment, the signal intensity reads:

$$I_s(L) = I_s(0) \exp(-\alpha(L_1 + L_2)) \exp\left(I_0 \left[g_{B2}(\nu_2) L_{2eff} + g_{B1}(\nu_1) L_{1eff} \exp(-\alpha L_2)\right]\right), \quad (4.23)$$

where g_{B1} and g_{B2} are the Brillouin linear gains of each fiber segment respectively, L_1 and L_2 are the lengths of the fiber segments, and L_{1eff} and L_{2eff} are their corresponding usual nonlinear effective lengths [8]. Hence the total gain spectrum observed at the output of fiber2 is the superposition of the gain spectra accumulated along the two fibers, with different weights depending on the relative ordering of the fiber segments, their length and a possible different Brillouin linear gain. Assuming a small loss, the two resonances will show nearly identical strength for equally long fiber segments.

This way two separate gain or loss windows with arbitrary bandwidth can naturally appear in the Stokes and the anti-Stokes regime. These, in turn, can induce anomalous dispersion or normal dispersion in the middle of the gain or loss doublets, respectively. Hence, signal advancement and fast light can be observed when the signal is spectrally placed at the center of the gain doublet. On the contrary, an equivalent temporal delay or slow light can be produced as well by simply tuning the signal frequency in between the absorption

doublet. The optimum delay-bandwidth product for the two-resonance scheme is achieved for a particular ratio between the separation of the resonances and their width, thereby this relationship should be approximately $(\nu_{B1}-\nu_{B2})/\Delta\nu_B \approx 3$. In this experiment, $\nu_{B1} - \nu_{B2}$ is approximately 120 MHz, so it was necessary to broaden the spectrum of the Brillouin interaction from its characteristic value of 27 MHz to approximately 40 MHz, so that it could match the optimum delay-bandwidth product conditions. This is done simply by introducing a noise modulation of the current passing through the pump laser, in a similar way to the one developed in [16] and later extended to extreme bandwidths in [17,18].

4.2.3.2   Broadband window in the center of gain-doublet

Figure.4.2.6 depicts the schematic diagram of the experimental set-up. Two segments of different single-mode optical fibers with similar length (approximately 2 km) were appended to be used as the SBS gain medium. These two fibers are both step index single mode fibers, but constituted with a 20 % difference in core doping concentration and in the core radius. These conditions lead to a Brillouin shift difference of 120 MHz between the two Brillouin resonances while showing basically identical Brillouin bandwidth of approximately 27 MHz [10]. Two conventional temperature and current-controlled distributed-feedback (DFB) lasers operating at a wavelength of 1532 nm are used to generate the pump and probe beams, respectively. The pump laser is directly modulated using a noise generator in order to broaden its spectral linewidth through the current-frequency dithering effect. Then the pump power is amplified using an erbium doped fiber amplifier (EDFA) and the output power of the EDFA is adjusted by a variable optical attenuator (VOA) before routing via a circulator to pump the cascaded optical fibers. The spectral width of the pump is simply controlled by varying the amplitude of the noise signal. When the pump modulation is turned off, two well separated natural SBS gain/loss resonances are observed with a central frequency spacing of
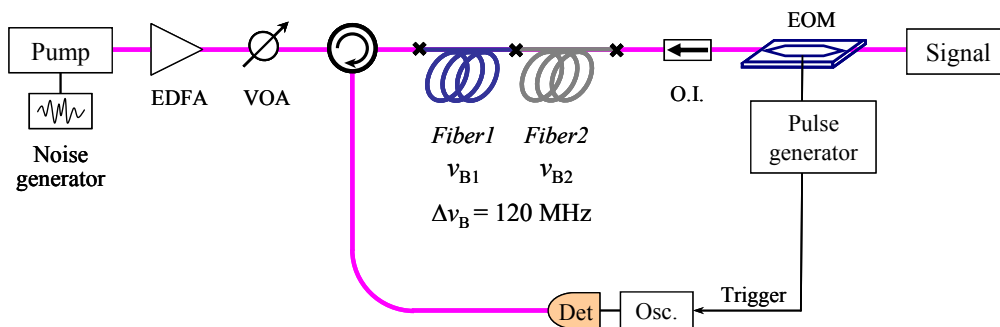
Figure 4.2.6: Experimental setup to realize fast light propagation with low distortion, by appending two optical fibers showing different Brillouin shift and a spectrally broadened pump laser. EDFA: erbium doped fiber amplifier, VOA: variable attenuator; EOM: electro-optic modulator, PC: polarization controller.
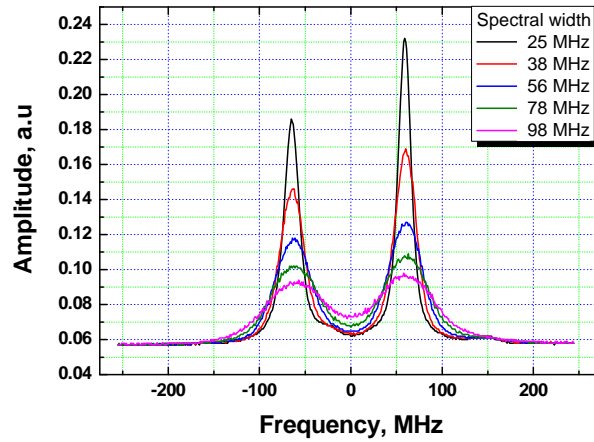
Figure 4.2.7: The spectral profiles of gain-doublets as a function of frequency for different spectral widths of the pump while the pump power is kept constant.

about 120 MHz (ν_{B1} - ν_{B2}). The frequency separation remains perfectly stable in this experiment since there is no applied strain and/or temperature variations around the fibers. It must be pointed out that a temperature variation would only cause a global spectral shift of the 2 resonances, but their frequency difference would remain constant [10].

To observe the shape of the gain doublet, the signal amplitude at the end of the concatenated fibers was measured while the signal frequency was swept linearly in time. In the proposed method, SBS gain doublets were clearly observed for different values of the pump spectral width while the pump power is kept constant, as shown in Figure 4.2.7. It is seen that the two gain peaks of Brillouin amplification are slightly mismatched mainly as a result of the pump attenuation after propagation in the first fiber segment, but the measurement experimentally confirms the adequacy of the expression in Eq.(4.23). It turns out that the global gain is given by the superposition of the individual gains in each fiber.

Signal advancements in the center of gain doublet

To generate a signal pulse train, a distinct DFB laser is optically gated using a fast external electro-optic modulator. The signal then enters the compound fiber in opposite direction to the pump beam. The frequency of the signal is precisely tuned by adjusting the temperature and current settings applied to the laser, so that the center frequency of the signal is accurately placed in the middle of the two Brillouin gain resonances. The temporal advancements and amplitudes of the signal pulses after propagating through the fiber cascade are measured and displayed on a digital oscilloscope for different values of pump power and pump linewidth. Optimized results are found when the width of the effective gain curves of the fiber segments reaches approximately 40 MHz. The FWHM width of signal pulse used in this experiment is about 25 ns and the pulses have a Gaussian-like intensity profile with
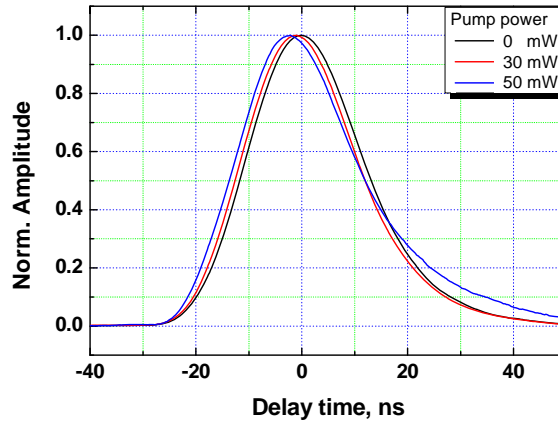
Figure 4.2.8: Normalized temporal traces of the signal pulses after propagating through the concatenated fibers for different pump powers, showing clear signal advancements.

smooth edges, though showing a somehow longer trailing edge. Figure.4.2.8 shows the normalized time waveforms of the signal pulses after experiencing the fast light propagation through concatenated fibers for different pump powers at 0 mW, 30 mW and 50 mW, respectively. It is clearly observed that signal advancement is achieved with minor signal distortion, resulting from the spectral filtering (high-pass filtering) in a fast light process. The largest signal advancement achieved is about 2 ns with 2.7 dB signal amplification at the pump power of 50 mW. Evaluating the FWHM spectral width of the valley through simple arithmetics to be approximately 80 MHz, an equivalent delay would be associated with a 6.4 dB gain or loss using a standard single resonance configuration, showing clearly that the output power variation is substantially reduced.

      To accurately determine the amount of signal advancement induced by the proposed scheme, a sinusoidally modulated light was used to avoid any biasing due to a possible
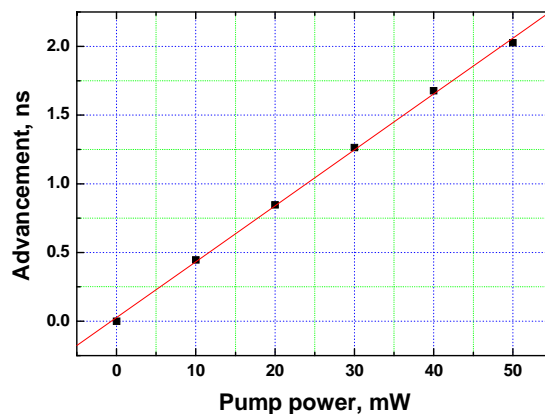
Figure 4.2.9: Signal advancements for a 1 MHz sine modulated signal as a function of the pump power in the optimum delay-bandwidth conditions (resonance separation: 120 MHz, effective resonance width 40 MHz).

distortion. This way it unambiguously measures the real time advancement without any arbitrary criterion, by measuring the phase shifts of the sine wave. Figure.4.2.9 shows the achieved time advancement as a function of the pump power, showing that the signal advancement has a linear dependence along the pump power with a slope efficiency of approximately 0.04 ns/mW.

Bandwidth limitation

Using this concept, the bandwidth limitation is determined by the spectral distance between the two Brillouin shifts. It is not difficult to find two fibers whose Brillouin shift is separated by at least 1 GHz, such as standard and dispersion compensating fibers, extending the data rate to at least 1 Gbit/s. For a larger separation, one can elongate one of these two fibers in order to shift the Brillouin frequency by 500 MHz/% [10], resulting in a further extended bandwidth. Higher resonance separation would require fibers manufactured in different materials, such as fluoride and chalcogenide glasses showing Brillouin shifts several GHz lower than silica [24,25].

Signal delays it the center of loss doublet

This technique cascading fibers can also be applied to produce slow light, by simply placing a signal spectrally in the center of a loss doublet, occurring in the Brillouin loss regime. In this condition a large normal dispersion is observed in the valley of the two peaks and the refractive group index is increased with pump power. In this case, the pump source was also spectrally broadened by means of direct modulation in order to optimize the characteristics of the slow light medium. This configuration was also experimentally tested and Figure.4.2.10 shows the obtained delays. The insert presents the measured Brillouin loss doublet created in
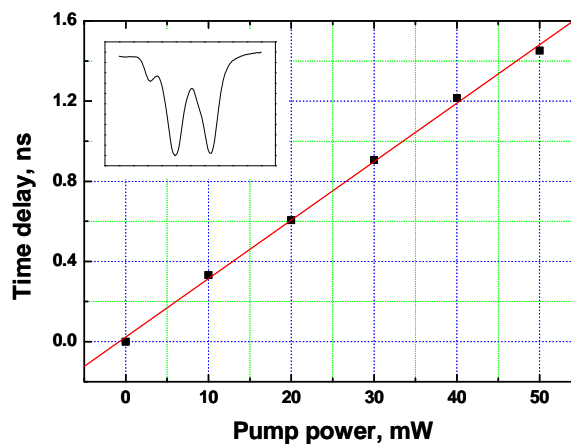
Figure 4.2.10: Signal delays for 1 MHz sine modulated signal with respect to the pump power after propagating through two different optical fibers. Insert shows the Brillouin loss doublet created in the Brillouin loss regime.

the Brillouin loss regime while the pump propagates through the cascaded fiber segments. As anticipated, a linear dependence of the time delay on the pump power was observed, showing a slope efficiency of approximately 0.03 ns/mW.

4.3 Transparent Brillouin slow light

The bandwidth of SBS-based slow light can be made arbitrarily large by actively broadening the pump spectrum using random direct current modulation of the pump laser [15-18] or by using SBS gain/loss doublets [20-22]. However, all these techniques still suffer from the drawback of a significant amplitude change associated with the delaying effect, which may be highly impairing in a real system. Indeed, the delaying effect in slow & fast light is intimately related to a narrowband gain or loss process. With typical SBS characteristics in a standard single-mode fiber, 1-bit delay for a pulse with 30 ns FWHM duration gives rise to a large 30dB pulse amplitude change [1,2,26].

This problem was soon identified as severe in the early experiments on slow & fast light using atomic absorptions, the high loss rendering the output signal unobservable for large delays. Elegant solutions were proposed to open transparency windows in narrow atomic absorption lines such as coherent population oscillation [7] and electromagnetically-induced transparency [27], this latter demonstrating large delay with much reduced amplitude change. In this thesis work, it was demonstrated that the high flexibility of SBS can offer the possibility to synthesize a gain spectral profile, so that a signal delay or advancement is achieved with an absolute null amplitude change [28]. This can be obtained by the combination of gain and loss spectral profiles with identical depth but different width, resulting in a net zero gain and a differential delaying effect. The possibility to finely tune independently the depth of each spectral profile results in a perfect compensation of gain and loss and induces an ideal electromagnetically-induced transparency window in the spectral profile. This way continuously tunable optical delays with nearly zero amplitude change are experimentally achieved using slow and fast light.

4.3.1 Principle

In Brillouin slow light, a signal propagating in a medium showing a linear gain G will experience a net amplitude change by a factor $\exp(G)$, together with an extra delay T, due to the associated group velocity change. For a SBS gain or loss process following a Lorentzian spectral distribution, linear gain G and delay T are simply given by:

$$G = g_o I_p L_{eff} \quad \text{and} \quad T = \frac{G}{2\pi\Delta\nu},$$ (4.24)

where $\Delta\nu$ is the full width at half maximum of the Lorentzian distribution, g_o is the peak value of the Brillouin gain, L_{eff} is the effective length of fiber and I_p is the intensity of the pump. The delay T thus depends on two parameters: the linear gain G (negative sign for loss)
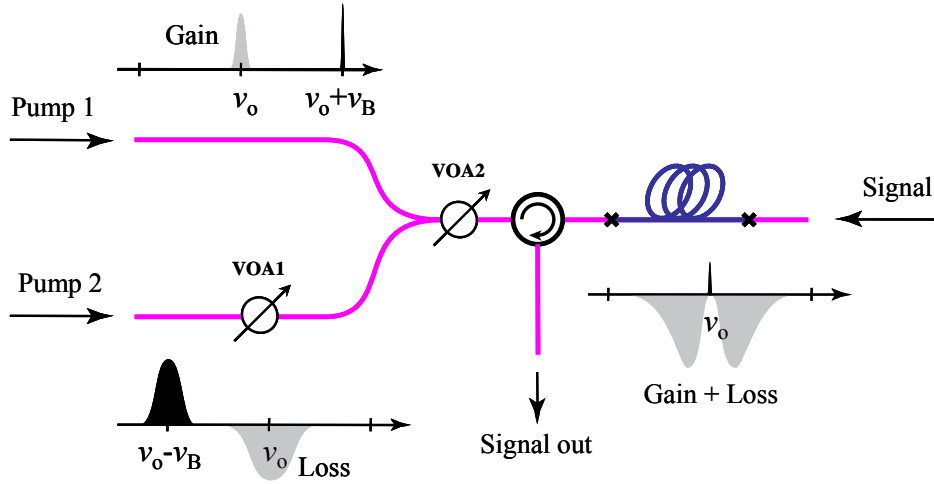
Figure 4.3.1: Principle of the experimental configuration to generate transparent spectral resonances where two distinct optical pumps were used to produce Brillouin gain and loss, respectively.

and the bandwidth Δv of the gain or loss process. Two optical resonances can be generated by two distinct pump lasers placed at a frequency $\pm v_B$ above and below the signal frequency v, respectively. Then the bandwidth of each pump Δv can be arbitrarily broadened and controlled using the scheme proposed in [16-18]. A gain is generated using SBS by placing a pump frequency at frequency $+v_B$ above the signal frequency, v_B being the Brillouin shift. On the contrary, an equivalent loss at the same frequency can be also generated simply by placing the pump frequency at frequency $-v_B$ below the signal frequency. Now let superpose in the frequency domain a SBS gain with linear gain $+G_1$ and a bandwidth Δv_1 on a SBS loss with negative linear gain (thus loss) $-G_2$ and a bandwidth Δv_2, as shown in Figure.4.3.1. In consequence, the resulting linear gain G_{net} and the overall delay T_{net} must be modified as:

$$G_{net} = G_1 - G_2 \qquad \text{and} \qquad T_{net} = \frac{G_1}{2\pi\Delta v_1} - \frac{G_2}{2\pi\Delta v_2}. \qquad (4.25a)$$

If $G_1 = G_2$, then:

$$G_{net} = 0 \qquad \text{and} \qquad T_{net} = \frac{G_{1,2}}{2\pi}\left(\frac{1}{\Delta v_1} - \frac{1}{\Delta v_2}\right). \qquad (4.25b)$$

If the bandwidths of the gain and loss spectra are substantially different, e.g. $\Delta v_2 \gg \Delta v_1$, it is possible to obtain a significant time delay T_{net} with nevertheless a zero linear gain G_{net}. The effect is fully comparable to electromagnetically-induced transparency or coherent population oscillation, in which a transparency window is opened in the middle of an absorption line. The configuration offers a large flexibility, since a spectral hole can be similarly created in a gain line by swapping the spectral positions of the broad and narrow pumps, to generate fast light. In addition the supplementary degree of freedom offered by the possibility to tune the

pumps spectral width makes possible to control to a wide extent the slope between signal delay T_{net} and the pump powers.

4.3.2   Transparency in Brillouin gain resonance

Figure.4.3.2 shows the schematic diagram of the experimental set-up used to demonstrate the transparent delays. As Brillouin gain medium, a conventional 2-km-long optical fiber was used, showing a Brillouin shift of 10.8 GHz and a spectral width of 27 MHz. Pump 1 was kept unmodulated and spectrally placed at a frequency $v+v_B$ above the signal at frequency v, so that the frequency difference between Pump 1 and signal is equal to the Brillouin frequency shift v_B. To secure a high stability of the frequency difference between Pump 1 and signal, these two optical waves were generated through modulation of the CW light from one commercial DFB laser diode emitting at a wavelength of 1532 nm. This is achieved by modulating the laser light using an electro-optic Mach-Zehnder intensity modulator (EOM) at half the Brillouin frequency shift (5.4 GHz). The DC bias voltage on the modulator is adequately set to achieve a full extinction of the carrier. Therefore, the optical spectrum at the output of the modulator contains only the two modulation sidebands, exactly separated by the Brillouin frequency shift of 10.8 GHz. The higher frequency component is then amplified by a first Erbium-doped fiber amplifier (EDFA) to a maximum power of 17 dBm. On the contrary, the lower frequency sideband was modulated either sinusoidally or as a signal pulse train using a second EOM. This technique secures a total absence of spectral drift between Pump 1 and the signal, together with a perfect centering of the signal in the gain spectrum [10]. Pump2 was generated from a distinct DFB laser diode, operating at the same 1532 nm wavelength. This laser was directly modulated by superposing the random noise signal on the
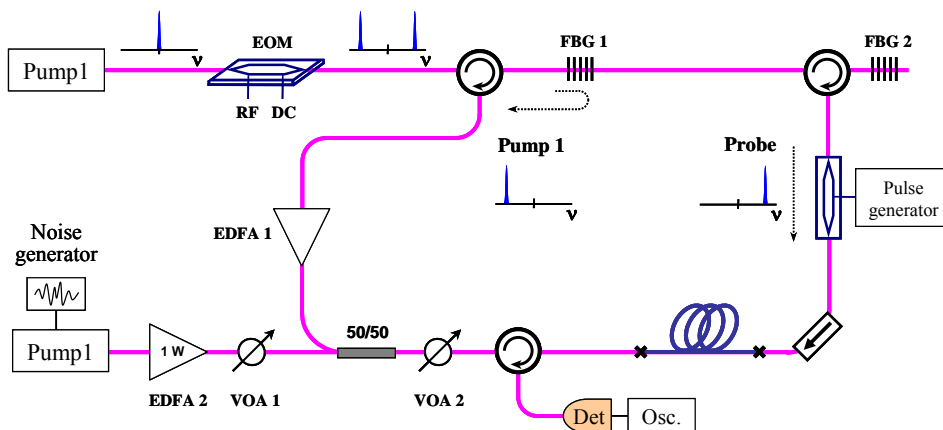
Figure 4.3.2: Experimental setup to realize transparent slow light via optical fibers, by spectrally superposing a gain spectrum over a loss spectrum, generated from distinct sources showing different linewidths. VOA: variable attenuator; BPF: band-pass filter; FBG: fiber Bragg grating; EDFA: Erbium-doped fiber amplifier.

DC bias current in order to substantially broaden its optical spectrum through the current-to-frequency dithering effect. This way the linewidth of pump2 Δv_2 could be obtained up to 312 MHz. The center frequency of pump2 was set below the signal frequency, at a frequency of $v\text{-}v_B$, so that this pump generates a broadband loss through SBS at the signal frequency v, following the principle sketched in Figure 4.3.2.

Since the spectral width Δv_2 is about 12-fold broader than the natural Brillouin linewidth Δv_1 induced by the pump1 the frequency setting of pump2 is less critical and just requires a fine tuning by adjusting the DC bias current and temperature applied to the laser. The broadened pump was strongly boosted using a high power EDFA with a saturation power of ~1 W since the pump2 power must be larger than the pump1 power by a factor identical to the broadening factor $\Delta v_2 / \Delta v_1$ to make the peak gain/loss generated by the two pumps identical [16]. A variable optical attenuator (VOA1) was used to adjust the pump2 power to perfectly match G_2 to G_1. This adjustment was carried out by substituting to the signal the light from a frequency-sweeping laser and by monitoring the signal amplitude at the fiber output. G_1 and G_2 are equal when the signal amplitude at the peak of the narrow band gain is equal to the amplitude of the signal far away from the broadband loss spectrum, as shown in Figure.4.3.3. It clearly demonstrates that the obtained spectral transmission profile of the probe after propagating through the test fiber is very similar to an ideal EIT profile. It must be pointed out that the procedure using the frequency sweeping signal is also useful to center the gain and loss spectra generated by the two pumps. It illustrates that a good compensation of gain and loss can be obtained by using two optical pumps via stimulated Brillouin scattering in optical fibers. The light from the two pumps is combined through a 3dB directional coupler and their state of polarization is aligned to get a stable and evenly distributed double SBS interaction along the fiber. The VOA 2 is then used to vary
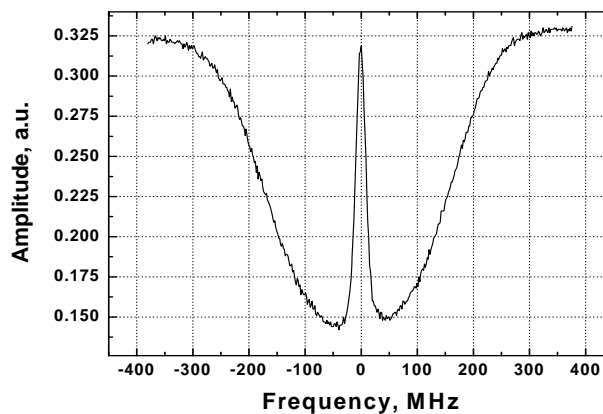
Figure 4.3.3: Variation of the amplitude of the probe signal as a function of frequency after propagation through a 2-km fiber, showing the achievement of a well-compensated SBS gain/loss profile.

simultaneously and identically the power of the two pumps, so that the gain/loss compensation is maintained at any pumping level.

4.3.3 Signal delay with small amplitude change

In typical SBS slow light, the temporal delay induced by the slow & fast light effect was normally measured as a function of the SBS gain/loss, as a consequence of the direct and simple relationship between these two quantities in Eq.(4.10). However, by essence it turns out to be conceptually inappropriate in this experimental configuration since only a small residual gain/loss of the signal is observed as a result of the peak gain compensation. Hence the delays were rather evaluated as a function of the pump1 power while the pump2 power varies proportionally. Since the gain G_1 is proportional to the pump1 power, a linear relation must also be observed between the induced delays and this power. It also makes comparisons possible with the standard technique by simply measuring delays using the same procedure after turning off the pump2.

Delays and amplitudes of signal pulse after propagation through a 2-km standard single-mode fiber were precisely measured while incrementing the pump1 power from 0 mW to 19 mW. The duration of signal pulse used in this experiment was 50 ns FWHM and typical traces are shown in Figure.4.3.4. It must be pointed out that the signal pulses are shown with non-normalization using a fixed scope vertical scale, demonstrating a moderate amplitude change due to a slight mismatch between peak gain and loss. The effect of the mismatch logically increases for higher pump levels and a perfect balance would experimentally require a dedicated feedback control circuit that was not implemented for this simple demonstration of the experimental principle. The effect of a negative mismatch was also observed as
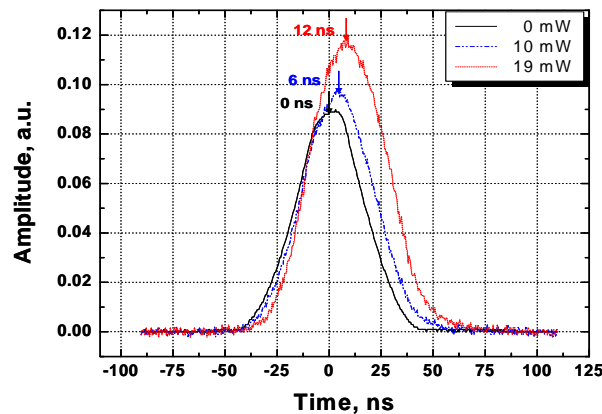
Figure 4.3.4: Time traces of signals after propagation in a fiber with a transparent profile for different pump1 powers, showing a clear delay and a minor amplitude change. Traces are non-normalized and measured in unmodified experimental conditions. Arrows indicate the pulses peak position.

decreasing pulse amplitudes for increasing pump levels, with no noticeable effect on the observed delays. An equivalent maximum delay using the non-compensated standard technique would result in a 12 dB amplitude change using the ~1 ns/dB delay versus gain relationship commonly observed using SBS in standard single mode fibers [1]. However, the possible strong noise, caused by the high power erbium doped amplifying process, should be considered for practical applications. Also, two-fold SBS processes could generate significant spontaneous noise, which would be imposed onto the signal.

Since the signal experiences non-negligible distortion and pulse broadening, a sinusoidally modulated light was used to precisely determine the delays induced by the group velocity change. This way it makes possible to unambiguously obtain the real delays induced by the group velocity change without applying any arbitrary criterion, by measuring the difference between the phases of the sine modulation with and without the pump power. Delays and amplitudes for a 1 MHz sine modulated signal were measured for different pump levels, as shown in Figure.4.3.5. It clearly demonstrates that the delaying effect is maintained and fully comparable in magnitude to those obtained using the standard method [1], while observing a maximum amplitude change of 0.9 dB that can be reasonably considered as a flat response. The largest induced delay was limited by the onset of the amplified spontaneous Brillouin scattering generated by the spectrally broadened pump2. The observed threshold is well below the theoretical expectation, when taking into account the broadening effect. This is certainly due to a residual coherence in the spectral properties of the pump2, the noise-generated broadening effect being not perfectly optimized in terms of frequency and amplitude to result in a fully chaotic linewidth enhancement. Modifications of the noise generator parameters towards optimization raised significantly Brillouin threshold for the pump2 and this strongly supported the validity of the explanation. A full and careful
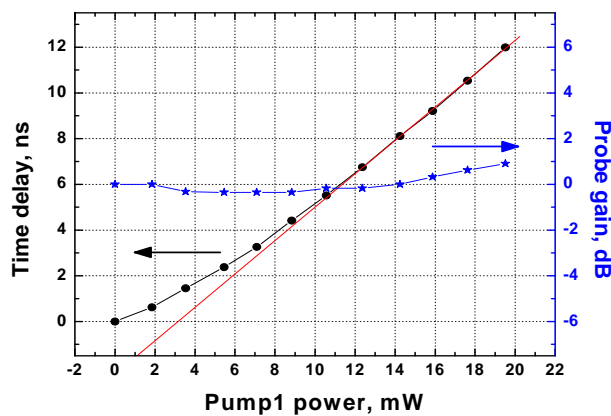
Figure 4.3.5: Delays and amplitudes for a 1 MHz sine modulated signal as a function of the pump1 power in a transparent slow light configuration. The pump2 power is 12 times larger than the pump1 power.

optimization of the noise-generated broadening would lead to delays comparable to those obtained with no gain compensation.

The broadband SBS gain induced by the spectrally broadened pump2 can be replaced by any broadband amplification process based on another type of interactions such as Raman scattering and parametric amplification, but also using doped fibers. However, the operation of the delay line would be in this case less convenient since the signal and the SBS pump1 will both be subject to the bidirectional broadband gain. This demonstrates the key role and the excellent suitability of SBS for the generation of slow & fast light in optical fibers due to its directivity and its unique narrowband and flexible spectral property.

Effect of spectrally broadened pump on efficiency

The effect of gain compensation results in a decrease of the slope efficiency between the pump1 power and delay by a factor $(\Delta v_2 - \Delta v_1)/\Delta v_2$ when compared to the standard technique. The validity of the model could be verified by measuring the slope efficiencies with the pump2 turned on (gain compensation) and off (no compensation) and comparing with the expected slope reduction as calculated from the gain linewidths. The slope efficiency deduced from the linear fit was 0.709 ns/mW when the pump2 is on and rises to 0.776 ns/mW when the pump2 is off. Experimentally the slope is thus reduced by a factor 0.913. Using the measured broadened linewidth Δv_2=312 MHz, such a slope reduction would be obtained after calculation with a gain linewidth Δv_1=27 MHz, that is equal to the Brillouin natural gain linewidth in standard single mode fibers. This shows the perfect adequacy between the simple model and the experimental results.

Polarization effect on SBS slow light

In Figure 4.3.5, the relationship between delay and pump power is not perfectly linear and deviates from the linear fit in particular for low pump levels. This effect results from the residual random birefringence in the fiber that makes the counter-propagating probe and pump waves mostly interacting with unmatched polarization, thus the efficiency of SBS decreases. However, it turns out that this penalizing effect is substantially reduced for high gain since the Brillouin interaction transfers photons from the pump to the probe. These coherently transferred photons keep the polarization property of the pump, so that they pull the probe polarization state towards the pump polarization, resulting in a better polarization matching [29,30].
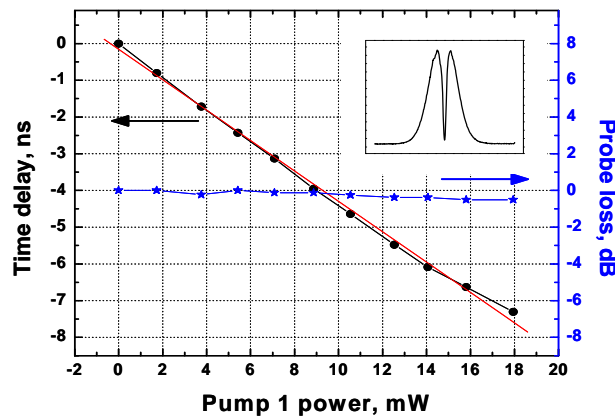
Figure 4.3.6: Advancements and amplitudes for a 1 MHz sine modulated signal as a function of pump1 power in a transparent fast light configuration. Power of Pump2 is 8 times larger than power of Pump 1. The insert shows the measured SBS gain/loss profile in this configuration.

Signal advancements with negligible amplitude change

The gain compensation technique can also be applied to generate fast light, by simply swapping the frequency positions of the pump1 and pump2. In such environmental conditions, the broadened pump generates a gain at the signal frequency and the narrow pump burns a hole at the center of the gain spectrum. This configuration was also experimentally tested and resulted in a successful fast light propagation with nearly zero loss, as shown in Figure.4.3.6. A larger pump1 power could be used through a smaller broadening of the pump2 ($\Delta\nu_2$=210 MHz) that resulted in a better coherence reduction. The gain and loss compensation is nearly perfect in this case, but a substantial slope efficiency reduction was observed when compared to slow light, by nearly a factor 2 down to -0.414 ns/mW. It can only be partly explained by a smaller broadening of Pump2 that would result in a 10 % reduction of the slope efficiency. The explanation certainly lies in the interplay between line broadening through the random frequency dithering of the pump2 and polarization dragging effect: as a result of the frequency dithering Brillouin gain - and thus polarization dragging of the probe - occurs only at limited and random locations, so that most of the time the probe polarization is only subject to random birefringence. Matching between pump and probe polarizations is thus poorly improved even for high gain and the slope efficiency is reduced substantially, accordingly. This explains the asymmetric behavior between slow and fast light and this observation is certainly an important contribution for guiding the future design of fiber optics delay line based on spectrally-broadened SBS.

4.4   Optimized shape of signal for Brillouin slow light

Since the first demonstration of Brillouin slow light, many solutions towards the objective of a real implementation solutions were proposed to enlarge the bandwidth of the Brillouin resonance [16-18] and to optimize its dispersion characteristics [31-33]. All these experiments modified the Brillouin spectrum by slightly modulating the current applied to the pump laser, so that the effective gain spectrum is broadened to contain the entire signal spectrum. Although such SBS slow light systems appear to be very promising timing tools, they clearly need a set of optimizations to get the maximum benefits for a given bandwidth, since a broader resonance results in a lower delaying efficiency that can be only compensated at the expense of a higher pump power.

In this section, an optimization based on the time-domain intensity profile of a signal will be introduced in order to modify its spectrum for a best fit within the Brillouin gain bandwidth. It must be noticed that this approach in the context of a delay line is mainly for tunable timing purposes and not for the transmission of information through a continuous data stream. In this particular case, it is assumed that a train of isolated pulses is transmitted to carry the timing information that is extracted when the pulse amplitude crosses a preset level, typically 50 % of its peak amplitude. Clearly the scope of this study is definitely more oriented to metrology applications than the telecommunication domain. Since the overlap between adjacent pulses is inexistent, the issues related to inter-symbol interferences can be ignored. In addition, the relevant quantities to characterize the pulse for this class of applications will be the position of its peak (or front edge) and its FWHM temporal and spectral widths. This method is therefore distinct from a recent complete study [34], in which the signal shape is optimized for a continuous data stream for communication applications. In this latter case relevant quantities characterizing the signal are different and in particular RMS temporal and spectral widths have to be considered. This leads to optimal signal shapes substantially different in the two studies.

4.4.1   Optimization of the signal spectral width

The relationship between a pulse shape and its optical spectrum can be characterized by its time-bandwidth product K. This parameter is essentially given by the product of Δv and Δt, here defined as the full widths at half maximum (FWHM) of the spectral and temporal distributions, respectively. Table.1 shows the values of K for various pulse shapes in the case of transform-limited pulses [11]. It turns out that, for a given pulse duration, its spectral width can be substantially modified by properly shaping the pulse envelope. Thereby a significant

Shape	$\varepsilon(t)$	K
Gaussian function	$exp[-(t/t_0)^2/2]$	0.441
Exponential function	$exp[-(t/t_0)/2]$	0.140
Rectangular function	$u(t+t_0/2) - u(t-t_0/2)$	0.892
Lorentzian function	$[1+(t/t_0)^2]^{-1}$	0.142

Table 4.1: Values of the FWHM time-bandwidth product K for various pulse shapes. $u(t)$ is the unit step function at the origin..

narrowing of the effective spectral width in terms of FWHM can be obtained. The signals can therefore be spectrally well confined in the center of the Brillouin resonance where a perfect linear transition in the effective refractive index is observed. As a result, larger delays of the pulse peak or front edge could be achieved through Brillouin slow light systems.

In a simulation test, three different pulse intensity profiles were defined with identical FWHM duration, showing successively exponential, Gaussian and rectangular temporal distributions. The spectra of the pulses were numerically obtained through a Fourier transform of the pulse waveforms, as shown in Figure.4.4.1. It is clearly observed that as anticipated the different pulses show different spectral widths. Then, to demonstrate the validity of the proposed approach, the three different pulse shapes were experimentally generated with identical 14 ns FWHM duration by using an arbitrary waveform generator. The spectral widths of the differently shaped pulses were measured by the typical delayed self-homodyne method based on a Mach-Zehnder interferometer in which one arm contains a delay line to break the coherence of the analyzed beat signal. The measured pulse spectra show a good agreement with the numerical predictions, clearly illustrating the spectral width dependence on the pulse time-domain waveform. Unavoidable small deviations remain in the
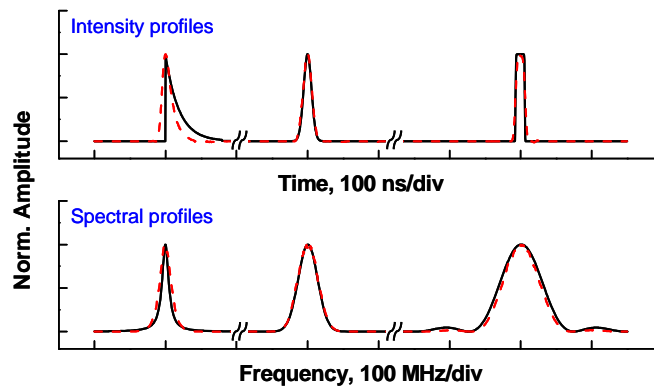
Figure 4.4.1: Signal pulses under study (exponential, Gaussian and rectangular time distribution from left to right with corresponding spectra on bottom chart). Numerical and measured results are shown in solid and dashed lines, respectively.

spectral width, which are induced by the smoothed rising and falling edges of the pulses. Among these intensity profiles, the exponential pulse offers the narrowest FWHM spectral width of 18 MHz, while the Gaussian and Rectangular pulses show a measured spectral width of 35 MHz and 58 MHz, respectively.

4.4.2   Enhanced signal delay

Figure.4.2.2 depicts the schematic diagram of the experimental setup. As a Brillouin gain medium a 1-km-long standard single mode fiber was used. The Brillouin characteristics of this fiber were measured, showing a Brillouin shift of 10.8 GHz and an SBS gain bandwidth of 27 MHz. The experimental validation has been realized using the natural Brillouin gain without engineered broadening, since the bandwidth issues are less critical for timing applications and the gain spectral characteristics are fully stable and accurately known. However, the approach can be extrapolated to any gain spectral distribution, in particular when the spectrum is synthetically broadened.

A commercial distributed feedback (DFB) laser diode operating at 1532 nm was used as a light source and its output was modulated through an electro-optic Mach-Zehnder intensity modulator at half the Brillouin frequency shift to generate two first-order sidebands. The DC bias on the modulator was well set, so that the carrier was completely suppressed and only two sidebands are present at the output. Each sideband was then filtered and directed to a distinct fiber using a set of 2 fiber Bragg gratings associated with 2 circulators. The higher frequency sideband was amplified using an Erbium doped fiber amplifier (EDFA) to play the role of the Brillouin pump and its power was precisely controlled by a variable optical
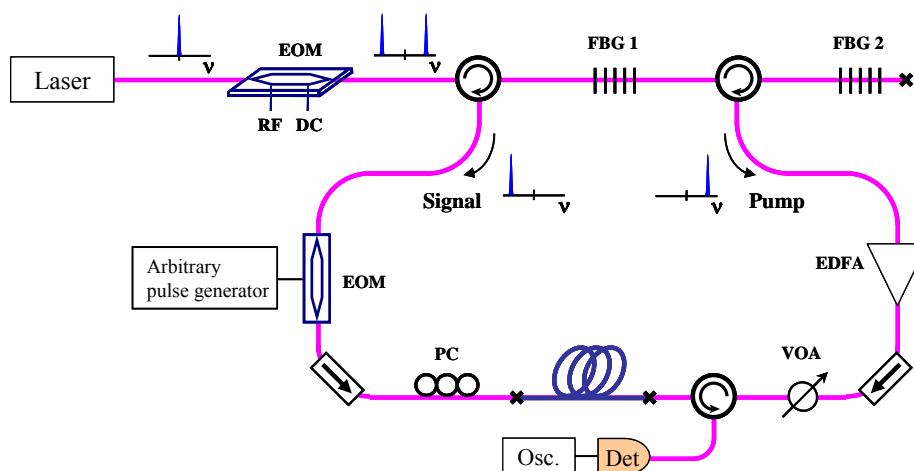
Figure 4.4.2: Experimental setup to demonstrate the effect of the signal shape on the time delay. FBG: fiber Bragg grating, EDFA: erbium doped fiber amplifier, VOA: variable optical attenuator, PC: polarization controller.

attenuator. The lower frequency sideband was launched into another external modulator to properly shape the signal pulse, so that trains of signal pulses with distinct intensity profiles are generated showing identical 14 ns FWHM pulse duration.

To observe the delaying effect induced by the Brillouin gain, the pump power was varied from zero to 50 mW. The temporally delayed signals after propagation through the fiber were measured as a function of the pump power using a fast detector and displayed on a digital oscilloscope. Figure.4.4.3 shows the normalized time waveforms of the signal pulses with different pulse envelope for a set of fixed pump levels: 0 mW, 20 mW, 35 mW and 50 mW. In all situations the signals experience more delay for an increasing pump power, as expected from a SBS slow-light system, but it is clearly observed that the exponentially shaped pulse achieves the largest delay. When rectangular and Gaussian pulses exit the fiber, significant distortion is imposed onto the signal pulses and a reduced time delay is observed, since these two pulses suffer by essence a stronger spectral filtering effect by the narrower Brillouin resonance.
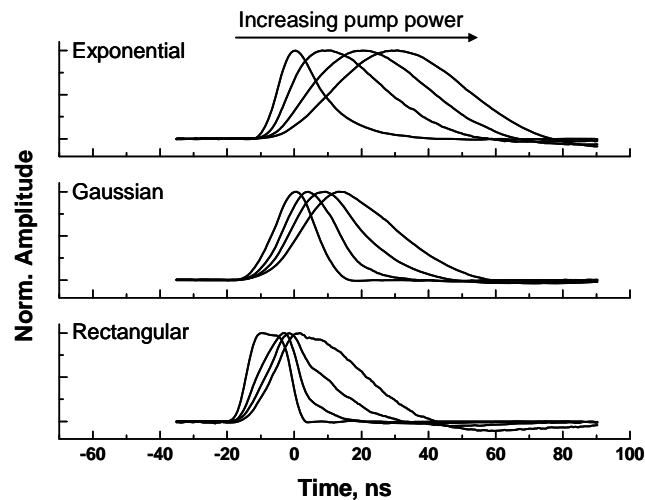
Figure 4.4.3: Normalized time traces of the signal pulses with pump power at 0 mW, 20 mW, 35 mW and 50 mW, showing a clear time-delay dependence on the signal shape.

In previous works [1,2,26], temporal delays induced by SBS were evaluated in terms of Brillouin gain. But, in this experiment the signal delays are rather plotted as a function of the pump power for a flat comparison between the time delays obtained in the three different cases, as shown in Figure 4.4.3, the effective gain value being substantially different for different pulse shapes. To evaluate the amount of time delay, the peak position of the signal pulse was used. It is interesting to immediately point out that, for a given pump power and fixed input pulse duration, the obtained time delay is larger with a reduced distortion when the pulse shaping results in a smaller FWHM spectral width. However, the signal delaying
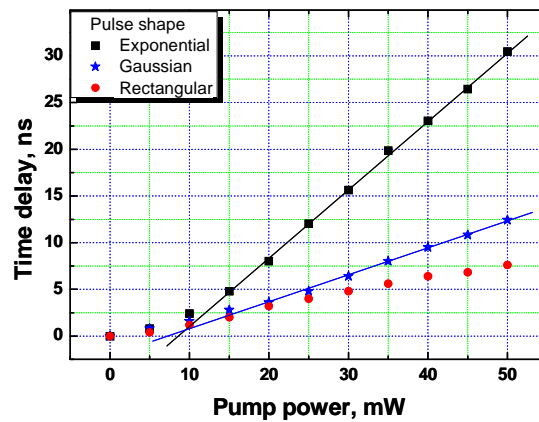
Figure 4.4.4: Comparison of the temporal delays as a function of the pump power for the signal pulses with three different shapes.

remains unavoidably accompanied by a pulse broadening as a result of the spectral filtering (low-pass filter) in the slow light process. The largest time delay achieved by the exponential pulse is about 31 ns (or a fractional delay of 2.1) with a broadening factor of 3. For comparison it was calculated that in a typical SBS slow light system an equivalent delay for 14 ns FWHM Gaussian pulses would result in a broadening factor of 3.4. The advantage may look minor in terms of broadening, but the main benefit of the optimized pulse shape turns out to be the following: the signal delay shows a linear dependence on the pump power with a slope efficiency of 0.73 ns/mW for the exponential pulse. In the Gaussian case, this slope efficiency is observed to be 0.28 ns/mW, resulting in a 2.5 times decrease when compared to the exponential pulse.

It must be noticed that this description is justified when the FWHM widths of the time and spectral distributions are considered, the product of the RMS time and spectral widths keeping of course minimized for Gaussian pulses. This approach is justified for timing applications when a transition threshold is defined to determine the pulse arrival time. It must also be pointed out that the exponential pulse also offers another spectral optimization in the sense that its spectral distribution is Lorentzian as the natural Brillouin gain spectrum. This also indicates that a particular pulse shape is certainly optimal for a given gain spectral shape.

4.5 Reduced broadening Signal delay in Brillouin slow light

In order to overcome the trade-off relation between signal delay and signal distortion, several linear slow light schemes have been theoretically and experimentally investigated [16,22,31-39]. In particular, tailoring the shape of the spectral resonance to optimize the dispersive properties in the material could partially reduce the induced distortion while keeping the fractional delay. However, this approach could not fully eliminate the strong distortion, thus the maximum achievable signal delay remains limited to a few pulse durations. In parallel, the limits of delay and distortion have been explored for several kinds of slow light systems [40-42], and recent studies seem to indicate that linear slow light systems will never be candidates for making distortionless (or zero-broadening) slow light systems [43]. Nevertheless, the vast majority of the slow light systems proposed up to now in the literature can be considered linear in terms of the signal propagation. Therefore, a general scheme to achieve slow light without distortion for any arbitrary fractional delay is still under investigation, but the results of these papers seem to indicate that nonlinear elements should be essential for this task. In a recent work [44], a possible solution to mitigate the broadening effect was put forward using a depleted (therefore nonlinear) Brillouin amplifier as slow light system. Even though the signal broadening issue was improved, the compensation of the broadening was certainly not complete, and the saturation in the amplification had the unwanted outcome of reducing also the delaying effect.

In this thesis work, a new configuration to compensate the inherent signal broadening in all slow light systems was proposed and experimentally demonstrated. The demonstration is based on an all-fiber setup, rendering the system very attractive for future applications in the field of optical communications. It makes use of the combination of a conventional SBS linear slow light system and a nonlinear fiber loop mirror (NOLM) as broadening compensation element. The NOLM plays the role equivalent to a fast saturable absorber. In the Brillouin slow light segment, the signal pulse experiences both a time delay and the usual broadening. Then this delayed signal is delivered into the nonlinear fiber loop mirror, where it experiences a compression as a result of the nonlinear transmission (the peak of the signal experiences a larger transmission than both tailing parts). In this experiment, a fractional delay above unity could be effectively achieved with no signal broadening in the SBS slow light delay line. Additionally, this regeneration element can eliminate most of the background noise introduced by the Brillouin amplifier when the signal is "off", therefore improving the contrast between the ones and the zeros in a transmission system. There is in principle no limitation to cascade this system and achieve large fractional delays with very minor distortion.

4.5.1 Compensation of signal distortion

Stimulated Brillouin scattering in optical fibers is usually described as a nonlinear interaction between two counter-propagating waves, a strong pump and a weak probe wave. However, it can be shown that the effect of the amplification/loss on the signal wave can be treated as a linear effect (in absence of pump depletion) and therefore modeled through a linear transfer-function approach [43]. Thus, as a linear low-pass system, the signal pulse is broadened and this limits the maximum delay that can be achieved with a reasonable distortion. To avoid this effect, one can use a nonlinear regeneration element at the output. In the time domain, this nonlinear element should sharpen the shape of the pulse. In the frequency domain, the role of this element will be to broaden the signal spectrum and re-generate the frequencies that have been filtered out by the slow light element.

The experimental scheme comprises two basic building blocks: an SBS slow light delay line and a nonlinear optical loop mirror (NOLM) that acts as a regeneration element. Upon propagation through the SBS slow light line, the signal essentially experiences distortion. In the proposed configuration, the NOLM acts similarly to a fast saturable absorber. The transmission of the NOLM is larger for higher input powers and decays rapidly as the input power is reduced. When a signal enters into the compensation element, the peak of the signal experiences a larger transmission coefficient than the wings, leading to a sharpening in its shape. By using only the input power to the NOLM as control variable, one can also accommodate the sharpening of the signal in the NOLM, and potentially one can discuss on achieving a complete regeneration of the signal. This way the system can allow the delayed signal to have effectively no broadening at the output of the nonlinear element for large delays in the SBS delay line.

The NOLM basically consists of a Sagnac loop, in which an attenuator is placed at one loop end and thus introduces a large power imbalance between the clock-wise and counter-clockwise fields while they propagate in the loop. A polarization controller was used in the loop to match the states of polarization (SOP) so as to maximize the visibility of the interference and secure a total absence of transmission at low powers. In linear operation, the Sagnac mirror acts as a perfect mirror. The input signal is split by a directional coupler into two counter-propagating electric fields, as shown in Figure.4.5.1. The two fields are in turn re-combined at the coupler after propagation through the optical fiber loop. Since they travel the same path but opposite direction, the optical path length is identical to both propagating fields, resulting in the same linear phase shift. As a result, the input signal is totally reflected into the input port. Therefore, for low input powers the loop acts as a perfect mirror, and no light exits through the output port. In the high power regime, however, the refractive index of
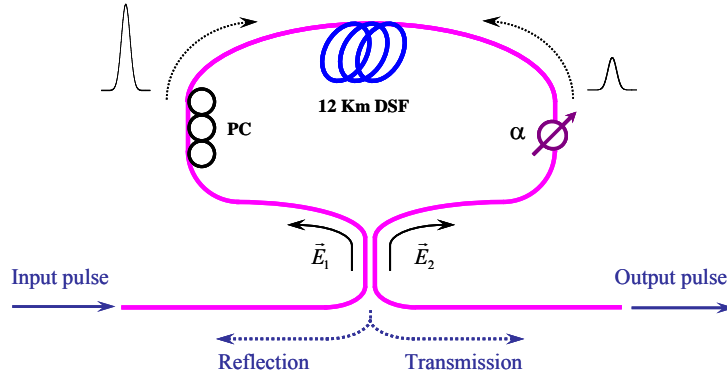
Figure 4.5.1: Schematic diagram of an attenuation imbalanced nonlinear optical fiber loop to compress the shape of signal. E_1 and E_2 present clock and counter-clock wise electric fields of pulses, respectively. DSF; dispersion shifted fiber, PC; polarization controller and α; an attenuation factor.

the fiber depends on the light intensity. This means that the imbalance in the optical power of the two arms caused by the attenuator will lead to a difference in the effective optical path length for the clockwise and counter-clockwise signals [45].

In this experiment, the input light was equally split as required for maximum contrast, but 1-dB attenuation was set for the counter-clock wise field prior to its propagation through the loop using a variable optical attenuator. In addition, a 12-km dispersion shifted fiber (DSF) was used as a nonlinear medium over which the two fields experience a differential phase shift, mainly caused by Kerr effect. The clock and counter-clockwise electric fields E_1 and E_2 before entering the DSF can be written as:

$$E_1 = \sqrt{1/2}\, A_{in} \qquad \text{and} \qquad E_2 = i\sqrt{\alpha/2}\, A_{in}, \tag{4.26}$$

where A_{in} presents the amplitude of the input electric field and α is the attenuation factor for the E_2. Upon recombination in the coupler, the signal at the output port will depend on the input power and the power imbalance between the two arms. In this circumstance, the electric fields after a single pass via the loop are given by the expressions:

$$E'_{1out} = \frac{\sqrt{\alpha}}{2} A_{in} \exp\left[i\frac{1}{2}\varphi\right] \qquad \text{and} \qquad E'_{2out} = -\frac{\sqrt{\alpha}}{2} A_{in} \exp\left[i\frac{\alpha}{2}\varphi\right] \tag{4.27}$$

The nonlinear phase shift φ is defined as $\varphi = \gamma P_o L$ where γ is the nonlinear coefficient, P_o is the optical power of the light at the input port and L is the fiber length. Therefore, the transmission coefficient T can be written as:

$$T = \frac{\alpha}{2}\left[1 - \cos\left(\frac{1-\alpha}{2}\varphi\right)\right] \simeq \frac{\alpha(1-\alpha)^2}{16}\varphi^2 \qquad \text{for } \varphi \ll 1, \tag{4.28}$$

and the system turns out to be equivalent to a saturable absorber: the transmission grows for higher input powers, with a quadratic dependence on the power for small accumulated nonlinear phase shifts. Since the power in the peak of the signal is larger than in the wings, the output pulse will be sharper than that at the input, resulting in pulse compression [46]. However, due to the nonlinear response of the phase shift induced by self-phase modulation across the signal, a negative frequency chirp will be imposed through the signal. It shows presumably that the delayed signal can be further compressed, probably to a very small extent, by placing a dispersive medium with anomalous dispersion, such as dispersion compensated fiber.

4.5.2 Nearly non-broadened signal delay

The schematic diagram of the experimental scheme is depicted in Figure.4.5.2. As a Brillouin gain medium a 1-km-long standard single-mode fiber was used. The Brillouin characteristics of this fiber were measured, showing a Brillouin shift of 10.8 GHz and an SBS gain bandwidth of 27 MHz. A commercial distributed feedback (DFB) laser diode operating at 1532 nm was used as the light source and its output was split using an optical coupler. Then one branch was amplified using an erbium-doped fiber amplifier (EDFA) to play the role of Brillouin pump, and its power was precisely controlled by a variable optical attenuator before entering into the delaying fiber segment. The other branch was modulated through an electro-optic Mach-Zehnder intensity modulator (EOM) at the Brillouin frequency of the fiber so as to generate two first-order sidebands. The DC bias of the modulator was adequately set to obtain complete suppression of the carrier. Therefore, only two sidebands were present at the output of the modulator. Only lower-frequency sideband was then filtered by a fiber Bragg
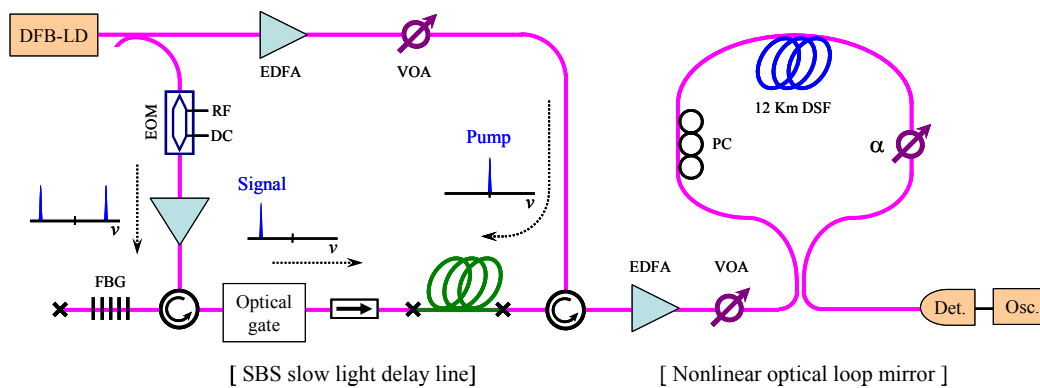
Figure 4.5.2: Experimental setup to produce non-distorted signal delays, by combining a nonlinear generation element with a typical Brillouin slow light system. EDFA; erbium doped fiber amplifier, EOM; electro-optic modulator, FBG; fiber Bragg grating, VOA; variable optical attenuator, DSF; dispersion shifted fiber, PC; polarization controller and α; an attenuation factor.
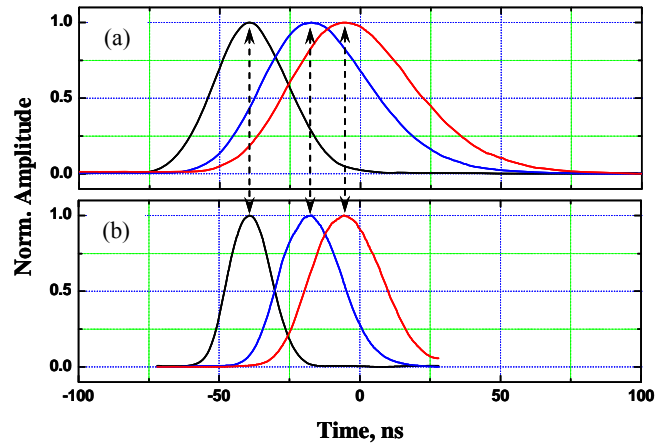
Figure 4.5.3: (a) Normalized waveforms of signals that experienced time delays through SBS slow light and (b) normalized waveforms of transmitted signals through a saturable absorber, showing noticeable pulse compression.

grating via a circulator, and this wave was optically gated using a fast external modulator to generate a signal pulse train. Consequently, a signal pulse train was generated at frequency downshifted from the pump frequency by the Brillouin frequency. The signal pulse showed duration of 27 ns FWHM at a repetition rate of 200 kHz.

To produce relative time delays, the signal was sent into the SBS delay line while the pump power was increased from 0 to 30 mW. Figure.4.5.3a shows the normalized time waveforms of the signal pulses at the output of the Brillouin delay line. As in any typical Brillouin slow light system, it is clearly observed that the signal delay increased a function of pump power. Also, the pulse exiting from the delay line was temporally both delayed and broadened with respect to the pump power. This way the largest signal delay achieved was about 36 ns (corresponding to 1.3-bits delay) at the pump power of 30 mW and the delayed pulse was significantly broadened by a factor of 1.9. After passing through the delay line, the delayed signal was amplified using another EDFA and delivered into the nonlinear loop. In practice, the NOLM acts as a saturable absorber as previously described. Consequently, the shape of the broadened signal was sharpened at the output, as shown in Figure.4.5.3b. Moreover, it must be pointed out that the unwanted background components imposed onto the pulse train (mainly amplified spontaneous emission from the EDFAs and the Brillouin amplifier) were cleaned up since they were rejected for the transmission. It is clearly observed that the output signal is compressed at the output of the loop, nevertheless fully preserving the time delays achieved in the previous stage, SBS delay line. Figure.4.5.4 shows the measured fractional delay and signal broadening as a function of signal gain. This system allows producing fractional delays of up to 1.3-bits without any broadening. This result is fully consistent with the prediction for a transmission depending quadratically on the
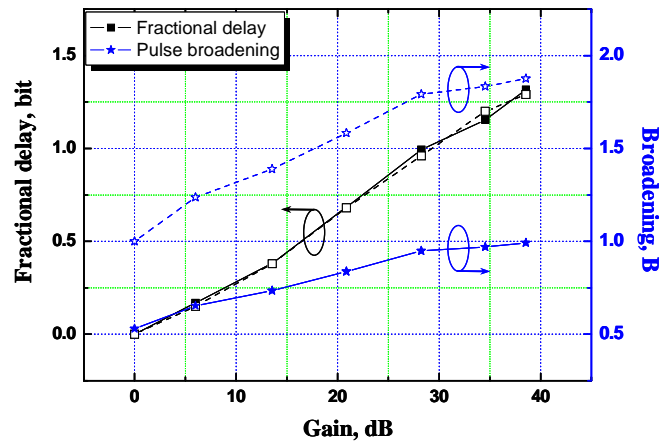
Figure 4.5.4: Factional delays and broadening factors of signal pulses, respectively, with square and star symbols as a function of signal gain when the nonlinear loop mirror is present (filled symbols) or absent (opened symbols).

intensity, which gives a compression by a factor $2^{-\frac{1}{2}}$ when applied to a signal with a Gaussian intensity profile. Of course the non-delayed signal is also compressed, but this should not be an issue in detection, since the detection system is inherently band-limited. Another advantage takes into account the signal-to-noise ratio of the setup. It was observed that the output pulse contained amazingly very clean zero background level, which is rather unusual in Brillouin amplifier setups. This zero-background level can be very helpful in real transmission systems to enhance the contrast between the "on" and "off" states in the detection process.

4.6 Self-advanced Brillouin fast light

Stimulated Brillouin scattering offers unmatched flexibilities for an all-optical control of the signal delay in a fiber. However, considering practical issues, Brillouin slow light shows two actual drawbacks: first, this scheme inevitably requires an external pump source; second, the frequency separation between the pump and probe lasers has to be constant and precisely controlled within typically a 1 MHz uncertainty. These requirements force a certain complexity in the experimental system, which should be preferably avoided in many practical applications. In this section, key contribution of this thesis will be demonstrated, that is, a light signal with a sufficient average component can make itself speed up along the fiber without any external pump source. The working principle is the following: when the signal power grows beyond a certain critical power - commonly denominated Brillouin threshold - a significant Stokes component is generated at a frequency down-shifted ν_B below the signal. This Stokes wave, in turn, acts as Brillouin pump to create an absorption peak in the transmission spectrum of the fiber at the signal frequency, hence creating relative advancement on the signal. In other words, simply controlling the power of the signal entering the fiber eventually determines its advancement. This configuration is considerably simpler than all previously reported techniques and may serve as a practical basic concept for several applications.

4.6.1 Noise-seeded stimulated Brillouin scattering

The process of SBS can be initiated without the need of an external probe wave. The background energy present in the fiber in ambient conditions causes the presence of thermally activated acoustic waves that spontaneously scatter the light from the pump. This noise-scattered seed light initiates the stimulation and is thus gradually amplified if it lies within the SBS gain spectrum. This can eventually lead to a considerable amount of power that is back-reflected at the Stokes wavelength ν_{pump}-ν_B. A useful quantity in this case is the Brillouin critical power P_c, which is conventionally defined as the power of the input CW light necessary to have an equal amount of power present in the backscattered Stokes wave in the fictitious case of an absence of depletion. For a uniform fiber, this critical power can be estimated [47] as $P_c=21A_{eff}/(g_BL_{eff})$, where g_B is the Brillouin gain coefficient, A_{eff} is the nonlinear effective area of the fiber and L_{eff} is the nonlinear effective length. In long conventional optical fibers with $L > L_{eff}$, this critical power is about 5 mW at a wavelength of 1550 nm and can thus be easily reached using a conventional distributed feedback lasers.
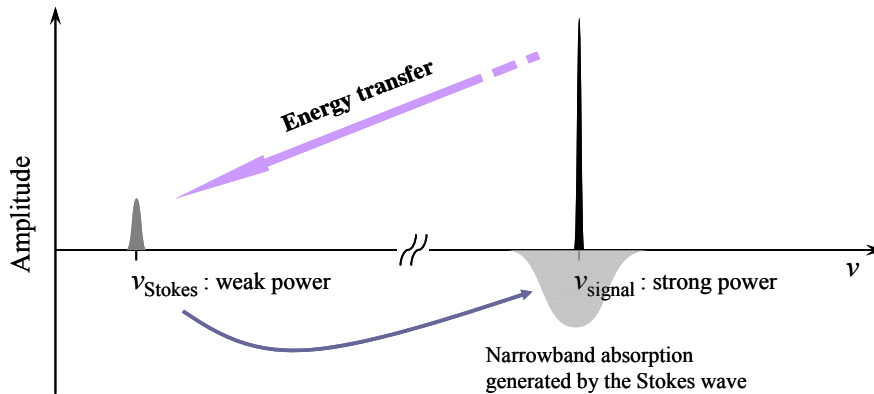
Figure 4.6.1: Principle of the configuration to generate self-advanced fast light. The signal power is high enough to generate a strong amplified spontaneous Stokes wave, which in turn depletes the signal wave. The depletion is assimilated to a narrowband loss spectrum.

The basic idea of the self-induced fast light scheme is to avoid using a distinct pump wave to modify the signal propagation conditions through SBS. This is simply realized by delivering a sufficiently powerful average signal into the fiber, above the Brillouin critical power P_c. Seeded by noise, the process of stimulated Brillouin scattering will generate a substantial Stokes signal, which in turn will induce through depletion a narrowband loss for the signal, as depicted in Figure.4.6.1. Associated to this narrowband loss, a spectral region of anomalous dispersion is induced, in which the temporal envelope of the signal will experience advancement through fast light.

The advantage of this configuration is that the signal is continuously and accurately centered in the spectrum of the loss resonance created by the spontaneously amplified Stokes wave. The pump-signal frequency difference automatically compensates for any environmental and wavelength changes and remains perfectly stable without the need of any optical component or instrument (such as external modulators, microwave generators, etc.) typically used in other configurations [1,2,19,28]. Moreover, in case of very large gain as in the present situation, the polarization state of the Stokes wave is precisely parallel to that of the signal at the fiber input since the SBS interaction coherently transfers photons from the pump to the Stokes wave and preserves their states of polarization [30]. Thus, in these conditions, the polarization of the strongly amplified Stokes wave experiences a pulling effect and eventually aligns to the pump polarization. This holds for a common standard fiber with a reasonably low birefringence value. This secures a maximum efficiency and stability for the interaction, and hence the highest possible advancement for a given input power.

When addressing the delay-bandwidth characteristics and the efficiency of a slow and fast light scheme, it is important to know the spectral width of the Brillouin resonance. The bandwidth of the gain/loss process is obtained from the convolution of the intrinsic

Brillouin spectral distribution with the pump spectrum [16]. In this configuration, it is important to realize that the Stokes signal is not purely monochromatic, since it builds up from a noise-seeded SBS process and will therefore present a certain spectral distribution [48]. For low input power the spontaneous Brillouin noise shows a linewidth close to the intrinsic Brillouin linewidth $\Delta \nu_B$. However, for higher input power, the linewidth experiences a dynamic narrowing. This narrowing stabilizes when the critical power is reached and a significant depletion of the input signal is observed [48]. In this case, significant advancement of the signal starts to take place when the signal power exceeds the Brillouin critical power, hence when significant pump depletion starts to occur. In these conditions, the spectral width of the amplified spontaneous Brillouin emission should remain moderate and constant for all input powers [48]. Therefore, a power-invariant loss spectral distribution for the signal must be expected, since it is essentially given by the convolution of the Stokes wave spectrum with the natural Brillouin gain, both being constant for all the relevant input powers in the present experimental conditions.

The power of the signal must also be considered as constant when time-averaged during transit in the fiber, so that an amplified spontaneous Stokes emission showing a constant power is generated and no time jitter is observed on signal delays. Practically, this condition requires that the fiber length must be much longer than the typical periodicity of the signal, or equivalently a large number of symbols (> 100-1000) forming the data pattern must simultaneously propagate through the fiber. Under this condition each separate symbol in the data stream taken individually has a negligible impact on the amplitude of the Stokes wave and therefore experiences a Brillouin loss actually similar to that produced by an external constant pump. This makes the system behave identically to a standard Brillouin fast light configuration in terms of distortion and limitation.

4.6.2 Characteristics of spontaneous Stokes wave

The experimental setup realized to demonstrate the self-advanced fast light through SBS is shown in Figure.4.6.2. A 12-km-long conventional dispersion shifted fiber (DSF) with a Brillouin shift of 10.6 GHz and a FWHM gain bandwidth of approximately 27 MHz is used as the SBS gain/loss medium. To generate the signal a commercial distributed feedback laser diode was used, operating at a wavelength of 1532 nm. The output of the laser is modulated using an external electro-optic modulator to produce a signal pulse train with a width of 45 ns (FWHM) at a repetition rate of 5 kHz. With this periodicity, only one pulse is present at a time over the entire optical fiber, so that any cross-interaction between adjacent pulses during propagation is avoided at a first stage. The signal includes a definite DC component obtained
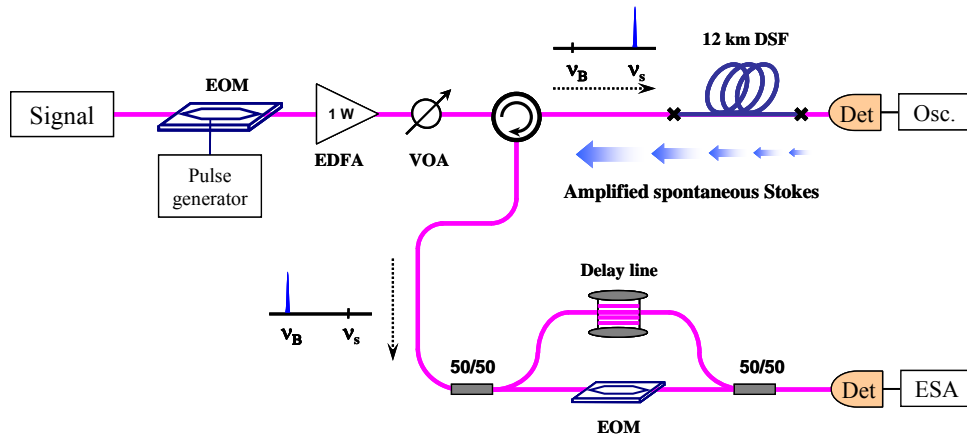
Figure 4.6.2: Experimental configuration to realize the self-pumped signal advancement based on both amplified spontaneous and stimulated Brillouin scattering. EOM; electro-optic modulator, EDFA; Erbium-doped fiber amplifier, VOA; variable optical attenuator, DSF; dispersion shifted fiber.

simply by adjusting the DC bias applied to the EOM. This DC component is essentially responsible for the generation of the Stokes wave. In a realistic fiber system, a sufficiently long pulse sequence present in the fiber would equally generate the Stokes component responsible of the signal advancement. The DC power is approximately 14 % of the peak power of the pulse, but creates a much larger integrated gain over the fiber length considering the very low pulse repetition rate. Then this compound signal is strongly boosted using a high power erbium-doped fiber amplifier (EDFA) with ~30 dBm saturation power before it is launched into the DSF. The signal power is controlled with a variable optical attenuator (VOA) after being amplified by the EDFA. The strong DC component present on the signal generates a strong backward Brillouin Stokes at a frequency downshifted ν_B below the pulse signal frequency. This Stokes wave causes an absorption peak in the spectral transmission of the fiber at the frequency of the input signal, which consequently experiences fast light conditions. This is observed at the fiber output by measuring the temporal advancement of the pulse signal for different input signal powers. To perform this measurement the amplitude of the pulse at the input of the detector was controlled using a variable optical attenuator, so as to avoid any possible biasing of the trace from an amplitude-dependent time response of the detector. The higher the input power, the stronger the Stokes wave, the deeper the peak absorption is and the faster the pulse will travel.

The Stokes power as a function of the input signal power is shown in Figure.4.6.3a. It is seen that there is no significant Stokes component below the Brillouin critical power, while an abrupt change is observed over this threshold power. For higher signal power all the light intensity in excess of the threshold power is transferred to the Stokes waves, making the output signal power saturated at a constant value. For even higher input power exceeding
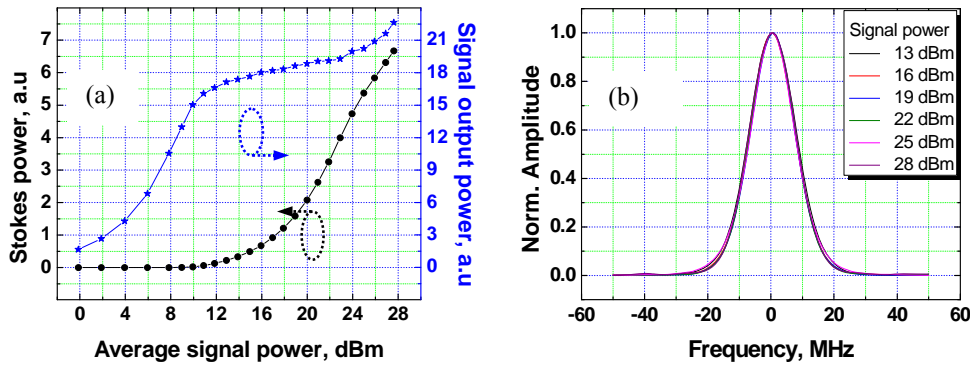
Figure 4.6.3: (a) Measured optical powers of the Stokes waves and transmitted signals. (b) Linewidths of the generated Brillouin Stokes waves recorded in the ESA, by use of the delayed homo-heterodyne system.

twice the Brillouin threshold the Stokes waves is powerful enough to generate its own Stokes wave co-propagating with the signal. This turning point at approximately 24 dBm input power is observed as an apparently resumed growth of the signal output power. The linewidth of the Stokes wave with respect to the signal power was characterized. The spectral width of the Stokes wave was measured by the delayed self-heterodyne method [49]. This method is an interferometric method, and is based on a Mach-Zehnder interferometer in which one arm contains a frequency shifter (EOM2) and the other is used as a delay line to break the coherence of the analyzed beat signal. The beating is recorded using a fast detector connected to an electrical spectrum analyzer. Figure.4.6.3b shows the spectral profiles of the generated Stokes wave for different input signal powers, all of them over the SBS critical power. The spectra show no linewidth change of the Stokes wave for all the relevant input powers, hence the spectrum of the SBS-induced absorption will remain similar for all input powers, generated by a lightwave showing a linewidth of approximately 10 MHz.

4.6.3   Self-advanced signal propagation

Self-advancements for isolated signals

The signal delay induced by the SBS effect was typically measured as a function of the Brillouin gain/loss, as a consequence of the simple linear relationship between these two quantities. However, in this configuration, it turns out to be conceptually inappropriate since the signal pulse experiences fast-light propagation with no independent pump source. Additionally, the signal annihilates part of its power as a result of the Brillouin loss and saturates to a roughly constant value. Therefore, a direct measurement of advancement as a function of loss experienced by the signal is of limited interest and can not be easily extracted from the raw data. A more interesting quantity to plot, however, is the delay as a function of the input signal power. Figure.4.6.4 shows the measured time waveforms of the signal pulses
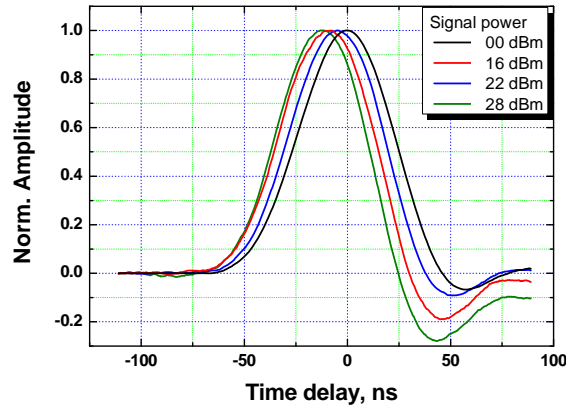
Figure 4.6.4: Temporal traces of the signal pulse after propagating through the dispersion shifted fiber for different input signal powers, showing clear advancements.
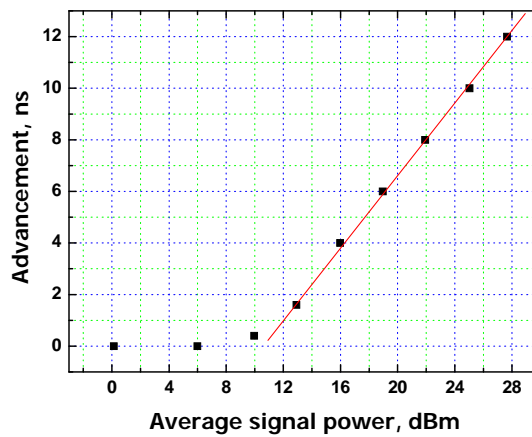
Figure 4.6.5: Temporal advancements of the signal pulses as a function of the signal average power, showing logarithmic dependence of delay on the signal power.

for different average powers of the input signal, ranging from 0 dBm to 28 dBm. It is clearly observed that the pulse experiences more advancement as the input power increases. Additionally, in all cases, the signal pulse experiences low distortion. The advanced pulses show a slightly sharper leading edge and a longer trailing edge, consistent with previous observations in SBS fast light [2]. The largest advancement induced by the proposed scheme is 12 ns (corresponding to a fractional delay 0.26) at a signal power 28 dBm. The signal power in this setup was limited by the saturation power of the EDFA. Longer delays could eventually be realized in this method with an EDFA with higher saturation power or with a fiber showing a smaller effective area. Figure.4.6.5 shows the advancement observed on the signal as a function of the input power. To determine the amount of signal advancement the position of the peak of the pulse was used. Notice that for low power levels, there is no visible advancement, since there is no significant loss of the signal below the Brillouin

critical power. When the signal power exceeds this critical value, the pulse train immediately experiences an observable advancement. In the range of measured values, the advancement depends logarithmically on the input power, with a slope efficiency of 0.69 ns/dBm.

This logarithmic dependence is actually a direct consequence of the total power transfer from the signal to the Stokes power above the Brillouin critical power P_c. The effective total loss A experienced by the signal is defined as

$$\frac{P_{out}}{P_{in}} = e^{-A}, \tag{4.29}$$

where P_{in} and P_{out} represents the input and output signal power, respectively. Since above the Brillouin threshold the signal output power P_{out} saturates to a constant value P_{sat}, the effective loss simply depends on the input signal power P_{in} following this relationship:

$$A(P_{in}) = -\ln\left(\frac{P_{out}}{P_{in}}\right) = -\ln\left(\frac{P_{sat}}{P_{in}}\right). \tag{4.30}$$

The temporal advancement being proportional to the effective total loss A and P_{sat} being constant, the logarithmic dependence on the input power comes out immediately from this simple description. It incidentally shows one more advantage of this scheme: the output signal power remains constantly fixed at the saturation power P_{sat} for any signal advancement, since all light over the critical level is scattered to build up the Stokes wave.

Self-advancements for a data stream

To demonstrate that this technique can also be used for a data stream with negligible DC component, the repetition rate of the signal pulse was modified to 20 MHz, so that it reasonably simulates a real sequence of bits when averaged over the fiber length. In this case, the pulses in this case have a FWHM of 14.22 ns, hence the duty cycle is 30 % and the DC component is reduced to a negligible fraction of the pulse peak power. Figure.4.6.6a shows
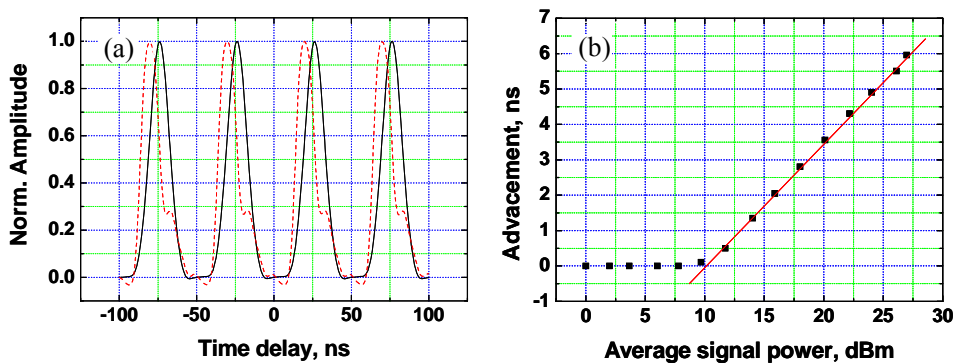
Figure 4.6.6: (a) Temporal traces of data streams for a signal power below the critical power (solid line) and at maximum signal power realized in our setup (dashed line). (b) Signal advancement as a function of the average signal power, showing the logarithmic dependence over the Brillouin critical power at 10 dBm.

the pulse train for 2 different signal powers - one below the critical power and the other at the maximum possible value using this setup - and the pulse advancement is again clearly visible. Figure.4.6.6b shows the advancement as a function of the signal power, with a maximal obtained fractional delay of 0.42. The slope is in this case 0.35 ns/dBm. It must be pointed out that the power of the data stream time-averaged over the fiber length must remain constant to avoid any timing jitter at the output, requiring a steady fraction of bits "1" with respect to the total number of bits.

The main limit for the maximum possible advancement in this configuration is caused by the onset of the 2nd order SBS amplified Stokes emission. Once the backward Stokes reaches its own critical power for SBS, there will be a forward Stokes wave downshifted by $2\nu_B$ below the frequency of the input signal. This wave will deplete the backward Stokes wave and hence make the advancement saturated. This places a fundamental limit to the range of signal power suitable to produce a delaying effect. Other limitations are related to the requirement of a permanent constant average power in the data stream to avoid fluctuations in the signal delay and amplitude.

4.6.4   Self-adapted signal bandwidth

A last aspect of self-pumping was investigated related to the capability of the Stokes amplified emission to adapt its spectral width to the signal bandwidth. For this purpose, the Stokes emission generated by a pulse train was observed while the pulse averaged power is well above the Brillouin critical power P_c. The initial pulse width was 50 ns at a repetition frequency of 4 MHz, corresponding to a normalized repetition rate of 5. Such a signal shows a measured FWHM bandwidth of 10 MHz that is substantially lower than the Brillouin natural linewidth. Then the pulse width was reduced while adapting proportionally the
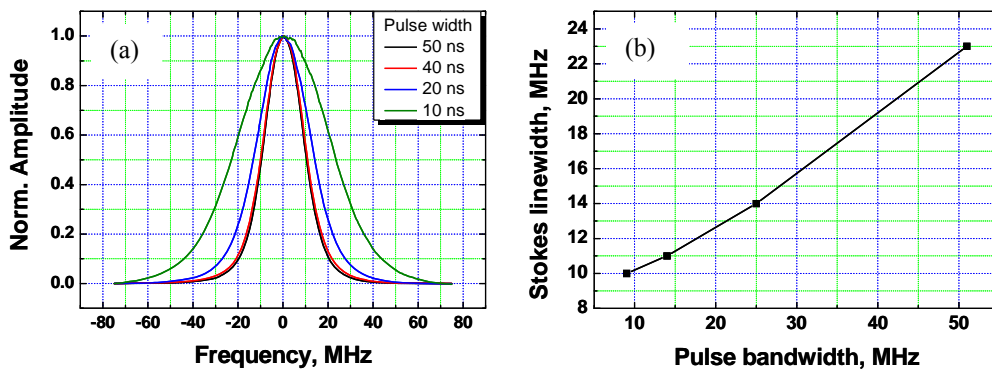
Figure 4.6.7: (a) Measured spectra of the Stokes emission by the delayed self-homodyne technique, for different signal widths at a constant normalized repetition rate. (b) Measured linewidth of back-scattered Stokes wave as a function of the measured signal bandwidth.

repetition frequency to maintain a constant normalized repetition rate. This way the average pump power is kept constant and the only modified relevant signal characteristic is its bandwidth. Figure.4.6.7a shows the measured Stokes spectra for different pulse width. From a floor value of 10 MHz the Stokes linewidth clearly self-adapts to the incremental broadening of the signal, as illustrated in Figure.4.6.7b. It must be pointed out that the Stokes linewidth represents only a fraction of the input signal bandwidth. It could be extrapolated from the measurements that this fraction corresponds asymptotically for a wideband signal to about 45 % of its bandwidth. Even after convolution with the natural Brillouin spectrum this fractional linewidth has certainly a substantial impact on the pulse distortion.

4.7   Dispersive delay line based on wavelength conversion

In this section, another approach for the development of all-optically controlled delay lines will be discussed that is entirely distinct from a slow light-based delaying scheme. In any slow light system the maximum time delay that a signal can experience is inherently limited to a few bits delay. It is mainly caused by the growing noise associated to the amplification process and the signal distortion, resulting from the frequency dependent Brillouin gain (spectral filtering effect) and the large dispersion induced by the slow light medium. Therefore, the scientific challenge to produce a large amount of signal delay with negligible distortion remains opened. To overcome this issue, an elegant solution was soon proposed, which makes use of the combination of wavelength conversion and group velocity dispersion [50-52]. This scheme allows tremendous signal delays for broadband signals. In the work of this thesis, the conversion-dispersion technique was also studied and experimentally demonstrated to improve to a large increment the fractional delay. The main progress in the configuration compared to the previous works is to simply and efficiently realize the wavelength conversion with a compact and low power concept. The wavelength of the signal was converted to a desired wavelength using cross gain modulation via a semiconductor optical amplifier. It must be noticed that this type of conversion offers the key advantage to be efficient over a much broader wavelength range than parametric processes. This technique extends the range of delays obtained by the dispersive line and a large range of optical delays with low distortion could be demonstrated experimentally up to tens of nanosecond for 100 ps optical pulses.

4.7.1   Wavelength conversion using cross gain modulation

Cross gain modulation (XGM) in a semiconductor optical amplifier (SOA) is usually described as a nonlinear interaction between two co- or counter-propagating beams, a strong pump wave at ν_{pump} and a weak probe wave at ν_{probe}. The principle to realize the wavelength conversion using XGM is depicted in Figure.4.7.1. Let suppose an intensity modulated pump light entering into an SOA and a continuous wave (CW) probe light simultaneously injected counter-directionally into the SOA. Due to the gain saturation, the pump light will modulate the gain inside the amplifier [53]. In turn XGM in the amplifier will impose the pump modulation on the probe. Consequently, the intensity of the probe at the target wavelength is inversely modulated and carries the complementary data pattern, so essentially the same information as the pump modulation. This way the wavelength of the signal can be converted with high conversion efficiency and no requirement for strict phase matching conditions,
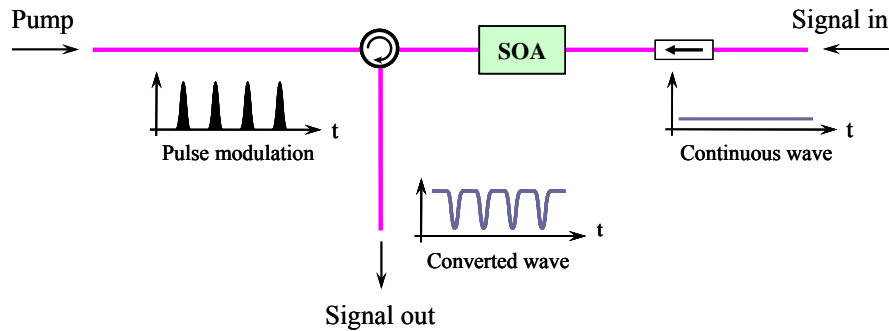
Figure 4.7.1: Schematic diagram of the principle to generate the XGM wavelength conversion, in which the pump and signal waves counter-propagate through semiconductor optical amplifier.

which are necessary to obtain parametric amplifications [50-52]. Moreover, this process can be polarization-independent if an SOA showing a polarization independent gain is employed.

After the first wavelength conversion is accomplished, the probe light exiting from the SOA is delivered into a highly dispersive optical medium such as long lengths of optical fiber [50,52] or even a highly dispersive Bragg grating [51]. The propagation velocity of the probe through the dispersive fiber is continuously varied by simply tuning the wavelength of the probe due to the wavelength dependence of the group velocity. As a result, the probe wave can exit the dispersive fiber with relative temporal delays or advancements. The amount of time delay achieved in the delay line can be simply estimated to first order as the product of probe wavelength change and the group-velocity dispersion (GVD) of the fiber. The delayed converted signal in turn experiences a second wavelength conversion through another SOA back to the original signal wavelength, restoring in the same process the original modulation pattern.

4.7.2   Continuous control of large fractional delay

The schematic diagram of the experimental setup is depicted in Figure.4.7.2. A commercial distributed feedback (DFB) laser diode operating at 1571 nm was used as a light source and its output was split by a 90/10 directional coupler. The higher power branch was optically gated using a fast electro-optic Mach-Zehnder intensity modulator (EOM) to produce a signal pulse train with duration of 100 ps FWHM at a repetition rate of 500 MHz. Then the pulse train was boosted using an erbium-doped fiber amplifier (EDFA) before entering into the first SOA, so that it could play the role of the pump in the first wavelength conversion. A weak continuous wave (CW) probe beam at a desired wavelength was generated by a tunable laser source (TLS) and was also simultaneously launched into the SOA, but in the direction opposite to the pulse direction. This way the converted probe signal could be simply
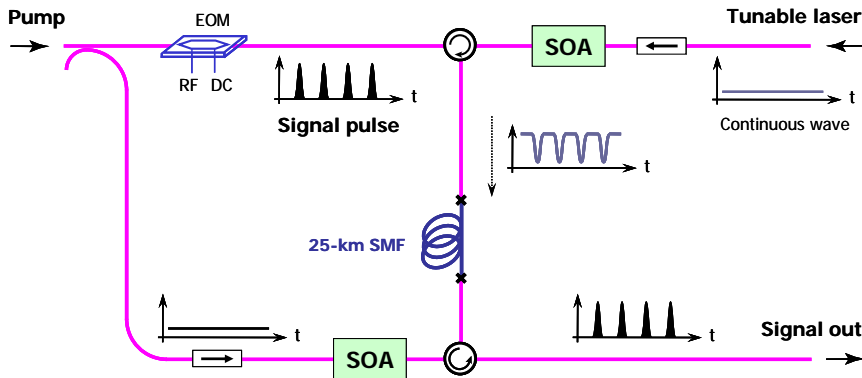
Figure 4.7.2: Experimental setup to generate a wide range of signal delays, using wavelength conversion through semiconductor optical amplifier and group velocity dispersion in optical fibers.

separated from the input pump pulse without any need of optical filters. According to the principle described above, XGM in the amplifier induces an intensity modulation on the probe, resulting in a wavelength converted signal that is inverted compared to the modulation pattern of the input pulses. The converted signal was then delivered to a dispersive medium to experience a relative time delays. In our setup, it was simply a 25 km-long single-mode fiber, showing the group velocity dispersion of ~180 ps/nm. After exiting from the dispersive fiber, the wavelength converted signal was amplified using another EDFA before entering into the second SOA. The lower power channel of the initial DFB laser was also launched into the SOA to play the role of the probe in the second wavelength conversion. Consequently, the original pattern of the signal pulse is restored and the signal returns to its original wavelength.

The normalized time waveforms of the signal pulses exiting from the delay line were measured and displayed on a digital oscilloscope for different wavelength of the TLS, as
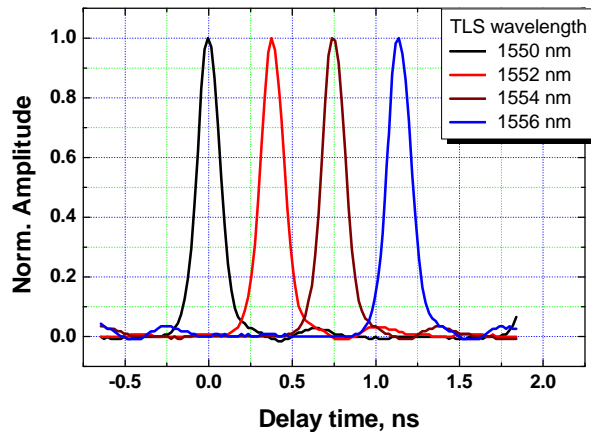
Figure 4.7.3: Time waveforms of the delayed signal pulse trains while the TLS wavelength was swept from 1550 nm to 1556 by 2 nm steps, showing clear delays of the signal pulse.
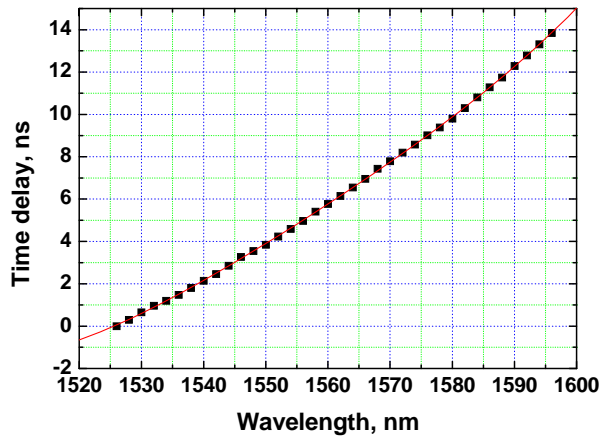
Figure 4.7.4: The relative signal delays as a function of the TLS wavelength and the red curve represents the result of the 4th order fitting.

shown in Fig.4.7.3. The pulse delays are clearly observed without significant broadening while the TLS wavelength is increased by 2 nm steps. To determine the amount of the signal delay the peak point of the pulse, as shown in Figure.4.7.4. The largest time delay achieved was 14 ns corresponding to a fractional delay of 140 while the TLS wavelength was swept from 1526 nm to 1596 nm. This ratio can certainly be further improved using a more dispersive delay line and an even broader wavelength scanning range.

It must be pointed out that the delay lines, based on wavelength conversion and group velocity dispersion, also suffer the trade-off relations between the maximum achievable delay and the associated signal distortion expressed by broadening. Since the chromatic dispersion is a key parameter to control the amount of signal delay, the frequency components of the signal travel through the medium at slightly different velocities. More specifically, blue components propagate faster than red components in the anomalous dispersion regime observed in standard single mode fibers in the minimum attenuation window. Therefore, the signal must experience a broadening effect after propagating through the material, limiting the signal bandwidth. This can be alleviated by imposing an extrinsic frequency chirp across the signal. Recently, Okawachi *et al.* demonstrated experimentally the possibility to completely compensate the large induced signal broadening using phase conjugation [54].

The anticipated signal broadening was calculated as a function of the GVD for the transform-limited Gaussian pulse with duration of 100 ps FWHM [55] and the wavelength change required to achieve 1000-bits delay, as shown in Figure.4.7.5. According to the simulation test, this delay line demands wavelength change of ~550 nm, which is far from real operational conditions. In an alternative way a larger GVD of the fiber can be replaced to
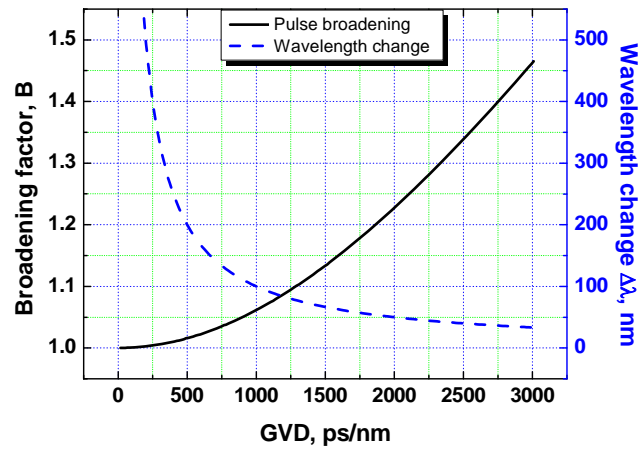
Figure 4.7.5: The associated signal broadening to achieve 1000-bits delay for a transform limited Gaussian pulse with a width of 100 ps FWHM and the required wavelength change as a function of group velocity dispersion.

compensate the small change of wavelength, but leading to more degradation on the data stream.

The maximum bit-rate of the data packet through this delay-line was restricted by the carrier recovery time of the SOAs used in this experiment. However, it must be pointed out that this delay-line can be applied for high speed networks since error-free wavelength conversion at 160 Gbit/s has been realized [56]. Moreover, the original signal wavelength is preserved while producing optical delays. The signal bandwidth can be moderately modified by the possible chirp effects by gain saturation in SOAs [57]. However, this scheme can be a promising timing tool for future communication and microwave photonics systems.

Bibliography

[1] K. Y. Song, M. Gonzalez-Herráez, and L. Thévenaz, "Observation of pulse delaying and advancement in optical fibers using stimulated Brillouin scattering," Opt. Express, **13**, 82-88 (2005).

[2] M. Gonzalez Herráez, K.Y. Song., and L. Thévenaz, "Optically controlled slow and fast light in optical fibers using stimulated Brillouin scattering," Appl. Phys. Lett., **87**, 081113 (2005).

[3] L. V. Hau, S. E. Harris, Z. Dutton, and C.H. Behroozi, "Light speed reduction to 17 meters per second in an ultracold atomic gas," Nature, **397**, 594-598 (1999).

[4] L. J. Wang, A. Kuzmich, and A. Dogariu, "Gain-assisted superluminal light propagation," Nature, **406**, 277-279 (2000).

[5] C. Liu, Z. Dutton, C. H. Behroozi, and L.V. Hau, "Observation of coherent optical information storage in an atomic medium using halted light pulses," Nature, **409**, 490-493 (2001).

[6] M. S. Bigelow, N. N. Lepeshkin, and R.W. Boyd, "Superluminal and slow light propagation in a room temperature solid," Science, **301**, 200-202 (2003).

[7] M. S. Bigelow, N. N. Lepeshkin, and R.W. Boyd, "Observation of ultraslow light propagation in a ruby crystal at room temperature," Phys. Rev. Lett., **90**, 113903 (2003).

[8] G. P. Agrawal, *Nonlinear Fiber Optics, 2nd ed.*, (Academic Press, San Diego, 1995).

[9] R. W. Boyd, *Nonlinear Optics, 2nd ed.*, (Academic Press, New York, 2003).

[10] M. Nikles, L. Thevenaz, and P.A. Robert, "Brillouin gain spectrum characterization in single mode optical fibers," J. Lightwave Technol. , **15**, 1842-1851 (1997).

[11] C. Rullière, *Femtosecond Laser Pulses*, (Springer-Verlag, Berlin Heidelberg 1998).

[12] S. Chin, M. Gonzalez-Herráez, and L. Thévenaz, "Self-advanced fast light propagation in an optical fiber based on Brillouin scattering," Opt. Express, **16**, 12181-12189 (2008).

[13] G. C. Calley, "A review of stimulated Brillouin scattering excited with a broad-band pump laser," J. Quantum Electron., **QE-22**, 704-712 (1986).

[14] Y. Aoki and K. Tajima, "Stimulated Brillouin scattering in a long single-mode fiber excited with a multimode pump laser," J. Opt. Soc. Am. B, **5**, 358-363 (1988).

[15] M. Denariez and G. Bret, "Investigation of Rayleigh wings and Brillouin stimulated scattering in liquids," Phys. Rev., **171**, 160-171 (1968).

[16] M. Gonzalez-Herráez, K. Y. Song, and L. Thévenaz, "Arbitrary-bandwidth Brillouin slow light in optical fibers," Opt. Express, **14**, 1395-1400 (2006).

[17] Z. Zhu, Andrew M. C. Dawes, Lin Zhang, A. E. Willner, and D.J. Gauthier, "Broadband SBS slow light in an optical fiber," J. Lightwave Technol., **25**, 201-206 (2007).

[18] K. Y. Song and K. Hotate, "25 GHz bandwidth Brillouin slow light in optical fibers," Opt. Lett., **32**, 217-219 (2007).

[19] K. Y. Song, M. Gonzalez-Herráez, and L. Thévenaz, "Gain-assisted pulse advancement using single and double Brillouin gain peaks in optical fibers," Opt. Express, **13**, 9758-9765 (2005).

[20] Z. Zhu and D.J. Gauthier, "Nearly transparent SBS slow light in an optical fiber," Opt. Express, **14**, 7238-7245 (2006).

[21] L. Thévenaz, S. Chin, and M. Gonzalez-Herraez, "Low distortion fast light in an optical fiber using stimulated Brillouin scattering," Slow and Fast Light, Technical Digest (CD), JTuA8 (2007).

[22] S. Chin, M. G. Herraez, and L. Thevenaz, "Simple technique to achieve fast light in gain regime using Brillouin scattering," Opt. Express, **15**, 10814-10821 (2007).

[23] N. Yoshizawa and T. Imai, "Stimulated Brillouin scattering suppression by means of applying strain distribution to fiber with cabling," J. Lightwave Technol., **11**, 1518-1522 (1993).

[24] K. Y. Song, K. S. Abedin, K. Hotate, M. Gonzalez-Herráez, and L. Thévenaz, "Highly efficient Brillouin slow and fast light using As2Se3 chalcogenide fiber," Opt. Express, **14**, 5860-5865 (2006).

[25] K. S. Abedin, "Observation of strong stimulated Brillouin scattering in single-mode As2Se3 chalcogenide fiber," Opt. Express, **13**, 10266-10271 (2005).

[26] Y. Okawachi, M. S. Bigelow, J. E. Sharping, Z. Zhu, A. Schweinsberg, D. J. Gauthier, R. W. Boyd, and A.L. Gaeta, "Tunable All-Optical Delays via Brillouin Slow Light in an Optical Fiber," Phys. Rev. Lett., **94**, 153902 (2005).

[27] A. Kasapi, M. Jain, G. Y. Yin, and S.E. Harris, "Electromagnetically induced transparency: propagation dynamics," Phys. Rev. Lett., **74**, 2447-2450 (1995).

[28] S. Chin, M. Gonzalez-Herráez, and L. Thévenaz, "Zero-gain slow & fast light propagation in an optical fiber," Opt. Express, **14**, 10684-10692 (2006).

[29] M. O. van Deventer and A.J. Boot, "Polarization properties of stimulated Brillouin scattering in single-mode fibers," J. Lightwave Technol., **12**, 585-590 (1994).

[30] Avi Zadok, Elad Zilka, Avishay Eyal, Luc Thévenaz, and M. Tur, "Vector analysis of stimulated Brillouin scattering amplification in standard single-mode fibers," Opt. Express, **16**, 21692-21707 (2008).

[31] A. Zadok, O. Raz, A. Eyal, and M. Tur, "Optically Controlled Low-Distortion Delay of GHz-Wide Radio-Frequency Signals Using Slow Light in Fibers," Photon. Technol. Lett., **19**, 462-464 (2007).

[32] M. Lee, R. Pant, and M.A. Neifeld, "Improved slow-light delay performance of a broadband stimulated Brillouin scattering system using fiber Bragg gratings," Appl. Opt., **47**, 6404-6415 (2008).

[33] R. Pant, M. D. Stenner, M. A. Neifeld, and D.J. Gauthier, "Optimal pump profile designs for broadband SBS slow-light systems," Opt. Express, **16**, 2764-2777 (2008).

[34] M. D. Stenner and M.A. Neifeld, "Optimal pulse design for communication-oriented slow-light pulse detection," Opt. Express, **16** 651-662 (2008).

[35] M. D. Stenner, M. A. Neifeld, Z. Zhu, A. M. C. Dawes, and D.J. Gauthier, "Distortion management in slow-light pulse delay," Opt. Express, **13**, 9995-10002 (2005).

[36] Z. Zhu, D. J. Gauthier, Y. Okawachi, J. E. Sharping, A. L. Gaeta, R. W. Boyd, and A.E. Willner, "Numerical study of all-optical slow-light delays via stimulated Brillouin scattering in an optical fiber," J. Opt. Soc. Am. B, **22**, 2378-2384 (2005).

[37] J. T. Mok, C. M. Sterke, I. C. M. Littler, and B.J. Eggleton, "Dispersionless slow light using gap solitons," Nature, **2**, 775-780 (2006).

[38] S. Sandhu, M. L. Povinelli, M. F. Yanik, and S. Fan, "Dynamically tuned coupled-resonator delay lines can be nearly dispersion free," Opt. Lett., **31**, 1985-1987 (2006).

[39] S. Chin and L. Thevenaz, "Optimized shaping of isolated pulses in Brillouin fiber slow light systems," Opt. Lett., **34**, 707-709 (2009).

[40] J. B. Khurgin, "Optical buffers based on slow light in electromagnetically induced transparent media and coupled resonator structures: Comparative analysis," J. Opt. Soc. Am. B, **22**, 1062-1073 (2005).

[41] R. W. Boyd, D. J. Gauthier, A. L. Gaeta, and A.E. Willner, "Maximum time delay achievable on propagation through a slow-light medium," Phys. Rev., A, **71**, 023801 (2005).

[42] David A. B. Miller, "Fundamental Limit to Linear One-Dimensional Slow Light Structures," Phys. Rev. Lett., **99**, 203903 (2007).

[43] M. Gonzalez-Herraez and L. Thévenaz, "Physical limits to broadening compensation in linear slow light systems," Optics Express, **17**, 4732-4739 (2009).

[44] Andrzej Wiatrek, Ronny Henker, Stefan Preußler, Max J. Ammann, Andreas T. Schwarzbacher, and T. Schneider, "Zero-broadening measurement in Brillouin based slow lihgt delays," Opt. Express, **17**, 797-802 (2009).

[45] N. J. Doran and D. Wood, "Nonlinear-optical loop mirror," Opt. Lett., **13**, 56-58 (1988).

[46] K. Smith, N. J. Doran, and P.G.H. Wigley, "Pulse shaping, compression and pedestal suppression employing a nonlinear-optical loop mirror," Opt. Lett., **15**, 1294-1296 (1990).

[47] R. G. Smith, "Optical power handling capacity of low loss optical fibers as determined by stimulated Raman and Brillouin scattering," Appl. Opt., **11**, 2489-2494 (1972).

[48] A. Yeniay, J-M. Delavaux, and J. Toulouse, "Spontaneous and Stimulated Brillouin Scattering Gain Spectra in Optical Fibers," J. Lightwave Technol., **20**, 1425-1432 (2002).

[49] D. Derickson, *Fiber Optic Test and Measurement*, (Prentice Hall PTR, New jersey, 1998).

[50] J. E. Sharping, Y. Okawachi, J. V. Howe, C. Xu, Y. Wang, A. E. Willner, and A.L. Gaeta, "All-optical, wavelength and bandwidth preserving, pulse delay based on parametric wavelength conversion and dispersion," Opt. Express, **20** 7872-7877 (2005).

[51] M. Fok and C. Shu, "Tunable Pulse Delay using Four-Wave Mixing in a 35-cm bismuth Oxide Highly Nonlinear Fiber and Dispersion in a Chirped Fiber Bragg Grating," in Proc. ECOC'06, Cannes, France (2006).

[52] Y. Okawachi, J. E. Sharping, C. Xu, and A.L. Gaeta, "Large tunable optical delay via self-phase modulation and dispersion," Opt. Express, **14**, 12022-12027 (2006).

[53] T. Durhuus, B. Mikkelsen, C. Joergensen, S. L. Danielsen, and K.E. Stubkjaer, "All-Optical Wavelength Conversion by Semiconductor Optical Amplifiers," J. Lightwave Technol., **14**, 942-954 (1996).

[54] Y. Okawachi, M. A. Foster, X. Chen, A. C. Turner-Foster, R. Salem, M. Lipson, C. Xu, and A.L. Gaeta, "Large tunable delays using parametric mixing and phase conjugation in Si nanowaveguides," Opt. Express, **16**, 10349-10357 (2008).

[55] G. P. Agrawal, *Fiber-optic Communication System, 3rd ed.*, (John Wiley & Sons, Inc., New York, 2002).

[56] Y. Liu, E. Tangdiongga, Z. Li, S. Zhang, H. Waardt, G. D. Khoe, and H.J. Dorren, "Error-Free All-Optical Wavelength Conversion at 160 Gb/s Using a Semiconductor Optical Amplifier and an Optical Bandpass Filter," J. Lightwave. Technol., **24**, 230-236 (2006).

[57] G. P. Agrawal and N.A. Olsson, "Self-phase modulation and spectral broadening of optical pulses in semiconductor laser amplifiers," J. Quantum Electron., **25**, 2297-2306 (1989).

Chapter 5

Slow light and linear light-matter interactions

The main target applications of slow light so far have been the achievement of all-optical timing tools such as all-optical delay lines, all-optical buffers and signal synchronization elements for future all-optical high capacity networks [1,2]. These target applications benefit from the group delay changes caused by the slow light element as an indirect consequence of the modification of the group velocity in the medium. However, the most remarkable feature of slow light media, in which extreme changes in the group velocity can be possibly achieved, remains unexploited. Recently, some research effort has been devoted to understanding the possibilities of slow light for enhancing light-matter interactions. For instance, the role of slow light for enhancing nonlinear effects has been theoretically investigated [3,4]. This enhancement is accomplished by two main contributions of slow light: the longer transit time of light through an optical medium and the higher energy density since the signal tends to be spatially compressed due to the increased group index. It has also been theoretically and experimentally proved that the extreme dispersion of slow light can lead to an enhancement of the spectral sensitivity of interferometers [5,6]. The role of slow light in gyroscopes has been also theoretically investigated [7]. Besides, recent works [8,9] have theoretically demonstrated that Beer-Lambert-Bouguer (BLB) absorption can be increased while light transmits through a special kind of microstructured photonic crystal (PC) cuvette. This absorption enhancement was attributed to the slow group velocity in the cuvette [8,9]. A simpler interpretation of these results would be that the PC structure acts as a quasi-cavity. In such a structural waveguide the incident light bounces back and forth several times, resulting in a longer interaction length of light with the liquid analyte. The experimental proof of these

theoretical results seems very challenging when considering the dimension of the microstructure and the degree of infiltration required.

In this thesis, the relationship between material slow light (slow light in traveling-wave media) and light-matter interactions was experimentally investigated and it is clearly observed that material slow light has no impact on Beer-Lambert absorption. This experimental demonstration was successfully achieved, using a special kind of gas cell. A photonic crystal fiber (PCF) with solid core plays the role of the gas cell as the fiber holes are filled with gaseous acetylene at reduced pressure. A small fraction of the mode field (the evanescent field) propagates through the holes and thus experiences Beer-Lambert absorption. The fiber is also used as a slow light medium. Since light mostly propagates through a solid silica core the group velocity of the light can be controlled by a nonlinear interaction between optical waves. The absorption can therefore be measured under normal and slow-light conditions without modifying the experimental implementation. By comparing the two regimes, one can observe if the slow light has any impact on the absorption by the gas. The results indicate that Beer-Lambert absorption is not at all affected by slow light. To the best of our knowledge, this is the first experimental observation of the effect of material slow light on light-matter interactions.

5.1 Principle

The absorption of a gas analyte is usually expressed by means of the Beer-Lambert (BL) law. When light with an intensity I_o propagates through the gas cell, the light experiences an exponential decaying and the transmitted intensity is given as $I=I_o\exp[-\alpha \cdot C \cdot L]$. C is the gas concentration, L is optical path length and α is the molar absorption coefficient, which is a unique property of the gas, related to the imaginary part of the refractive index. Previous papers (Ref [8], eq. 3) have suggested that the absorption coefficient is inversely proportional to the group velocity. However, in this work, it is experimentally shown that α is not related to the group velocity. To clarify the relationship between BL absorption and slow light, a solid-core microstructured optical fiber replaces the classical gas cell. There are two main reasons for this: first, in such fiber, the optical mode is mainly confined to the solid core. Thus, the velocity of light propagating through the PCF can be controlled by manipulating the material properties of the core using a narrowband gain process such as stimulated Brillouin scattering. The intrinsic fast light effect caused by the gas absorption resonance can be reduced to a negligible amount when compared to the effect of Brillouin gain (weaker linear absorption and much broader resonance width). Second, with a proper choice of the

fiber geometry, a non-negligible fraction of the guided light propagates through the air holes filled with gas, and hence can probe Beer-Lambert absorption. The key advantage of this setup is that the effects of slow light and absorption are totally de-coupled, so that it is possible to vary one without having a direct impact on the other. Under these conditions, the equation of BLB absorption can be slightly modified as:

$$I = I_o \exp[-N \cdot \sigma \cdot f \cdot L]$$

where N is the gas molecular density, σ is the absorption cross section, f is the fraction of light in holes and L is the optical length.

Figure.5.1a shows the SEM image of the single-mode PCF. Using the source-model technique (SMT) [10], the mode field distribution along the core cross section of the PCF was calculated at a wavelength of 1535 nm, as shown in Figure.5.1b. The evanescent part of the guided field propagating in the gas, representing 2.9 % of the total power, is shown in Figure.5.1c. The PCF was then filled with acetylene gas and hermetically sealed at a low pressure, using a normal arc fusion splicer. More details on the development of the gas cell are referred to the paper [11].
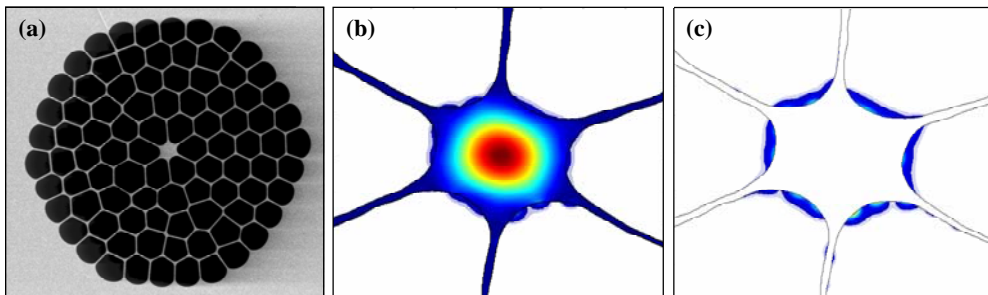
Figure 5.1: (a) SEM image of the solid-core microstructured photonic crystal fiber. (b) Calculated mode field distribution of the fundamental mode and (c) the small evanescent fraction of the guided field present in air holes.

5.2 Group velocity change through the fiber gas cell

As a Brillouin gain medium, a 9.18 m-long PCF was used. The Brillouin spectrum of this fiber was characterized, showing a Brillouin shift of 10.85 GHz and an SBS gain bandwidth of 38 MHz. Figure.5.2 depicts the experimental setup to clarify the relationship between slow light and BLB absorption. A commercial distributed feedback (DFB) laser diode, operating at 1535 nm, was used as a light source and its output was split using a directional coupler. One branch was strongly boosted using a high power erbium-doped fiber amplifier (EDFA) with
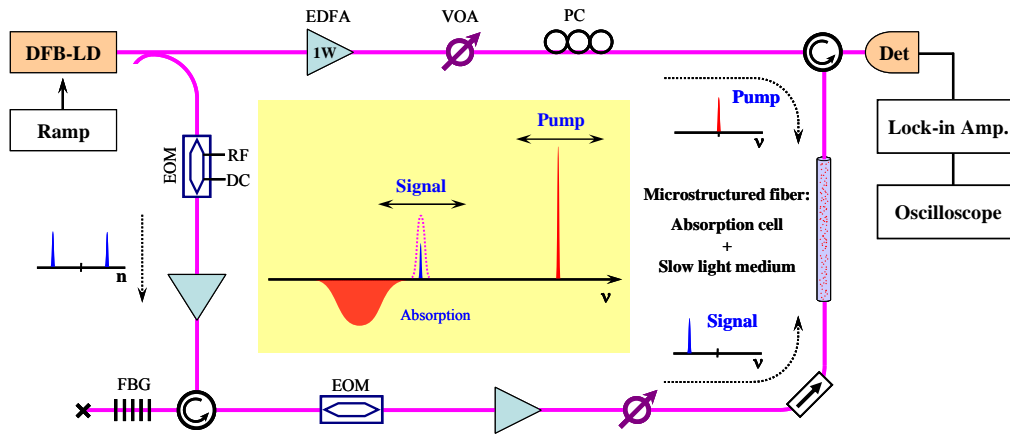
Figure 5.2: The experimental setup to verify the effect of slow light on BLB absorption. EDFA; erbium doped fiber amplifier, VOA; variable optical attenuator, PC; polarization controller, EOM; electro-optic modulator, FBG; fiber Bragg grating.

30 dBm saturation power so as to play the role of Brillouin pump. The output of the EDFA was then precisely controlled by a variable optical attenuator before entering into the gas cell. The other branch was modulated at the Brillouin frequency shift of the PCF through an electro-optic Mach-Zehnder intensity modulator (EOM) to generate two first-order sidebands and the DC bias of the modulator was adequately set for the complete suppression of the carrier. In consequence, the output of the modulator contains only two waves at frequencies of Brillouin Stokes and anti-Stokes. Only lower-frequency sideband was then precisely filtered by a fiber Bragg grating (FBG) and was launched into the fiber as signal.

The amount of group velocity change was first measured as a function of pump power. For this measurement, the frequencies of the pump and signal waves were spectrally placed in a region where absorption resonances are absent. As in typical Brillouin slow light the signal was clearly delayed with respect to the pump power, as shown in Figure.5.3a. To precisely determine the SBS-induced group delay, the signal was sinusoidally modulated at 1 MHz by another external EOM. The phase of the sine wave after propagation through the PCF was measured while the pump power was incremented from 0 to 600 mW by 100 mW steps. This way the group delay change achieved through the PCF for different pump powers was accurately determined from the difference of phase shift, as shown in Figure.5.3b. Additionally, the transit time through the fiber was also determined by making the same measurement with and without the PCF. The group velocity change is quantified by defining a slow-down factor S corresponding to the ratio between the transit times through the gas cell in slow light conditions (with pump) and in normal conditions (without pump), respectively. The largest time delay achieved through the PCF was 11.7 ns at a pump power of 600 mW, corresponding to an increment of the effective optical path length by 3.5 m and this time
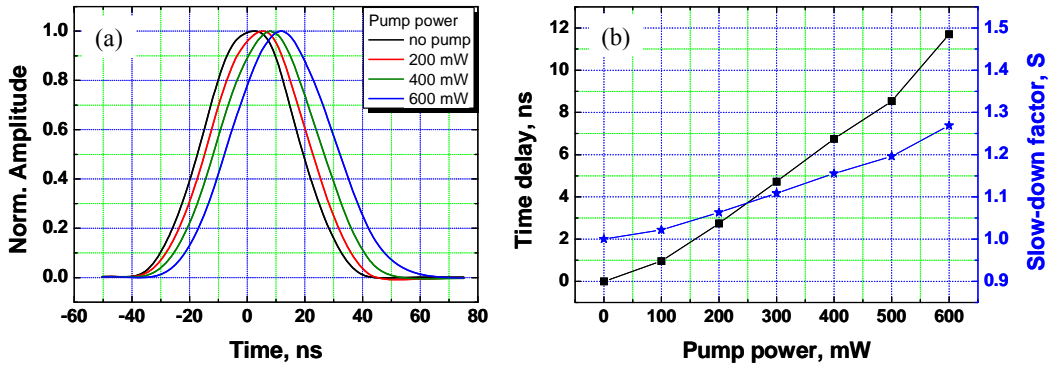
Figure 5.3: (a) Time waveforms of the signal after propagating through the PCF for different pump powers, showing clear signal delays and (b) the time delays achieved in this Brillouin delay line as a function of pump power and the associated slow-down factor.

delay is equivalent to a 26 % reduction of the group velocity.

5.3   Effect of slow light on Beer-Lambert absorption

To observe an absorption resonance of acetylene, the frequency of the signal was swept all over the absorption line, simply by introducing a slow variation of the current applied to the initial DFB laser. Since the signal and pump waves were generated from the same DFB laser source, the pump frequency was also swept with a perfect synchronization to the signal. This way the spectral distance between signal and pump was kept stable during frequency sweeping and matched the Brillouin shift. In consequence, the pump constantly generated a Brillouin gain resonance centered at the signal frequency, even though the signal frequency was swept across the absorption line. It results in a constant Brillouin gain for the signal while the frequency is swept, which means that the group velocity of the signal remains constant and simply controlled by the pump power. The intensity of the signal wave was also sinusoidally modulated at 100 kHz by an EOM to obtain a clean signal using a lock-in detection. The signal wave was then amplified using another EDFA, so as to even further improve the signal-to-noise ratio, still avoiding saturation of the Brillouin amplifier. The output power was then precisely adjusted before entering into the gas cell using a VOA in order to avoid any risk of saturation of the atomic transition [12].

The signal amplitudes after propagating through the fiber gas cell were recorded for different pump powers on a digital oscilloscope while the laser frequency was swept. Figure.5.4 shows the measured normalized absorption when the signal is centered in the P(17) absorption line at 1535.453 nm. The pump power was incremented following the same sequence as during the group delay calibration. Therefore, the curves are fully representative of the gas absorption while the signal propagates through the gas cell at different group

velocities. The absorption curves were normalized in logarithmic scale for a better comparison of the absorption levels. To evaluate the confidence level, measurements were repeated 5 times for each power levels, so that the mean value and the standard deviation of the peak attenuation due to the BL absorption could be accurately estimated. These values representing the absorption at the center of the molecular line are plotted as a function of the slow-down factor in Figure.5.5. It is clearly observed that BL absorption is totally independent on the slow-down factor S, hence group velocity change. The same experiment was also performed for the P(15) and P(19) absorption lines at 1534.158 nm and 1536.771 nm, respectively, resulting in very similar results despite fairly different magnitudes for their absorption coefficient α. The result of this experimental verification of the relationship

Figure 5.4: Variation of the signal amplitude in logarithmic scale after propagating through the PCF gas cell for different pump powers.

Figure 5.5: Measured optical power loss at the peak attenuation due to the Beer-Lambert absorption as a function of the slow-down factor. The error bars show the measured standard deviation on the attenuation measurement and the red line represents the hypothetical response expected for an absorption coefficient inversely proportional to the group velocity.

between absorption and group velocity could be at first glance anticipated, since the BL absorption law is obtained from light-matter interaction by only considering the phase velocity. The experimental results then unambiguously clarified that the linear interaction between light and matter is not influenced by group velocity changes, which is induced by modification of the material properties. However, it could be argued that the time delay (11.7 ns) induced by slow light is negligible compared to the signal period (10 μs) of the sine wave used for the measurements, and thus does not expand substantially the interaction time to lead to an observable effect on the BL absorption. Besides, in this environment, the sine wave acts as a quasi continuous wave which propagates through the gas cell at the phase velocity. To decisively clarify this issue, this experiment was repeated using an optical pulse as signal. The duration of the pulse was 22 ns FWHM, which is shorter than the propagation
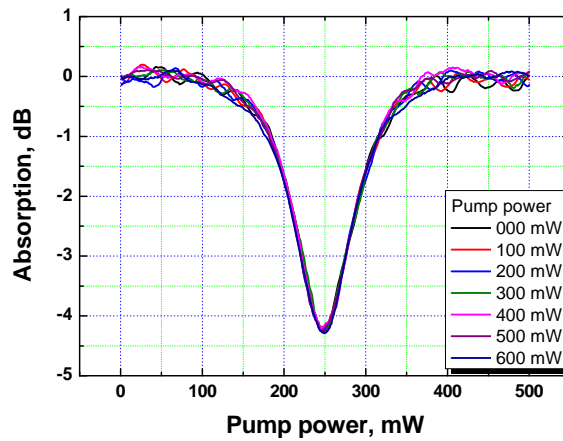
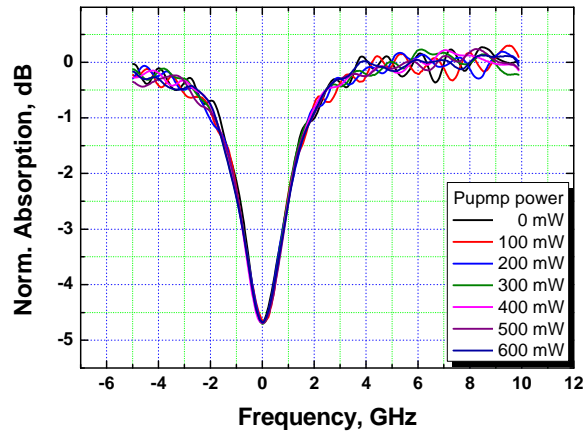Figure 5.6: Amplitude variation of the pulsed signal in logarithmic scale after propagating through the PCF gas cell for different pump powers.
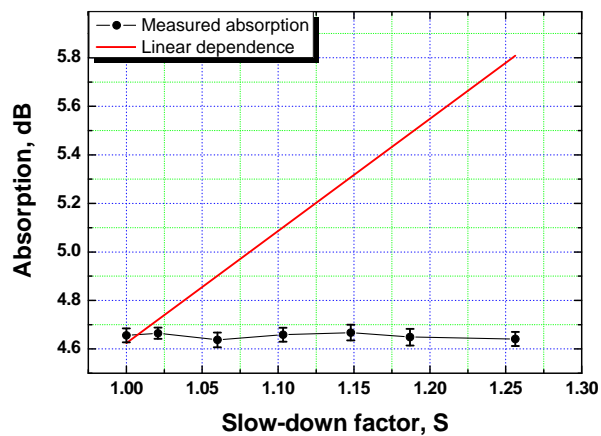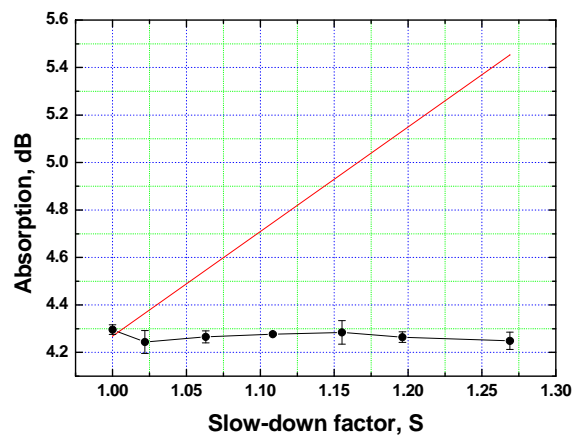
Figure 5.7: Measurement of pulsed signal power loss at the peak attenuation due to the Beer-Lambert absorption as a function of the slow-down factor.

time (45 ns) through the gas fiber cell. This way the interaction time of the signal pulse with the gas is clearly and noticeably modified by slow-light effect. However, this experiment resulted in the same flat response, as shown in Figure 5.5 and Figure 5.6. As a result, it confirms that BL absorption is not influenced by group velocity since photons interacting with gas atoms can be considered as propagating through the material at phase velocity.

These results decisively lead to the evidence that material slow light does not bring any benefit for this kind of sensing, and the same conclusion can be extrapolated with a good confidence to all types of linear light-matter interaction. In fact, in case of material-related slow light the electric field itself may be not enhanced while its energy density is basically condensed due to increased group index in a proportional manner. The extra energy is then transferred into the material to reinforce the acoustic wave, so that the electric field remains constant. However, it must be pointed out that an entirely different conclusion will be probably drawn for structural slow light, like that created in coupled resonators or using the dispersion in a properly designed waveguide structure. In such systems the optical path length is artificially extended through loop recirculation or multiple reflections, causing primarily an apparent slowing of light but also a longer interaction length for light-matter interaction. In that case the apparently enhanced absorption can always be interpreted with classical arguments, out of the framework of slow light theory.

Bibliography

[1] J. B. Khurgin and R.S. Tucker, *Slow Light: Science and Applications*, (CRS Press Boca Raton, 2009).

[2] R. W. Boyd and D.J. Gauthier, *"Slow and Fast Light"*. 2002, Elsevier: Amsterdam. p. 497-530.

[3] M. Soljacic, S. G. Johnson, S. H. Fan, M. Ibanescu, E. Ippen, and J.D. Joannopoulos, "Photonic-crystal slow-light enhancement of nonlinear phase sensitivity," J. Opt. Soc. Am. B, **19**, 2052-2059 (2002).

[4] C. Mohat, B. Corcoran, M. E. Heidari, C. Grillet, B. J. Eggleton, T. P. White, L. O'Faolain, and T.F. Krauss, "Slow light enhancement of nonlinear effects in silicon engineered photonic crystal waveguides," Opt. Express, **17**, 2944-2953 (2009).

[5] A. L. Gaeta, "Slow light: Putting the brakes on images,," Nature Photonics, **1**, 140-141 (2007).

[6] Z. Shi, R. W. Boyd, D. J. Gauthier, and C.C. Dudley, "Enhancing the spectral sensitivity of interferometers using slow-light media," Opt. Lett., **32**, 915-917 (2007).

[7] M. Terrel, M. J. F. Digonnet, and S. Fan, "Performance comparison of slow-light coupled-resonator optical gyroscopes," Laser & Photon. Rev., 1-14 (2009).

[8] N. A. Mortensen and S. Xiao, "Slow-light enhancement of Beer-Lambert-Bouguer absorption," Appl. Phys. Lett., **90**, 141108 (2007).

[9] K. H. Jensen, M. N. Alam, B. Scherer, A. Lambrecht, and N.A. Mortensen, "Slow-light enhanced light-matter interactions with applications to gas sensing," Opt. Commun., **281**, 5335-5339 (2008).

10] A. Hochman and Y. Leviatan, "Efficient and spurious-free integral-equation-based optical waveguide mode solver," Opt. Express, **15**, 14431-14453 (2007).

[11] I. Dicaire, J. C. Beugnot, and L. Thévenaz, "Suspended-core fibers as optical gas sensing cells: study and implementation," SPIE proceeding, **7357**, paper 30 (2009).

[12] J. Henningsen, J. Hal, and J.C. Petersen, "Saturated absorption in acetylene and hydrogen cyanide in hollow-core photonic bandgap fibers," Opt. Express, **13**, 10475-10482 (2006).

Chapter 6

Conclusions and Perspectives

Brillouin slow and fast light has shown an unprecedented flexibility to offer an all-optically controlled delaying element for modern optical telecommunication systems based on high speed networks. However, it has been proved that any slow light system, based on a large dispersion induced by a spectral resonance, presents a critical deadlock in terms of optical storage capacity. As already discussed in many studies [1-3], the maximum achievable time delay in such slow light-delay lines is strictly limited up to a few periods of the signal. Actually, the storage of more than 5-bits of information remains unrealistic, since it requires a tremendous pump power in order to achieve such an amount of time delay, and tends to being subject to a significant noise induced by the amplification process. For this main target application, slow light based on micro-ring resonators could be implemented to extend the maximum delay to 10-bits, but remains restricted to a system, in which the wavelength of a light signal is controlled and very well-defined [4,5]. Also, coherent optical storage seems to be a better approach for the generation of tunable delaying. Recently, it was reported that SBS can transform the information encoded by a bit sequence to an acoustic excitation and retrieve the signal information at a later time, resulting in a considerable delaying effect. From a practical point of view, dispersive delay lines based on wavelength conversion looks like more promising solution to obtain a multi-bits delay. This technique has already shown the capability to delay a full sequence of more than 1000-bits at 10 Gbit/s transmission [6-9]. As a result, although slow light was initially motivated as a scientific challenge to realize an all-optical buffer for future all-optical routers, in practice, it has been proved to be an insufficient timing tool when compared to other methods mentioned above. According to this conclusion the slow-light community started to reconsider potential applications of slow light, where one can take the maximum benefit of the real slowing of light.

Optical storage is just one aspect of slow light applications. Slow light-delay lines can be implemented as a robust solution for retiming applications in digital communications, in which only error-free 1-bit delay is required. In a wavelength-division multiplexing transmission, a light signal in each channel can be independently delayed, so that one channel can be precisely synchronized to other ones using a single bit delaying [10,11]. Moreover, as far as analog signals are concerned in communication systems, slow light is possible to produce tunable delays slightly more than one signal period or 2π phase shift. It turns out that this tunable range is sufficient for the development of optical switches and modulators [12], and also for the generation of true time delays for microwave photonic applications such as photonic microwave filters [13] and phased-array antenna systems [14]. It must be pointed out that the intrinsic linear response of Brillouin amplification can further support the applications to analog signals as linearity is another essential requirement in analog systems.

In slow light conditions, light actually propagates slowly through a medium, so that the transit time turns to be longer. This fascinating fact may potentially lead to a longer interaction length between light and matter. According to this particular feature of slow light, a significant enhancement of light-matter nonlinear interactions has been already demonstrated when light propagates through the optical medium with a reduced group velocity [15-18] and the enhancement of nonlinear effects must scale as the square of slowing-down factor. Additionally, it is anticipated that the spectral sensitivity of interferometers or optical sensors can be considerably improved when a slow light medium is involved in these systems [19-23]. The key point of such applications is that transformations and functions based on optical nonlinearities could be observed in miniaturized structures, showing identical nonlinear efficiency. For instance, if the propagation velocity of light is reduced by a tenth of its normal group velocity, a 1 m-long nonlinear medium under test could be replaced by a 1 cm-long one for an equivalent nonlinear effect. However, this point must be cautiously addressed since particular waveguide structures such as photonic crystal and coupled resonator lead to a longer transit time of light in the medium by increasing the effective path length through multiple reflections (or a similar effect), resulting in a longer interaction time of light with material. A reduced group velocity induced by structural slow light is not a fundamental cause of the sensitivity or nonlinearity enhancement in these implementations. Naturally, structural slow light will give rise to such an enhancement since delaying and enhanced interaction result from the same effect, i.e. an extended effective optical path length.

Nevertheless, some exotic and unexpected applications as well as all these anticipated applications will be discovered in coming years through innovative and creative

solutions, and such scientific challenges makes slow light yet a very fascinating field of research.

Bibliography

[1] R. S. Tucker, P. C. Ku, and C. J. Chang-Hasnain, "Slow-light optical buffers: Capabilities and fundamental limitations," J. Lightwave Technol., **23**, 4046-4066 (2005).

[2] R. W. Boyd, D. J. Gauthier, A. L. Gaeta, and A.E. Willner, "Maximum time delay achievable on propagation through a slow-light medium," Phys. Rev., A, **71**, 023801 (2005).

[3] J. B. Khurgin, "Power dissipation in slow light devices: A comparative analysis," Opt. Lett., **32**, 163-165 (2007).

[4] Khurgin, J.B., "Optical buffers based on slow light in electromagnetically induced transparent media and coupled resonator structures: Comparable analysis," J. Opt. Soc. Am. B, **22**, 1062-1074 (2005).

[5] F. Xia, L. Sekaric, and Y. Vlasov, "Ultracompact optical buffers on a silicon chip," Nature Photonics, **1**, 65-71 (2007).

[6. J. E. Sharping, Y. Okawachi, J. V. Howe, C. Xu, Y. Wang, A. E. Willner, and A.L. Gaeta, "All-optical, wavelength and bandwidth preserving, pulse delay based on parametric wavelength conversion and dispersion," Opt. Express, **20**,7872-7877 (2005).

[7] M. Fok and C. Shu, "Tunable Pulse Delay using Four-Wave Mixing in a 35-cm bismuth Oxide Highly Nonlinear Fiber and Dispersion in a Chirped Fiber Bragg Grating," in Proc. ECOC'06, Cannes, France (2006).

[8] S. Chin and L. Thévenaz, "Large multi Gbit/s delays generated in an all-optical tunable delay line preserving wavelength and signal bandwidth," in Slow and Fast Light, Technical Digest (CD), SMC3 (2008).

[9] Y. Okawachi, M. A. Foster, X. Chen, A. C. Turner-Foster, R. Salem, M. Lipson, C. Xu, and A.L. Gaeta, "Large tunable delays using parametric mixing and phase conjugation in Si nanowaveguides," Opt. Express, **16**, 10349-10357 (2008).

[10] B. Zhang, L. S. Yang, J. Y. Yang, I. Fazal, and A.E. Willner, "A Single slow-light element for independent delay control and synchronization on multiple Gb/s data channels," Photon. Technol. Lett., **19**, 1081-1083 (2007).

[11] B. Zhang, L. Zhang, L. S. Yan, I. Fazal, J. Y. Yang, and A.E. Willner, "Continuously-tunable, bit-rate variable OTDM using broadband SBS slow-light delay line," Optics Express, **15**, 8317-8322 (2007).

[12] D. M. Beggs, T. P. White, L. O'Faolain, and T.F. Krauss, "Ultracompact and low-power optical switch based on silicon photonic crystals," Opt. Lett., **33**, 147-149 (2008).

[13] J. Capmany, B. Ortega, D. Pastor, and S. Sales, "Discret-time optical processing of microwave signals," J. Lightwave Technol., **23**, 702-723 (2005).

[14] J. Capmany and D. Novak, "Microwave photonics combines two worlds," Nature Photonics, **1**, 319-330 (2007).

[15] M. M. Kash, V. A. Sautenkov, A. S. Zibrov, L. Hollberg, G. R. Welch, M. D. Lukin, Y. Rostovtsev, E. S. Fry, and M.O. Scully, "Ultraslow group velocity and enhanced nonlinear optical effects in a coherently driven hot atomic gas," Phys. Rev. Lett., **82**, 5229-5232 (1999).

[16. A. B. Matsko, Y. V. Rostovtsev, H. Z. Cummins, and M.O. Scully, "Using slow light to enhance acoustooptical effects: Application to squeezed light," Phys. Rev. Lett., **84**, 5752-5755 (2000).

[17] M. Soljacic, S. G. Johnson, S. H. Fan, M. Ibanescu, E. Ippen, and J.D. Joannopoulos, "Photonic-crystal slow-light enhancement of nonlinear phase sensitivity," J. Opt. Soc. Am. B, **19**, 2052-2059 (2002).

[18] M. Soljacic and J.D. Joannopoulos, "Enhancement of nonlinear effects using photonic crystals," Nature Mater., **3**, 211-219 (2004).

[19] L. Thévenaz, K. Y. Song, S. Chin, and M. Gonzalez-Herraez, "Light Controlling Light in an Optical Fibre: From Very Slow to Faster-Than-Light Speed," in IEEE Int. Symposium Workshop on Intelligent Signal Processing, Madrid, Spain (2007).

[20] M. González-Herráez, O. Esteban, F. B. Naranjo, and L. Thévenaz, "How to play with the spectral sensitivity of interferometers using slow light concepts and how to do it practically," in Third European Workshop on Optical Fibre Sensors, Napoli, Italy, SPIE Proc., **6619**, 661937 (2007).

[21] Z. Shi, R. W. Boyd, D. J. Gauthier, and C.C. Dudley, "Enhancing the spectral sensitivity of interferometers using slow-light media," Opt. Lett., **32**, 915-917 (2007).

[22] Z. Shi, R. W. Boyd, R. M. Camacho, P. K. Vudyasetu, and J.C. Howell, "Slow-Light Fourier Transform Interferometer," Phys. Rev. Lett, **99**, 240801 (2007).

[23] M. Terrel, M. J. F. Digonnet, and S. Fan, "Performance comparison of slow-light coupled-resonator optical gyroscopes," Laser & Photon. Rev., 1-14 (2009).

Nomenclature

List of symbols

α	Attenuation coefficient
γ_e	Electrostrictive constant
ε_o	Electric permittivity in vacuum
ε	Dielectric constant
$\Delta\varepsilon$	Scalar fluctuations of the dielectric constant
κ	Thermal conductivity
λ	Optical wavelength
μ_o	Magnetic permittivity in vacuum
μ	Dielectric constant
$\Delta\rho$	Density variations
σ	Absorption cross section
τ_p	Average life time of acoustic phonons
ν_p	Optical frequency of the pump wave
ν_s	Optical frequency of the signal wave
ν_B	Brillouin frequency shift
$\Delta\nu_B$	Bandwidth of Brillouin resonance
ϕ	Phase of optical wave
χ_j	j-th order susceptibility
ω_p	Angular frequency of the pump wave
ω_s	Angular frequency of the signal wave
$\delta\omega$	Frequency detuning of the signal wave
Γ	Acoustic damping coefficient
Γ_B	Bandwidth of Brillouin scattering
K	Bulk modulus, Time-bandwidth product

Ω	Angular frequency of the acoustic wave
$\Phi_{p,S}^{SBS}$	Nonlinear phase shift induced by the Brillouin process
c	Light velocity in vacuum
c_p	Specific heat at a constant pressure
f	Electrostrictive force
$g_B(\nu)$	Brillouin gain spectrum
$g_{eff}(\nu)$	Effective Brillouin gain spectrum
k_p	Wavevector of the pump wave
k_S	Wavevector of the Stokes wave
k_1	Group velocity
k_2	Group velocity dispersion
k_3	Dispersion slope
n	Refractive index
n_g	Group index
p_{st}	Electrostrictive pressure
Δp	Pressure fluctuations
q	Wavevector of the acoustic wave
Δs	Entropy fluctuations
t_o	Pulse duration factor
t_{in}	Pulse FWHM duration
Δu	Energy density fluctuations
v_p	Phase velocity
v_g	Group velocity
v_a	Acoustic velocity
A	Amplitude of the acoustic wave
A_{eff}	Effective area
C_s	Adiabatic compressibility
$\tilde{E}$	Fourier transform of the field envelope function
E_p	Field amplitude of the pump wave
E_S	Field amplitude of the Stokes wave
G	Linear Brillouin gain
I	Optical intensity
L_{eff}	Effective length
N	Gas molecular density

P_c	Critical power
P_{in}	Input signal power
P_{out}	Output signal power
$\mathbf{P}_L$	Linear polarization vector
$\mathbf{P}_{NL}$	Nonlinear polarization vector
T	Transfer function
ΔT_d	Effective time delay

List of acronyms

BLB	Beer-Lambert-Bouguer
CPO	Coherent population oscillation
CW	Continuous wave
DC	Direct current
DFB	Distributed-feedback
DSF	Dispersion shifted fiber
EIT	Electromagnetically-induced transparency
EDF	Erbium-doped fiber
EDFA	Erbium-doped fiber amplifier
EOM	Electro-optic modulator
FBG	Fiber Bragg grating
FWHM	Full width at half maximum
GVD	Group velocity dispersion
IFT	Inverse Fourier transform
NOLM	Nonlinear optical loop mirror
PC	Photonic crystal, Polarization controller
PCF	Photonic crystal fiber
RMS	Root mean square
SBS	Stimulated Brillouin scattering
SOA	Semiconductor optical amplifier
SOP	State of polarization
TLS	Tunable laser source
VOA	Variable optical attenuator
XGM	Cross gain modulation

Sanghoon Chin

Address : 89, Route Neuve, Ecublens VD, Switzerland

Phone : (+41) 021 693 68 77

Email : sanghoon.chin@epfl.ch

Civil Status : Married   Gender: Male

Nationality : South Korea   Date of Birth: 27 May 1977

Education

2006.01 onwards	**Ph.D Candidate** in Electrical and Electronics Engineering
	Ecole Polytechnique Fédérale de Lausanne (EPFL), Switzerland
	Group for Fiber Optics, directed by Prof. Luc Thévenaz
Thesis title:	Governing the speed of a light signal in optical fibers: Brillouin slow and fast light
	Experimental research for the development of all-optical buffers
Research interests:	slow & fast light, optical storage, optical fiber sensors, nonlinear fiber optics, light source generation
2003.03 ~ 2005.02	**Master Degree** in Information and Communications
	Gwangju Institute of Science and Technology, South Korea
	Photonic Device Measurement Lab., by Prof. Dug Young Kim
Thesis title:	New method for characterization of nonlinear phase chirp of a laser pulse by fitting its autocorrelation trace
	Experimental research for the generation and characterization of ultra-short optical pulse, generated by Figre-8 EDFL and gain-switched method.
1996.03 ~ 2003.02	**Diploma** in Physics
	Chonnam National University, South Korea
	Major in Optics

Awards and fellowships

2009.06.24	**Conference Grant for Early Stage Researchers**
	ICT domain in COST
2003.03 ~ 2005.02	**Scholarship**
	Korea Ministry of Education

Project involved

2008.09 onwards	**European Project** (219299)
	Governing the Speed of Light (GOSPEL)
2009.01 onwards	**Swiss National Science Foundation** (200020-121860)
	Optical storage
2006.01 ~ 2008.02	**Swiss National Science Foundation** (200021-109773)
	Slow and fast light in optical fibers
2005.05 ~ 2005.10	**European Space Agency** (17267/03/NL/CH)
	Tunable frequency stabilization scheme

Work experience

2006.02 ~ 2009.06	**Teaching assistant**
	Ecole Polytechnique Fédérale de Lausanne, Switzerland
	Preparation of experimental demonstrations for teaching lectures.
2005.05 ~ 2005.10	**Academic Host,**
	Ecole Polytechnique Fédérale de Lausanne, Switzerland
Main activities:	Relative frequency stabilization of semiconductor diode lasers, using mode-locking method and spectral resonance
	Development of a fiber gas cell: sealing CO_2 gas in a photonic crystal fiber at low pressure
2001.06 ~ 2001.08	**Assistant teacher**
	Ivanhoe grammar school, Melbourne, Australia
Main activities:	Teaching assistant for mathematics in a sixth grade class.

1997.04 ~ 1999.06	**Military service**
	South Korea
	Administrative soldier

Languages

Mother tongue	**Korean**		
	Understanding	Speaking	Writing
English:	Fluent in listening and reading	Fluent	Fluent
French:	Intermediate in listening and reading	Intermediate	Intermediate

Non professional skill

Computer skill	Competent with most MS office programmes, Matlab, Origin and Labview (data acquisition, instrument control and step-motor control), and some experience with Mathematica.
Sport and activity	football, ski, hiking and travel

Publications

Journal paper

1. **S. Chin**, Y. J. Kim, H. S. Song and D. Y. Kim, "Complete chirp analysis of a gain-switched pulse using an interferometic two-photon absorption autocorrelation," Appl. Opt. **45**, 7718-7722 (2006).

2. **S. Chin**, M. Gonzalez-Herraez and L. Thevenaz, "Zero-gain slow & fast light propagation in an optical fiber," Opt. Express, **14**, 10684-10692 (2006).

3. **S. Chin**, M. Gonzalez-Herraez and L. Thevenaz, "Simple technique to achieve fast light in gain regime using Brillouin scattering," Opt. Express, **15**, 10814-10821 (2007).

4. **S. Chin**, M. Gonzalez-Herraez and L. Thevenaz, "Self-advanced fast light propagation in an optical fiber based on Brillouin scattering," Opt. Express, **16**, 12181-12189 (2008).

5. **S. Chin**, and L. Thevenaz, "Optimized shaping of isolated pulses in Brillouin fiber slow light systems," Opt. Lett., **34**, 707-709 (2009).

6. A. Zadok, **S. Chin**, L. Thevenaz, E. Zilka, A. Eyal and M. Tur, "Stimulated Brillouin scattering induced polarization mode dispersion in slow light setups," submitted to Opt. Lett.

7. **S. Chin**, and L. Thevenaz, "Large multi Gbit/s delays generated in an all-optical tunable delay line preserving wavelength and signal bandwidth," Photon. Technol. Lett., under submission.

8. **S. Chin**, M. Gonzalez-Herraez and L. Thevenaz, "Complete compensation of pulse broadening in a linear slow light system using a non-linear regeneration element," Opt. Express, under submission.

Invited presentation

1. L. Thévenaz, **S. -H. Chin**, K. -Y. Song, and M. Gonzalez-Herráez, "Flexible Slow and Fast Light in Optical Fibers," LEOS 19th Annual Meeting 2006, Montreal QC, October 29 – November 2 2006, Paper MA3, pp. 18-19, Invited.

2. M. Gonzalez-Herráez, K. -Y. Song, **S. -H. Chin**, and L. Thévenaz, " Progress in Brillouin Slow Light and Its Impact in Fiber Sensing," 18th International Conference on Optical Fiber Sensors, Cancún, Mexico, October 23-27 2006, OSA Technical Digest (CD) (Optical Society of America, 2006), paper TuC1, Invited.

3. L. Thévenaz, M. Gonzalez-Herráez, K. -Y. Song, **S. -H. Chin**, "La lumière lente et rapide: une future pièce maîtresse pour la photonique", 25e Journées Nationales d'Optique Guidée JNOG'06, Metz F, November 7-9, 2006, Invited.

4. L. Thévenaz, K. Y. Song, **S. Chin** and M. Gonzalez-Herráez, " Light controlling light in an optical fibre: from very slow to faster-than-light speed", IEEE International Symposium on Intelligent Signal Processing WISP 2007, Alcala de Henares, Spain, October 3-5 (2007), Plenary talk.

5. **S. Chin**, K. Y. Song, M. Gonzalez-Herráez and L. Thévenaz, "Slow and fast light in optical fibers, based on stimulated Brillouin scattering," Seminar, University of Chosun, South Korea, August 7, (2008), Invited.

6. L. Thévenaz, M. Gonzalez-Herráez, **S. Chin**, "Potentialities of show and fast light in optical fibers," Proceedings Photonic West, SPIE, **7226**, 72260C (2009), Invited.

Presentation in conferences

1. **S. Chin**, Y. J. Kim, H. S. Song and D. Y. Kim, "Non-linear phase chirp retrieval of a 1.55 um gain switched pulse laser using two photon absorption autocorrelation," CLEO Pacific/Rim, **CWAB3-P10** (2006)

2. L. Thévenaz, **S. H. Chin**, M. Gonzalez-Herráez, "Zero-Gain Slow Light in Optical Fibres", Proceedings of the 32nd European Conference on Optical Communication ECOC'2006, Sept. 24-28, 2006, Cannes, F, paper Tu1.1.2.

3. L. Thévenaz, **S. -H. Chin**, K. -Y. Song, and M. Gonzalez-Herráez, "Flexible Slow and Fast Light Using Tailored Brillouin Spectra in Optical Fibers," in Slow and Fast Light, Technical Digest (CD) (Optical Society of America, 2006), paper TuB4.

4. R. Matthey, C. Affolderbach, G. Mileti, S. Schilt, D. Werner, **S.-H. Chin**, L. Abrardi, L. Thévenaz, "Frequency-stabilized laser reference system for trace-gas sensing applications from space", 6th International Conference on space Optics, Noordwijk, Netherlands, June 27-30, 2006.

5. R. Matthey, C. Affolderbach, G. Mileti, S. Schilt, D. Werner, **S.-H. Chin**, L. Abrardi, L. Thévenaz, "Water vapour DIAL optical frequency laser reference system", 23rd International Laser Radar Conference, Nara, Japan, July 24-28, 2006.

6. **S. Chin**, M. Gonzalez-Herráez and L. Thévenaz, "Simple scheme for realizing fast light with low distortion in optical fibers," Research day & Photonics day, EPFL, **Poster section** (2006).

7. **S. Chin**, M. Gonzalez-Herráez and L. Thévenaz, "Simple scheme for realizing fast light with low distortion in optical fibers," European Conference on Lasers and Electro-Optics, June 17-22, **CD9-4-Fri** (2007).

8. **S. Chin**, M. Gonzalez-Herráez and L. Thévenaz, "Self-advanced propagation of light pulse in an optical fiber based on Brillouin scattering," in Slow and Fast Light, Technical Digest (CD), **SWC5** (2007).

9. L. Thévenaz, **S. Chin** and M. Gonzalez-Herráez and, "Low distortion fast light in an optical fiber using stimulated Brillouin scattering," in Slow and Fast Light, Technical Digest (CD), **JTuA8** (2007).

10. **S. Chin**, L. Thévenaz and M. Gonzalez-Herráez, "Self-advanced fast light in an optical fiber based on Brillouin scattering," Research day & Photonics day, EPFL, **Poster section** (2008).

11. J. P. Dakin, **S. Chin**, L. Thévenaz, "A multiplexed CW Brillouin system for precise interrogation of a sensor array made from short discrete sections of optical fiber," 19th international conference on Optical Fiber Sensors, **7004**, 70046L-4 (2008).

12. **S. Chin**, and L. Thévenaz, "Enhancement of Brillouin slow-light in optical fibers through optical pulse shaping," in Slow and Fast Light, Technical Digest (CD), **JMB10** (2008).

13. L. Thévenaz and **S. Chin**, "Self-pumped optical delay line based on Brillouin fast light in optical fibers," in Slow and Fast Light, Technical Digest (CD), **STuC5** (2008).

14. **S. Chin**, and L. Thévenaz, "Large multi Gbit/s delays generated in an all-optical tunable delay line preserving wavelength and signal bandwidth," in Slow and Fast Light, Technical Digest (CD), **SMC3** (2008).

15. **S. Chin**, M. Gonzalez-Herráez and L. Thévenaz, "Complete broadening compensation in a slow light system using a non-linear regeneration element," in Slow and Fast Light, Technical Digest (CD), **JWB2** (2009).

16. **S. Chin**, I. Dicaire, J. C. Beugnot, S. Foaleng-Mafang, M. Gonzalez-Herráez and L. Thévenaz, "Material slow light does not enhance Beer-Lambert absorption," in Slow and Fast Light, Technical Digest (CD), **SMA3** (2009).

17. L. Thévenaz, **S. Chin**, I. Dicaire, J. C. Beugnot, S. Foaleng-Mafang and M. Gonzalez-Herráez, "Experimental verification of the effect of slow light on molecular absorption," 20th international conference on optical fiber sensors (2009), <u>accepted</u>.

18. A. Zadok, **S. Chin**, E. Zilka, A. Eyal, L. Thevenaz and M. Tur, "Polarization dependent pulse distortion in stimulated Brillouin scattering slow light systems," <u>submitted to the post-deadline for Slow and Fast Light, Technical Digest (CD) (2009)</u>.